



LIBRARY
Michigan State
University

This is to certify that the

dissertation entitled

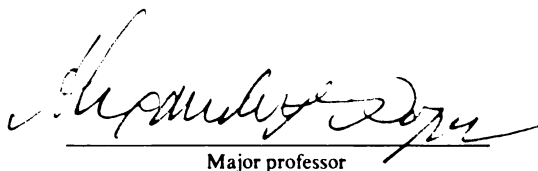
*Mechanisms of Crown Ether Complexation
Reactions With Na^+ and Cs^+ Ions*

presented by

Bruce Owen Strasser

has been accepted towards fulfillment
of the requirements for

Ph.D. degree in Chemistry



Major professor

Date 11-19-84



RETURNING MATERIALS:
Place in book drop to
remove this checkout from
your record. FINES will
be charged if book is
returned after the date
stamped below.

MAY 11 2000

MECHANISMS OF CROWN ETHER COMPLEXATION
REACTIONS WITH Na^+ and Cs^+ IONS

By

Bruce Owen Strasser

A DISSERTATION

Submitted to
Michigan State University
in partial fulfillment of the requirements
for the degree of

DOCTOR OF PHILOSOPHY
Department of Chemistry

1984

ABSTRACT

MECHANISMS OF CROWN ETHER COMPLEXATION REACTIONS WITH Na^+ and Cs^+ IONS

By

Bruce Owen Strasser

The kinetics of complexation of sodium ion with the ligand 18-crown-6 (18C6) were studied in six solvents or solvent mixtures by a complete sodium-23 nuclear magnetic resonance line-shape analysis. The salt used was sodium tetraphenylborate or the thiocyanate. The solvent systems were tetrahydrofuran, methanol, propylene carbonate, methanol-tetrahydrofuran mixture (40-60 mole %) and propylene carbonate-tetrahydrofuran mixtures (20-80 and 60-40 mole %).

In tetrahydrofuran solutions, the exchange mechanism is determined by the degree of contact ion pairing of the sodium salt and of its complex with 18C6. When SCN^- is the counterion the solvated and complexed sodium ions form contact ion pairs and higher ionic aggregates. This ionic association reduces the charge-charge repulsion of the sodium ions in the transition state of the bimolecular exchange mechanism and allows this process to predominate. When BPh_4^- or AlEt_4^- are the counterions, contact ion pairing is minimal and the predominant exchange mechanism is the dissociative process.

In methanol, in the methanol-tetrahydrofuran mixture, and in the 20-80 mole % propylene carbonate-tetrahydrofuran mixture, the predominant exchange mechanism is the dissociative process. However, in propylene carbonate and in the 60-40 mole % propylene carbonate-tetrahydrofuran mixture, the predominant exchange mechanism is the bimolecular exchange process.

A correlation has been found between the Gutmann donor number of the solvent and the free energy of activation for the dissociative step in systems in which the dissociative mechanism has been found to predominate. In those cases in which the bimolecular mechanism is predominant, the free energy of activation for the process is independent of solvent.

The kinetics of complexation of cesium thiocyanate with the ligands dibenzo-21-crown-7 (DB21C7) and dibenzo-24-crown-8 (DB24C8) were studied in acetone and in methanol solutions by a complete cesium-133 nuclear magnetic resonance lineshape analysis. In all systems, the bimolecular exchange process has been found to be predominant.

Isosolvation studies of sodium ion in methanol-tetrahydrofuran and in propylene carbonate-tetrahydrofuran solutions have been done using sodium-23 nuclear magnetic resonance chemical shifts. The salts were sodium tetraphenylborate and sodium perchlorate. In all systems, the solvent with the higher Gutmann donor number has the lowest concentration at the isosolvation point.

This Thesis is
Dedicated
To My Parents

ACKNOWLEDGMENT

Sincere gratitude is extended to Tom V. Atkinson whose computer wizardry has greatly reduced the time and frustration needed for the completion of this dissertation. Your patience, dedication, and friendship have not gone unappreciated.

Many thanks go to the Popov group. Our long philosophical discussions, whether over coffee or wine, have made my stay here quite memorable.

One cannot forget the dedication of the "happy hour gang". The weeks flew by in anticipation of Fridays at 5:00 p.m. Where do you want to go?

The efforts of the nmr group - Klaas, Kermit, and Long - must be fully acknowledged. Your contributions to the nmr facility and the work presented in this thesis have not gone unnoticed.

Finally, thanks Alex. Your guidance and friendship throughout my stay here at Michigan State are warmly appreciated. Don't forget to save room for (Meg's) dessert.

TABLE OF CONTENTS

Chapter	Page
LIST OF TABLES	vii
LIST OF FIGURES.	xii
LIST OF ABBREVIATIONS.	xix
CHAPTER 1. HISTORICAL REVIEW.	1
Introduction	2
Complexation Kinetics of Alkali Cation- Crown Ether Complexes.	3
CHAPTER 2. EXPERIMENTAL PART.	21
A. Salt and Ligand Purification	22
B. Instrumental Measurements and Data Handling.	24
1. Instruments.	24
2. References and Corrections	24
3. Temperature Calibration and Control.	27
4. Linewidth Measurements	30
5. Data Acquisition and Signal Processing	32
6. Data Transfer.	33
CHAPTER 3. MISCELLANEOUS.	35
A. Ion-Pairing in Tetrahydrofuran Solutions.	36
Introduction	36
Results and Discussion	38
1. Conductance Measurements	38
2. Infrared Studies	40
3. NaAlEt ₄ -18C6 Exchange in THF	42

Chapter	Page
Conclusions.	42
B. Isosolvation Studies	45
Introduction	45
Results and Discussion	47
CHAPTER 4. KINETICS OF COMPLEXATION OF SODIUM ION WITH 18-Crown-6 IN NONAQUEOUS SOLVENTS	54
A. Introduction	55
B. Choice of Solvents and Salts	55
C. Results and Discussion	59
1. Measurements in the Absence of Exchange.	59
2. Fourier Transform NMR Exchange Equations.	77
3. Mechanisms of Exchange	84
4. Results in THF Solutions	86
5. Results in Methanol Solutions.	98
6. Results in PC Solutions.	105
7. Comparison of Results in Neat Solvents	107
8. Results in MeOH-THF Mixture.	116
9. Results in PC-THF Mixtures	121
CHAPTER 5. COMPLEXATION KINETICS OF CESIUM ION WITH DB 21C7 AND WITH DB24C8	130
Introduction	131
Results and Discussion	132
A. Measurements in the Absence of Exchange	132
B. Kinetic Results.	142

Chapter	Page
APPENDICES	
APPENDIX A - DATA TRANSFER PROGRAMS FOR THE WH-180 NMR	155
APPENDIX B - FT-NMR TWO-SITE EXCHANGE EQUATIONS MODIFIED TO INCLUDE LINE BROADENING AND DELAY TIME.	159
APPENDIX C - SUGGESTIONS FOR FUTURE WORK	165
REFERENCES	169

LIST OF TABLES

Table		Page
1	Exchange Mechanisms Postulated or Observed for Alkali Metal Ion-Crown Ether Complexation	5
2	Kinetic Parameters for Relaxation of 18C6 in Various Solvents	8
3	Kinetic Parameters for Com- plexation of Na ⁺ Ion with Crown Ethers at 25°C	13
4	Kinetic Parameters for K ⁺ Ion Complexa- tion with 18C6 in Various Solvents at 25°C	15
5	Kinetic Parameters for Complexation Kinetics of Cs ⁺ Ion at 25°C.	17
6	Kinetic Parameters for Complexation of Cs ⁺ Ion with Several Crown Ethers in Methanol and in Acetone Solutions at 25°C	18
7	Temperature Calibration of the WH- 180 Spectrometer	28
8	Temperature Calibration of the DA-60 Spectrometer	29

Table		Page
9	Equivalent Conductances of Various Tetrahydrofuran Solutions at 25°C.	39
10	Sodium-23 Chemical Shift vs. Composition of THF/PC Binary Mixtures at 25°C	48
11	Sodium-23 Chemical Shifts vs Com- position of THF/MeOH Binary Mixtures at 25°C.	49
12	Selected Properties of Some Solvents at 25°C.	57
13	Sodium-23 Chemical Shifts and Relaxa- tion Rates of NaBPh ₄ and of its Com- plex with 18C6 in THF Solutions.	60
14	Sodium-23 Chemical Shifts and Relaxation Rates of NaSCN and of its Complex with 18C6 in THF Solu- tions.	61
15	Sodium-23 Chemical Shifts and Relaxa- tion Rates of NaBPh ₄ and of its Com- plex with 18C6 in PC Solutions	62
16	Sodium-23 Chemical Shifts and Relaxa- tion Rates of NaSCN and of its Com- plex with 18C6 in MeOH	63
17	Sodium-23 Chemical Shifts and Relaxa- tion Rates of NaBPh ₄ and of its Com- plex with 18C6 in a 40-60 mole %	

Table		Page
	MeOH-THF Mixture	64
18	Sodium-23 Chemical Shifts and Relaxa- tion Rates of NaBPh ₄ and of its Com- plex with 18C6 in a 80-20 mole %	
	THF-PC Mixture	65
19	Sodium-23 Chemical Shifts and Relaxa- tion Rates of NaBPh ₄ and of its Com- plex with 18C6 in a 60-40 mole %	
	PC-THF Mixture	66
20	Sodium-23 Results for Solvated Na ⁺ in Selected Solvents	73
21	Sodium-23 Results for Complexed Na ⁺ in Selected Solvents	74
22	Mean Lifetimes as a Function of Temperature for the System NaBPh ₄ · 18C6 in THF Solutions.	87
23	Mean Lifetimes as a Function of Temperature for the System NaSCN· 18C6 in THF Solutions.	88
24	Kinetic Parameters for the Com- plexation of Na ⁺ with 18C6 at 25°C	92
25	Weighted Average List of Kinetic Parameters for Complexation of Na ⁺ with 18C6 at 25°C.	95

Table		Page
26	Kinetic Results for the System NaAlEt ₄ ·18C6 in THF Solutions at 25°C	97
27	Mean Lifetimes as a Function of Temperature for the System NaSCN· 18C6 in MeOH Solutions	100
28	Kinetic Parameters for the Complexa- tion of NaSCN by Several Crown Ethers in MeOH Solutions at 25°C	103
29	Mean Lifetimes as a Function of Temperature for the System NaBPh ₄ · 18C6 in PC Solutions	106
30	Mean Lifetimes as a Function of Temperature for the System NaBPh ₄ · 18C6 in a 60-40 Mole % THF-MeOH Mixture.	117
31	Mean Lifetimes as a Function of Tem- perature for the System NaBPh ₄ ·18C6 in a 20-80 Mole % PC-THF Mixture	122
32	Mean Lifetimes as a Function of Tem- perature for the System NaBPh ₄ ·18C6 in a 60-40 Mole % PC-THF Mixture.	123
33	Cesium-133 Chemical Shifts and Relaxa- tion Rates of CsSCN and of its Complexes with DB21C7 and with DB24C8 in MeOH Solutions.	133

Table		Page
34	Cesium-133 Chemical Shifts and Relaxation Rates of CsSCN and of its Complexing with DB21C7 and with DB24C8 in AC Solutions.	135
35	Mean Lifetimes as a Function of Temperature for CsSCN-Crown in MeOH Solutions.	143
36	Mean Lifetimes as a Function of Temperature for CsSCN-Crown in AC Solutions.	144
37	Kinetic Parameters for the Complexation of Cs ⁺ with Several Crown Ethers in AC and in MeOH Solutions at 220°K	151

LIST OF FIGURES

Figure		Page
1	Some synthetic and naturally occurring macrocycles	4
2	Types of ion pairs in solution.	37
3	Room temperature infrared spectra of tetrahydrofuran solutions containing NaSCN. I) 0.126 <u>M</u> NaSCN + 0.140 <u>M</u> 18C6: Spectrum of $\text{Na}^+ \cdot 18\text{C}6 \cdot \text{NCS}^-$. II) 0.074 <u>M</u> NaSCN, (a) $\text{Na}^+ \cdot \text{NCS}^- \cdot \text{Na}^+$; (b) $\text{Na}^+ \cdot \text{NCS}^-$; (c) $(\text{Na}^+ \cdot \text{NCS}^-)_2$. Assign- ments from Reference 56	41
4	Sodium-23 nmr of a solution containing [NaAlEt ₄]/[18C6] ≈ 1.9 in THF at several temperatures.	43
5	Sodium-23 chemical shift <u>vs.</u> composition of THF/PC mixtures. (o) 0.1 <u>M</u> NaBPh ₄ ; (x) 0.1 <u>M</u> NaClO ₄ ; (*) (+) isosolvation points.	50
6	Sodium-23 chemical shift <u>vs.</u> composition of THF/MeOH mixtures. (o) 0.1 <u>M</u> NaClO ₄ ; (x) 0.1 <u>M</u> NaBPh ₄ ; (*) isosolvation point.	51
7	Semilog plots of $1/T_2$ <u>vs.</u> reciprocal temperatures for tetrahydrofuran	

	solutions containing solvated and 18C6 complexed Na^+ ion.	68
8	Semilog plots of $1/T_2$ <u>vs.</u> reciprocal temperatures for solutions containing solvated and 18C6 complexed Na^+ ion . . .	69
9	Semilog plots of $1/T_2$ <u>vs.</u> reciprocal temperatures for solutions containing solvated Na^+ ion. (x) 0.1 <u>M</u> NaBPh_4 in a 20-80 mole % PC-THF mixture; (o) 0.1 <u>M</u> NaBPh_4 in a 40-60 mole % MeOH-THF mixture; (+) 0.1 <u>M</u> NaBPh_4 in a 60-40 mole % PC-THF mixture	70
10	Semilog plots of $1/T_2$ <u>vs.</u> reciprocal temperatures for solutions containing 18C6 complexed Na^+ ion. (x) 0.1 <u>M</u> NaBPh_4 in a 60-40 mole % PC-THF mixture; (+) 0.1 <u>M</u> NaBPh_4 in a 20-80 mole % PC-THF mixture; (o) 0.1 <u>M</u> NaBPh_4 in a 40-60 MeOH-THF mixture	71
11	Computer fits of a sodium-23 nmr spectrum of a solution containing 0.2 <u>M</u> NaBPh_4 and 0.1 <u>M</u> 18C6 in THF at 25°C and a delay time of 800 μs . (x) experimental point; (o) calculated point; (=) no dif- ference between calculated and experimental	

	points within plot accuracy. (a)	
	no delay time correction; (b) with delay	
	time correction	80
12	Free induction decays with different	
	relaxation times.	81
13	Semilog plots of $1/\tau$ <u>vs.</u> $1/T$ at various	
	$[\text{NaBPh}_4]/[\text{18C6}]$ mole ratios in tetra-	
	hydrofuran solutions.	89
14	Semilog plot of $1/\tau$ <u>vs.</u> $1/T$ for $\text{NaSCN} \cdot$	
	18C6 in tetrahydrofuran solutions	90
15	Plot of $1/(\tau[\text{Na}^+]_{\text{total}})$ <u>vs.</u> the inverse	
	of the free sodium ion concentration for	
	$\text{NaBPh}_4 \cdot \text{18C6}$ in tetrahydrofuran solutions	
	at 25°C	93
16	Plots of $1/(\tau[\text{Na}^+]_{\text{total}})$ <u>vs.</u> the inverse	
	of the free sodium ion concentration for	
	$\text{NaSCN} \cdot \text{18C6}$ in tetrahydrofuran solutions at	
	several temperatures.	94
17	Plot of $1/(\tau[\text{Na}^+]_{\text{total}})$ <u>vs.</u> the inverse	
	of the free sodium ion concentration for	
	$\text{NaAlEt}_4 \cdot \text{18C6}$ in tetrahydrofuran solutions	
	at 25°C	99
18	Semilog plot of $1/\tau$ <u>vs.</u> $1/T$ for $\text{NaSCN} \cdot$	
	18C6 in methanol solutions.	101
19	Plot of $1/(\tau[\text{Na}^+]_{\text{total}})$ <u>vs.</u> the inverse	
	of the free sodium ion concentration for	
	$\text{NaSCN} \cdot \text{18C6}$ in methanol solutions at -4.7°C . 102	

20	Semilog plot of $1/(\tau[\text{Na}^+]_{\text{total}})$ <u>vs.</u> $1/T$ for $\text{NaBPh}_4 \cdot 18\text{C6}$ in propylene carbonate solutions	108
21	Plot of $1/(\tau[\text{Na}^+]_{\text{total}})$ <u>vs.</u> the inverse of the free sodium ion concentration for $\text{NaBPh}_4 \cdot 18\text{C6}$ in propylene carbonate solutions at -4.7°C	109
22	Semilog plot of k_{-2} <u>vs.</u> Gutmann donor number for Na^+ -crown in various solvents. (o) 18C6; (x) DB18C6; (+) DC18C6 (References 10, 25, 78)	112
23	Plot of ΔG_{-2}^\ddagger <u>vs.</u> Gutmann donor number for Na^+ -crown in various solvents. (o) 18C6; (x) DB18C6; (+) DC18C6 (References 10, 25, 78)	113
24	Semilog plot of $1/\tau$ <u>vs.</u> $1/T$ for $[\text{NaBPh}_4]/[\text{18C6}] = 1.91$ in a 40-60 mole % MeOH-THF mixture	118
25	Plot of $1/(\tau[\text{Na}^+]_{\text{total}})$ <u>vs.</u> the inverse of the free sodium ion concentration for $\text{NaBPh}_4 \cdot 18\text{C6}$ in a 40-60 mole % MeOH-THF mixture at 25°C	119
26	Plot of ΔG_{-2}^\ddagger <u>vs.</u> Gutmann donor number for Na^+ -crown in various solvents (References 10, 25, 78)	120

Figure		Page
27	Semilog plots of $1/\tau$ <u>vs.</u> $1/T$ for NaBPh ₄ ·18C6 in 60-40 mole % PC-THF solutions	124
28	Semilog plots of $1/\tau$ <u>vs.</u> $1/T$ for NaBPh ₄ ·18C6 in 20-80 mole % PC-THF solutions	125
29	Plot of $1/(\tau[\text{Na}^+]_{\text{total}})$ <u>vs.</u> the inverse free sodium ion concentration for NaBPh ₄ ·18C6 in 20-80 mole % PC- THF mixtures at 25°C.	126
30	Plot of $1/(\tau[\text{Na}^+]_{\text{total}})$ <u>vs.</u> the inverse free sodium ion concentration for NaBPh ₄ ·18C6 in 60-40 mole % PC- THF mixtures at 25°C.	127
31	Semilog plots of $1/T_2$ <u>vs.</u> $1/T$ for solvated and complexed cesium ion in methanol solutions. (x) 0.02 <u>M</u> CsSCN; (o) 0.02 <u>M</u> Cs ⁺ ·DB24C8, SCN ⁻ ; (+) 0.02 <u>M</u> Cs ⁺ ·DB21C7, SCN ⁻	136
32	Semilog plots of $1/T_2$ <u>vs.</u> $1/T$ for solvated and complexed cesium ion in acetone solutions. (o) 0.02 <u>M</u> CsSCN; (x) 0.02 <u>M</u> CsBPh ₄ (Reference 30); (●) 0.02 <u>M</u> Cs ⁺ ·DB24C8, SCN ⁻ ; (+) 0.02 <u>M</u> Cs ⁺ ·DB21C7, SCN ⁻	137

- 33 Semilog plots of $1/\tau$ vs. $1/T$ for
CsSCN·DB24C8 in methanol solutions.
(o)[CsSCN]/[DB21C7] = 3.18; (x)
[CsSCN]/[DB21C7] = 1.62; (●)
[CsSCN]/[DB24C8] = 1.61; (+)
[CsSCN]/[DB24C8] = 3.16; all DB24C8
data used for fit 145
- 34 Semilog plots of $1/\tau$ vs. $1/T$ for
CsSCN·DB21C7 and for CsSCN·DB24C8 in
acetone solutions. (●)[CsSCN]/[DB24C8] =
1.62; (+)[CsSCN]/[DB24C8] = 2.55; (x)
[CsSCN]/[DB21C7] = 2.97; (o)[CsSCN]/
[DB21C7] = 1.62 146
- 35 Plots of $1/(\tau[\text{Cs}^+]_{\text{total}})$ vs. the
inverse free cesium ion concentration
for CsSCN·DB21C7 in acetone solutions
at various temperatures. (o) 215°K;
(x) 200°K 147
- 36 Plots of $1/(\tau[\text{Cs}^+]_{\text{total}})$ vs. the
inverse free cesium ion concentration
for CsSCN·DB21C7 in methanol solutions
at various temperatures. (o) 220°K;
(x) 200°K 148
- 37 Plots of $1/(\tau[\text{Cs}^+]_{\text{total}})$ vs. the
inverse free cesium ion concentration

	for CsSCN·DB24C8 in acetone solutions at various temperatures. (x) 215°K; (o) 200°K	149
38	Plots of $1/(\tau[\text{Cs}^+]_{\text{total}})$ <u>vs.</u> the inverse free cesium ion concentration for CsSCN·DB24C8 in methanol solutions at various temperatures. (o) 214°K; (x) 206°K	150

LIST OF ABBREVIATIONS

THF	Tetrahydrofuran
PC	Propylene carbonate
MeOH	Methanol
EtOH	Ethanol
DMF	Dimethylformamide
DME	Dimethoxyethane

CHAPTER 1

HISTORICAL REVIEW

INTRODUCTION

The abundance of information available in the field of alkali metal ion complexation has grown dramatically since the discovery by Pedersen (1,2) of the macrocyclic ligands known as crown ethers and later the synthesis of cryptands by Lehn and coworkers (3-5). Yet, the knowledge of complexation kinetics of alkali metal ions with crown ethers is meager compared to what is currently known about complex stabilities. This is surprising considering the importance such information may provide as, for example, models for ion transport in biological membranes.

The role of the solvent in the kinetic process of complexation of alkali metal ions by crown ethers is, as yet, unknown. The influence of the ligand cavity size and of the counterion on the complexation kinetics remain unexplained. Whether or not the different alkali metal ions exhibit differences in their complexation kinetics with crown ethers has not been established. These are just a few of the unknowns which exist in this area. It is the intent of this dissertation to begin the process of unraveling these unknowns.

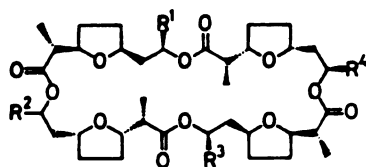
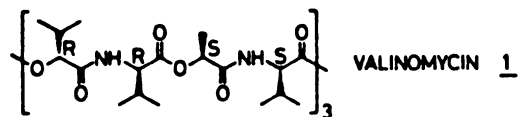
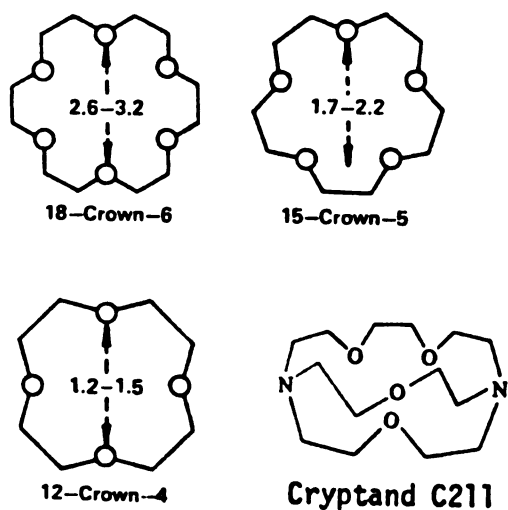
A review of current progress in the field of kinetics of complexation of alkali metal ion by crown ethers is necessary at this point.

COMPLEXATION KINETICS OF ALKALI CATION - CROWN ETHER COMPLEXES

The sparse information available for the kinetics of alkali metal ion complexation by macrocyclic ligands has been reviewed by Liesegang and Eyrins (6) (through 1978), by Schmidt (7) (through 1981) and by Szczygiel (8) (through 1984). Consequently, this survey will focus on the main concepts of alkali metal ion - crown ether kinetics discussed in these reviews, as well as review current progress in this field.

Several mechanisms have been postulated or observed for the complexation of alkali metal ions by crown ethers and cryptands (Figure 1). These mechanisms are listed in Table 1. The presence of the solvent, though not indicated, is implied.

Wong et al. (9) used proton nmr to study the exchange of sodium ion with dimethyldibenzo-18-crown-6 in deuterated tetrahydrofuran. Since an excess of the ligand was present in solution, exchange mechanism I was assumed in which the metal ion is simply exchanging between the crown ether molecules. An Arrhenius activation energy, E_a , of $12.5 \text{ kcal} \cdot \text{mol}^{-1}$ was calculated for this process. Replacement of the above crown by dicyclohexyl-18-crown-6 (DC18C6) resulted in a drop in the coalescence temperature from 2°C . In fact the coalescence was not observed although the measurements were carried down to -60°C . The difference



$R^1 = R^2 = R^3 = R^4 = \text{CH}_3$	NONACTIN	<u>2</u>
$R^1 = R^2 = R^3 = \text{CH}_3$ $R^4 = \text{C}_2\text{H}_5$	MONACTIN	<u>3</u>
$R^1 = R^3 = \text{CH}_3$ $R^2 = R^4 = \text{C}_2\text{H}_5$	DINACTIN	<u>4</u>
$R^1 = \text{CH}_3$ $R^2 = R^3 = R^4 = \text{C}_2\text{H}_5$	TRINACTIN	<u>5</u>
$R^1 = R^2 = R^3 = R^4 = \text{C}_2\text{H}_5$	TETRAACTIN	<u>6</u>

Figure 1. Some synthetic and naturally occurring macrocycles.

Table 1. Exchange Mechanisms Postulated or Observed
for Alkali Metal Ion-Crown Ether Complexation.

$M^+ \cdot C + \overset{*}{C} \xrightarrow{k_1} M^+ \cdot \overset{*}{C} + C$	I
$M^+ + C \xrightleftharpoons[k_{-1}]{k_1} M^+ \cdot C$	II
$M^+ + \overset{*}{M}^+ \cdot C \xrightleftharpoons{k_1} M^+ \cdot C + \overset{*}{M}^+$	III
$k_{-0} \overset{C'}{\underset{C}{\updownarrow}} k_0 + M^+ \xrightleftharpoons[k_{-1}]{k_1} M^+ \cdot C$	IV
$M^+ + C \xrightleftharpoons[k_{-1}]{k_1} M^+ \cdot C \xrightleftharpoons[k_{-2}]{k_2} M^+ C'$	V
$M^+ + C \xrightleftharpoons[k_{-1}]{k_1} M^+ \dots C \xrightleftharpoons[k_{-2}]{k_2} MC^+ \xrightleftharpoons[k_{-3}]{k_3} (MC)^+$	VI

in kinetic properties of the two crowns was postulated to be due to stronger ion-pairing of the dimethyldibenzo-18-crown-6 complex with the florenyl counterion which was used.

Shchori et al. (10) used ^{23}Na nmr to study the complexation kinetics of Na^+ by dibenzo-18C6 (DB18C6) in dimethylformamide (DMF). They found that in this case the exchange occurs by way of the associative-dissociative mechanism II rather than the bimolecular process III.

Chock (11) used temperature jump relaxation technique to study monovalent cation complexation by dibenzo-30-crown-10 in methanol (MeOH) solutions. The kinetic data were best described by mechanism IV. The crown ether undergoes a rapid transformation between two conformers. One of the conformers reacts readily with the cation to form the complex.

The conformational equilibria of the smaller crown ethers have been explored further. Liesegang et al. (12) measured relaxation of 18C6 in aqueous solutions with no salt present and found a relaxation time of $\tau_{-1} = 6.2 \times 10^8 \text{ s}^{-1}$ at 25°C . A relaxation rate of $\tau_{-1} = 1.4 \times 10^8 \text{ s}^{-1}$ was measured for aqueous solutions of 15C5 by Rodriguez et al. (13). In both cases the process was assumed to be a conformational change $\text{C}' \xrightleftharpoons[k_{-0}]{k_0} \text{C}$. The longer relaxation process for 15C5 as compared to 18C6 is consistent with a lower flexibility of the smaller crown.

The relaxation of 18C6 has also been measured in several other solvents and the kinetic data are summarized in Table 2. With the exception of water, the rate constants at 25°C have been calculated assuming ΔH^\ddagger and ΔS^\ddagger are independent of the temperature. It may readily be seen that there is a large dependence of ΔH^\ddagger and ΔS^\ddagger on the solvent. However, at 25°C with the exception of ethanol, k_{-0} is always $\sim 10^7 \text{ s}^{-1}$ at 25°C, and with the exception of water, k_0 is always $\sim 2 \times 10^9 \text{ s}^{-1}$. In the two exceptional cases the rate constants differ from the others by less than one order of magnitude. It is interesting to note that Chen and Petrucci (15) report that in methanol solutions one molecule of the solvent is eliminated during the isomerization process. Presumably, the open form of the crown is "solvated" or "complexed" with the methanol and releases one molecule during the conformational change. The importance of such crown - solvent interactions has been demonstrated by P. Boss (18).

Based on the observation of crown conformational equilibria in the absence of metal ions, one might expect similar conformational equilibria in the case of the crown - metal ion complex, i.e., mechanism V shown in Table 1. This mechanism fits best the results of Grell et al. (19) for the complexation of M^+ by the naturally occurring antibiotic valinomycin in methanol solutions. The first step involves a rapid diffusion-controlled collision between the ion and the valinomycin molecule which is followed by

Table 2. Kinetic Parameters for Relaxation of 18C6 in Various Solvents.

	$k_{-0}^{(f)}$	$k_0^{(f)}$	$\Delta H_{-0}^{\ddagger(g)}$	$\Delta S_{-0}^{\ddagger(h)}$	$\Delta H_0^{\ddagger(g)}$	$\Delta S_0^{\ddagger(h)}$
H ₂ O ^(a) (25°C)	1.0×10^7	6.2×10^8	10.2	7.7	7.4	7.7
DMF ^(d) (-10°C)	3.6×10^6	5.5×10^8	3.8	-13.8	7.5	10.2
(25°C)	9.9×10^6	3.3×10^9				
MeOH ^(c) (-20°C)	$\sim 3.0 \times 10^6$	3.1×10^8	3.2	-16.0	5.8	3.54
(25°C)	9.0×10^6	2.1×10^9				
EtOH ^(e) (-15°C)	1.9×10^6	4.8×10^8	1.1	-25.3	4.8	0
(25°C)	2.9×10^6	1.9×10^9				
Dioxane ^(b) (-20°C)		$\sim 2.0 \times 10^8$				

^aReference 12.

^bReference 14.

^cReference 15.

^dReference 16.

^eReference 17.

^fs⁻¹.

^gkcal·mol⁻¹

^he.u.

a rate limiting conformational rearrangement of the valinomycin to form a compact complex.

The first observation of a conformational rearrangement upon complexation for a crown ether was made by Chen and Petrucci (15) for the sodium ion with 18C6 in methanol using ultrasonic absorption. They determined a forward rate constant for this process to be $k_2 = 2.8 \times 10^8 \text{ s}^{-1}$. This is a slower process than the conformational change of the crown ether in the absence of sodium ($k_0 = 2.1 \times 10^9 \text{ s}^{-1}$). This is not surprising since the complex should be less flexible than the crown ether alone.

In two interesting publications Petrucci and coworkers (16,17) have postulated a third conformational arrangement of the 18C6 complex in ethanol and in DMF. They found that in some instances mechanism VI is applicable instead of mechanism V. The authors define $M^+...C$ as a solvent separated pair, MC^+ as a contact pair in which there is some coordination by the crown and $(MC)^+$ as an included species in which the ion is fully encapsulated by the crown.

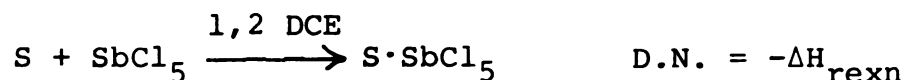
Two concentration independent relaxation processes were observed for the systems NaClO_4 -18C6 and KSCN-18C6 in DMF and LiClO_4 -18C6 in ethanol solutions instead of the single relaxations observed for NaClO_4 -18C6 and for KClO_4 -18C6 in ethanol and for LiClO_4 -18C6 in DMF. Thus, the authors concluded that the solvent strongly influences the complexation

kinetics. The first step of the complexation process was assumed to be a partial desolvation of the ion and ligand rearrangement. The second step is the encapsulation of the metal ion with the subsequent rearrangement of the crown.

The solvent influence was presumed to arise in the second step of complexation. At this point, cation desolvation should be complete in order for the 18C6 to encapsulate the ion. The observation of two relaxation processes for K^+ and for Na^+ with 18C6 in DMF but only one in ethanol is attributed to solvent differences. Chen and Petrucci concluded that the dielectric constants of the two solvents are not responsible for the observed solvent effect. They attributed the solvent influence to be due to differences in the solvating abilities of the solvent. The authors postulated that in the case of Na^+ and K^+ complexation in DMF the strong solvation of the ions sufficiently slows down the second step of complexation to make it observable for these ions. They speculate that the Li^+ ion is so strongly solvated that this step does not occur to an appreciable extent and thus, is not observed.

In ethanol, on the other hand, the metal ions are presumed to be less strongly solvated. Thus, the second step of complexation is too rapid to be observed for K^+ and for Na^+ complexation. With Li^+ the desolvation step is sufficiently fast to be observed. It should be mentioned that the Gutmann donor numbers (20) for ethanol and DMF

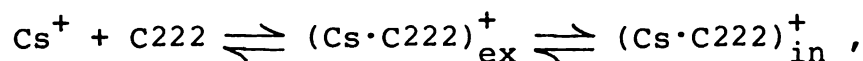
have been determined (20,21) to be 31.5 and 26.6, respectively. The Gutmann donor number is defined as the negative enthalpy upon complexation of the solvents with SbCl_5 in 1,2-dichloroethane, i.e.,



Therefore, according to this solvent donicity scale ethanol is a better solvator of the sodium ion than is DMF. This is in contrast to the conclusions just described.

The first direct conformational rearrangement of the 18C6 complex by nmr was reported by Dickert and Bumbrecht (22). They observed two conformers of the Co^{2+} complex by proton nmr at -1°C in CD_3NO_2 with small amounts of MeOH present. These two conformers were postulated to be the two species $\text{Co}(\text{18C6})^{2+}$ and $\text{mer}[\text{Co}(\text{18C6})(\text{MeOH})_3]^{2+}$.

Indirect nmr evidence of conformational rearrangement upon complexation has been observed by Mei et al. (23) in their ^{133}Cs studies with the cryptand C222·Cs complex in acetone (AC) and in propylene carbonate (PC) solutions. Their results of the exchange rate and chemical shift study suggested the existence of the following equilibria:



where ex and in refer to Cs^+ complexes where the Cs^+ ion only partially penetrates the cavity (exclusive), and where

the cation is completely inside the cavity (inclusive), respectively. Further studies showed (24) the formation of exclusive and inclusive complexes to be very dependent on the size of the cryptand and on the solvent. Exclusive complexes were found to form only when the equilibrium size of the cavity was slightly smaller than the Cs^+ ion. The precise nature of the solvent contribution to the formation of the exclusive complex is not completely clear. However, it was determined that strongly polar solvents tend to shift the equilibrium towards the inclusive complex. In solvents with low dielectric constants cation-anion interactions probably tend to prevent the cation from entering completely into the cavity.

Shchori et al. (10,25) investigated complexation kinetics of sodium ion with crown ethers DC18C6, DB18C6, and some derivatives of DB18C6 in DMF, MeOH, and in dimethoxyethane (DME) solutions by ^{23}Na nmr. In all systems studied the associative-dissociative mechanism was found to be predominant. Their results are listed in Table 3. The values for the decomplexation step ΔG_{-1}^\ddagger , ΔH_{-1}^\ddagger , and ΔS_{-1}^\ddagger have been calculated using their kinetic data and transition state theory. With the exception of DC18C6, regardless of solvent, all complexes studied were observed to have decomplexation Arrhenius activation energies of $\sim 12.5 \text{ kcal}\cdot\text{mol}^{-1}$. Thus, Shchori and coworkers surmised that the barrier to the decomplexation process is the

Table 3. Kinetic Parameters for Complexation of Na⁺ Ion with Crown Ethers at 25°C.

Crown	Sol.	K	E _a (e) -1	ΔH ₋₁ [‡] (e)	ΔS ₋₁ [‡] (f)	ΔG ₋₁ [‡] (e)	k ₋₁ (g)	E _a (e) -1	ΔH ₁ [‡] (e)	ΔS ₁ [‡] (f)	ΔG ₁ [‡] (e)	k ₁ (h)
DB18C6	DMF	600	12.6	12.0	4.7	10.6	1.0x10 ⁵	6.6	6.0	-2.7	6.8	6.0x10 ⁷
NDB18C6 ^(b)	DMF	115	12.5	11.9	5.7	10.2	2.0x10 ⁵	---	---	---	7.4	2.3x10 ⁷
AmDB18C6 ^(c)	DMF	615	13.1	12.5	7.7	10.2	1.9x10 ⁵	6.5	5.9	-1.7	6.4	1.2x10 ⁸
DB18C6	MeOH	23000	11.7	11.1	-2.3	11.8	1.4x10 ⁴	---	---	---	5.8	3.2x10 ⁸
DC18C6 ^(d)	MeOH	4800	8.3	7.7	-11.	11.0	5.2x10 ⁴	2.7	2.1	-13.	6.0	2.6x10 ⁸
DB18C6	DME	4500	13.3	12.7	3.0	11.8	1.5x10 ⁴	9.9	9.3	8.4	6.8	6.5x10 ⁷

^aResults calculated from data in References 10 and 25.

^bNDB18C6 = dinitrodibenzo-18C6.

^cAmDB18C6 = diaminodibenzo-18C6.

^dIsomer B.

^ekcal·mol⁻¹.

^fe.u.

^gs⁻¹.

^hM⁻¹ s⁻¹.

energy required for a conformational rearrangement of the complex. The lower activation energy for DC18C6 was thought to be due to greater flexibility of this crown ether as compared to DB18C6. It should be mentioned, however, that the observation of an activation energy independent of solvent may simply be accidental. Dimethoxyethane, DMF, and MeOH have very similar Gutmann donor numbers - 24, 26.6, and 25.7 respectively.

Shporer and Luz (26) used ^{39}K nmr to study complexation kinetics of the K^+ ion with DB18C6 in MeOH. The exchange mechanism was assumed to be the associative-dissociative process. An activation energy of $12.6 \text{ kcal}\cdot\text{mol}^{-1}$ and a dissociation rate constant of 610 s^{-1} were determined at -34°C . The Rb^+ exchange with DB18C6 was too fast to be measured by ^{87}Rb nmr.

Schmidt and Popov (27) determined the rate for the K^+ -18C6 exchange in acetone, 1,3-dioxalane, methanol, and an acetone/1,4-dioxane mixture by ^{39}K nmr. The results are listed in Table 4. Two interesting conclusions can be deduced from this study. First, the bimolecular exchange process, and not the associative-dissociative mechanism, was found to be predominant in 1,3-dioxalane and probably in the other solvent systems as well. This is the first time this mechanism has been shown to occur for crown ether complexes. The second interesting observation is the strong solvent dependence of the activation energy.

Table 4. Kinetic Parameters for K^+ Ion Complexation with 18C6 in Various Solvents at 25°C.^a

Solvent	E_a (b)	ΔH^\ddagger (b)	ΔS^\ddagger (c)	ΔG^\ddagger (b)	k_d (d)	Mech. (e)
AC	9.2(0.5)	8.6(0.5)	-4(2)	9.8(0.1)	4.1(0.9) $\times 10^5$	III
AC-1,4-dioxane	13.8(0.5)	13.2(0.5)	12(2)	9.6(0.1)	5.7(1.1) $\times 10^5$	III
MeOH	9.2(0.7)	8.6(0.7)	-3(3)	9.5(0.2)	6.8(2.7) $\times 10^5$	III
1,3-dioxalane	16.8(0.3)	16.2(0.3)	-8(3)	10.9(0.2)	6.8(2.7) $\times 10^4$ (f)	II
	15.5(0.7)	14.9(0.7)	11(2)	11.67(0.03)	1.74(0.09) $\times 10^4$	III

^aReference 27.

^bkcal·mol⁻¹

^ce.u.

^dM⁻¹s⁻¹

^eSee text for mechanism

^fs⁻¹.

The authors have suggested the large variation may be due to differences in solvation of K^+ in the transition state. The weaker solvents show larger activation energies because of the charge-charge repulsion which exists in the transition state is greater.

Mei et al. (28,29) studied Cs^+ ion complexation kinetics with 18C6 and DC18C6 in pyridine and in PC solutions by ^{133}Cs nmr. The results are listed in Table 5. The associative-dissociative mechanism was assumed to be operative. It is interesting to note that the rate data are essentially the same for the two 18C6 analogues despite the difference in solvents. The activation energy values are approximately the same as those found by Shchori et al. (25) for the Na^+ -DB18C6 exchange in methanol solutions. However, the activation energies are lower than those for the K^+ -18C6 complex.

Shamsipur (30) employed ^{133}Cs nmr to investigate Cs^+ complexation kinetics with the larger crown ethers DB21C7, DB24C8, and DB30C10 in methanol and in acetone. The results are listed in Table 6. The associative-dissociative mechanism was assumed to apply. In all cases, the activation energy for the decomplexation step was found to be larger in acetone than in methanol. The solvent dependence of the activation energy increases with decreasing cavity size of the ligand. The activation entropy, however, is more negative in methanol than in acetone with the result that in both solvents the free energy of activation, ΔG_{-1}^\ddagger ,

Table 5. Kinetic Parameters for Complexation Kinetics
of Cs^+ Ion at 25°C .^a

Sol.	Crown	$10^{-3}k_{-1}^{(b)}$	$E_a^{(c)}$	$\Delta H^\ddagger^{(c)}$	$\Delta S^\ddagger^{(d)}$	$\Delta G^\ddagger^{(c)}$
PC	DC18C6	11.	8.5	7.9	-14	11.94
PY	18C6	9.5	8.4	7.8	-14.2	12.03

^aReferences 28, 29.

^b s^{-1} .

^c $\text{kcal}\cdot\text{mol}^{-1}$

^de.u.

Table 6. Kinetic Parameters for Complexation of Cs^+ Ion with Several Crown Ethers in Methanol and in Acetone Solutions at 25°C.^a

Crown	Sol.	k_1 (b)	k_{-1} (c)	$E_{a,-1}^{(d)}$	ΔH_{-1}^\ddagger (d)	ΔS_{-1}^\ddagger (c)	ΔG_{-1}^\ddagger (d)	ΔH_1^\ddagger (d)	ΔS_1^\ddagger (e)	ΔG_1^\ddagger (d)
DB30C10	AC	3.0×10^8	2.1×10^4	6.1	5.5	-20.3	11.5	-8.00	-46.5	5.9
DB30C10	MeOH	7.5×10^8	3.5×10^4	5.2	4.6	-22.3	11.2	-8.00	-45.1	5.4
DB24C8	AC	6.7×10^8	10.3×10^4	8.2	7.6	-10.1	10.6	-3.8	-30.9	5.4
DB24C8	MeOH	4.4×10^8	8.7×10^4	6.3	5.7	-16.8	10.7	-4.1	-32.9	5.7
DB21C7	AC	7.1×10^8	5.9×10^4	9.3	8.7	- 7.5	10.9	-2.4	-26.1	5.4
DB21C7	MeOH	3.2×10^8	2.8×10^4	6.7	6.1	-17.7	11.4	-0.5	-21.2	5.8

^aResults calculated from or found in Reference 30.

^b $\text{M}^{-1} \text{s}^{-1}$.

^c s^{-1} .

^d $\text{kcal} \cdot \text{mol}^{-1}$

^ee.u.

is essentially the same for the three crown ether complexes. It is interesting to note that the activation energy for the complexation step is negative, i.e., the transition state is enthalpically more stable than the reactants. However, the large decrease in entropy results in a positive free energy of activation for the forward reaction.

In general, the cation exchange between free and complexed sites at room temperature is fast on the nmr time scale, and only one population-averaged nmr signal of the alkali metal nucleus is observed when the M^+ concentration is greater than that of a crown ether. However, Lin and Popov (31) have recently reported a slow exchange at room temperature for the system $NaBPh_4$ -18C6 in tetrahydrofuran and in 1,3-dioxalane solutions. But, when the counterion was ClO_4^- or I^- the exchange was fast. Although the kinetic parameters for these systems were not measured, there are two interesting observations which may be made from this study. First, this is the first known observation of slow exchange on the nmr timescale for an alkali metal ion with a crown ether at room temperature. Second, this is the first known occurrence of an anion influence on the exchange process.

In conclusion, while work is accelerating in the field of complexation kinetics of alkali metal ions with crown ethers a great deal of study is still required to

understand fully these processes in terms of solvent, cation, and anion influences to name a few.

CHAPTER 2

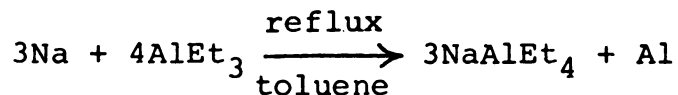
EXPERIMENTAL PART

A. Salt and Ligand Purification

Sodium tetraphenylborate (Aldrich, Gold Label) was dried under vacuum at room temperature for 48 hours. Reagent grade sodium thiocyanate (Mallinckrodt) was recrystallized from acetonitrile and dried under vacuum at 60°C for at least one day. Reagent grade sodium perchlorate and sodium iodide (Matheson Coleman & Bell) were dried at 110°C for several days. Cesium thiocyanate (Pfaltz and Bauer) was dried under vacuum at 60°C for at least two days.

Sodium tetraethylaluminate was originally donated by M. C. Day (32). Additional amounts of the salt were synthesized by the method of Hohn et al. (33). All glassware was cleaned and dried thoroughly. The reaction and all handling of materials were carried out under dry nitrogen atmosphere.

The reaction for the preparation of NaAlEt₄ is:



Forty ml of AlEt₃ were added by means of a dropping funnel to a refluxing solution containing 15 g of sodium metal in toluene. The solution was allowed to reflux for

two h after which time a hot filtration was carried out in a glove box yielding a clear solution. Upon cooling a white product precipitated which was the desired compound. The NaAlEt_4 was then recrystallized from toluene and stored under vacuum. All sample preparations involving this salt were done under a nitrogen atmosphere in a glove box. The melting point of the salt was 110-127°C (literature m.p. = 125°C (33)). It is likely that the solvent was not completely removed from the salt thus extending its melting point range. Day and coworkers (34) recommend rinsing the salt with hexane in order to help reduce trace amounts of toluene. This was not done since the product was only to be used for qualitative tests.

Tetrahydrofuran (Mallinckrodt) was refluxed over a mixture of potassium metal and benzophenone for at least 24 h. Methanol (Fisher) was refluxed over sodium methoxide for one day. Propylene carbonate (Aldrich) was refluxed over barium oxide under reduced pressure for at least one day. Acetone (Fisher) was refluxed over calcium sulfate for two days. In all distillations, only the middle 60 percent of the solvent fractions were kept. The solvents were stored over activated molecular sieves in a dry box under nitrogen atmosphere. Water content of the solvents was always less than 100 ppm as determined by gas chromatography.

The macrocyclic polyether 18-crown-6 (Aldrich) was

recrystallized from acetonitrile (35) and dried under vacuum for two days at room temperature. The purified ligand melted at 37-38°C (lit. m.p. 36.5-38.0°C (36), 38-40°C (37)). The crown ethers dibenzo-21-crown-7 and dibenzo-24-crown-8 (Parish) were recrystallized from n-heptane and dried under vacuum at room temperature for at least two days. The melting points were 107.0°C and 113.0°C (38), respectively, which are the same as the reported values.

B. Instrumental Measurements and Data Handling

1. Instruments. Sodium-23 nmr measurements were obtained on a Bruker WH-180 spectrometer operating at a field of 42.3 kG and a frequency of 47.61 MHz and on a modified (39) DA-60 spectrometer operating at a field of 14.09 kG and a frequency of 15.87 MHz. Both instruments were operated in the pulsed Fourier transform mode. A Nicolet 1180 computer was used to carry out data manipulation on the WH-180 while a Nicolet 1080 computer was used on the DA-60.

Cesium-133 nmr measurements were obtained on a Bruker WH-180 spectrometer operating at a field of 42.3 kG and a frequency of 23.62 MHz.

2. References and Corrections. The reported chemical shifts are referenced to infinitely dilute aqueous sodium chloride (sodium-23 nmr measurements) or to infinitely dilute aqueous cesium chloride (cesium-133 measurements).

Downfield chemical shifts are taken to be positive. The chemical shifts are corrected for differences in bulk diamagnetic susceptibility between samples and reference solvent according to the equations of Martin et al. (40). For a Fourier transform experiment utilizing an electromagnetic (DA-60):

$$\delta_{\text{corr}} = \delta_{\text{obs}} - \frac{2\pi}{3} (X_{\text{ref}} - X_{\text{samp}})$$

where X_{ref} and X_{samp} are the unitless volumetric susceptibilities of the reference and solvents, respectively, and δ_{corr} and δ_{obs} are the corrected and observed chemical shifts, respectively.

For a Fourier transform experiment utilizing a superconducting magnet (WH-180):

$$\delta_{\text{corr}} = \delta_{\text{obs}} + \frac{4\pi}{3} (X_{\text{ref}} - X_{\text{samp}})$$

where the symbols have the same meanings as above. It was shown by Templeman and Van Geet (41) that at low salt concentrations the contribution of the salt to the volumetric susceptibility of the solutions can be neglected. When mixed solvents were used the volumetric susceptibility of the solutions were calculated as follows (42):

$$X_{\text{AB}}^{\text{calc}} = \frac{V_{\text{A}}}{V_{\text{A}} + V_{\text{B}}} \cdot X_{\text{A}} + \frac{V_{\text{B}}}{V_{\text{A}} + V_{\text{B}}} \cdot X_{\text{B}}$$

where χ_{AB}^{calc} = volumetric susceptibility of the solution, V_A = volume of solvent A, V_B = volume of solvent B, χ_A = volume diamagnetic susceptibilities of pure solvent A, and χ_B = volume susceptibility of pure solvent B.

Two methods were employed for variable temperature experiments, depending on the instrument used, to reference all chemical shifts to 25°C. When the WH-180 was used the sample was placed in a 10 mm O.D. tube with a 5 mm tube containing lock solvent mounted coaxially inside. The sample was placed in the magnet and the lock maintained throughout the variable temperature experiment. At each temperature, only the fine Z shim control was adjusted to maintain lock and field homogeneity. Because the field was locked throughout the experiment chemical shifts at each temperature could be referenced to the one at 25°C. Finally, the chemical shifts could all be referenced to infinite dilution at 25°C by taking the spectrum of the sample with the appropriate reference at 25°C.

Chemical shift measurements as a function of temperature were much easier to do on the DA-60 spectrometer. This instrument has an external lock system which allows replacement of the sample with the reference solution while maintaining lock. The reference solution was placed in a 5 mm O.D. tube which was then vacuum sealed in a 10 mm O.D. tube as reported by Mei et al. (29). They showed this arrangement to be quite convenient for keeping the

reference solution at room temperature while inside the magnet for short periods of time. Thus, all chemical shift measurements determined in this manner are referenced to that at 25°C.

3. Temperature Calibration and Control. Temperature was controlled on the WH-180 with a Bruker B-ST 100/700 temperature control unit and measured to $\pm 1^\circ\text{C}$ with a calibrated Doric digital thermocouple placed about 1 cm below the sample. A N_2 flow rate of 50 SCFM was used and the temperature calibrated by means of the chemical shift difference between the methyl and hydroxyl protons of methanol (43). The data are listed in Table 7 and the resulting calibration curve was used to determine the sample temperature.

On the Varian DA-60 spectrometer, temperature was controlled with a Varian V-4540 temperature control. Sample temperature was measured with a calibrated Doric digital thermocouple placed about 1 cm below the sample. A N_2 flow rate of 40 SCFM was used. The Doric unit was calibrated by placing a calibrated thermometer in a 10 mm sample tube containing methanol and taking thermocouple and thermometer readings at various temperatures. The data are given in Table 8. Due to the close agreement between thermocouple and thermometer values, it was unnecessary to use a calibration curve.

Table 7. Temperature Calibration of the WH-180 Spectrometer.^a

Temperature Read (°C)	Actual Temperature (°C)
54.9	55.0(±1)
44.3	44.8
34.6	35.8
24.0	24.4
13.5	14.4
3.9	3.6
-5.7	-5.2
-15.2	-16.2
-25.0	-27.2
-35.6	-38.4
-45.7	-48.4

^a20 mm high frequency probe.

Table 8. Temperature Calibration of the DA-60 Spectrometer.

Temperature Read (°C)	Actual Temperature (°C)
47.3	47.0
36.9	36.6
23.3	23.4
12.6	13.0
2.5	3.0
-13.4	-13.5
-18.1	-18.0
-23.8	-23.5

4. Linewidth Measurements. Linewidth measurements on the WH-180 were done by either measuring the width at half height or by fitting the spectra to a Lorentzian function. On the DA-60 spectrometer, linewidths were measured by plotting the spectra and measuring the width at half height.

In order to correct the linewidths for daily differences in field homogeneity, two techniques were used, depending on the nmr spectrometer. On the WH-180 field homogeneity was checked by comparing the linewidth of a sample with that obtained on a previous day. In general, the linewidth was the same within experimental error. Total error in linewidth measurements (and thus, $1/T_2$'s since $1/(\pi T_2) = \Delta\nu_{1/2}$) is estimated to be 10% of the measured value.

Because the DA-60 spectrometer has an external lock it is possible to replace the sample with a reference solution as described in Section 2. Besides its use as a chemical shift reference, an aqueous 3 M NaCl solution was used as a linewidth reference. The observed linewidth of a nucleus can be viewed as the sum of the natural linewidth and the contribution from field inhomogeneity. Thus,

$$\left(\frac{1}{T_2}\right)_{\text{observed}} = \left(\frac{1}{T_2}\right)_{\text{natural}} + \left(\frac{1}{T_2}\right)_{\text{inhomogeneity}}$$

In order to determine the natural ^{23}Na linewidth for the aqueous 3 M NaCl reference the following procedure was performed. First, the ^7Li linewidth of an aqueous 4 M LiClO_4

solution was measured and found to be 1.56 Hz. The natural linewidth should be almost 0.0 Hz (44). Thus, the inhomogeneity contribution to the linewidth is 1.56 Hz. Next, the sodium-23 nmr of the 3 M NaCl solution was taken. Care was taken to ensure the geometry was the same as with the LiClO₄ solution. The field was kept locked between samples and there was no need to remove the probe. A ²³Na linewidth of 7.68 Hz was measured. Thus, for 3 M NaCl

$$\left(\frac{1}{T_2}\right)_{\text{natural}} = (7.68 - 1.56)\pi = 19.2 \text{ s}^{-1}$$

$$\text{or } \Delta\nu_{\frac{1}{2}} = 6.12 \text{ Hz.}$$

Eisenstadt and Friedman (45) found a concentration dependence of the ²³Na relaxation for aqueous NaCl solutions. The relationship has the form:

$$\frac{1}{T_2} = 17.55 + (0.55) C_{\text{NaCl}}$$

where C_{NaCl} = molarity NaCl. Though their maximum concentration was only 1 M NaCl, if an extrapolation is made to 3 M NaCl a first approximation of the relaxation rate may be obtained. A value of $1/T_2 = 19.2 \text{ s}^{-1}$ (or $\Delta\nu_{\frac{1}{2}} = 6.11 \text{ Hz}$) is calculated, which is the same as that measured above.

Thus, all ²³Na linewidths were referred to aqueous 3 M NaCl which was also used as a chemical shift reference.

Typically, corrections in linewidths were on the order of 1-3 Hz. Total error in these measurements is estimated to be 10% of the measured value.

Differences in sample susceptibilities (due to different solvents) will affect field homogeneities to different extents. Thus, the corrections made for field inhomogeneity may not yield true ($1/T_2$) values for a particular sample. However, the referencing procedure described above allows one to refer the linewidths to a common value and, thus, maintain consistency on a day to day basis.

5. Data Acquisition and Signal Processing. Several instrumental techniques were used to increase the signal to noise ratio and digital resolution. To increase signal/noise, two techniques were used: signal averaging and exponential line broadening of the free induction decay (FID). Typically, 100-10,000 scans were collected, depending on sample concentration and linewidth, and linebroadening of 10-40 Hz was applied to the FID.

To increase digital resolution the zero filling technique (46) was employed. In general, one collects an N-point FID and then adds 2-4 N zeroes to the end of the FID before Fourier transformation. This allows an increase in the point to point resolution without distorting the lineshape.

6. Data Transfer. For kinetic measurements it was desired to obtain theoretical fits of nmr lineshapes to extract the kinetic information present. The method of data transfer varied depending on the nmr instrument used, but ultimately was processed on a CDC-6500 mainframe computer.

6.a. WH-180. Data transfer from the WH-180 to the CDC-6500 occurred in 3 distinct stages. First, the transformed FID was stored on the hard disk used by the Nicolet 1180 computer. The data were transferred to a Digital Equipments Corporation (DEC) PDP-11 computer system via two programs. A program, MOVE, based on a program written by Walmsley and Atkinson (47), was written by K. Johnson and stored along with the computer language, BASIC, on the disk containing data to be transferred. The purpose of MOVE is to send the data out Serial Port B of the Nicolet 1180 computer. With the software update on the WH-180 in 1984 a new program, NTCDTL, was used to send data out this port of the computer. NTCDTL was provided by Nicolet with the new software package. A copy of MOVE as well as examples of the use of this program and of NTCDTL can be found in Appendix I.

A program CDC (48), operating on the DEC system, takes the data being transferred and stores the data on a floppy disk.

The second stage of data transfer involves taking the

data on the floppies and reformatting them to KINFIT (49) acceptable format. KINFIT is a nonlinear least squares fitting routine used for data analysis. The program NIC180 was used to reformat the data transferred by MOVE. NIC84 was used to reformat data transferred by NTCDTL. Both NIC180 and NICDTL were written by T. V. Atkinson (49).

The third stage consists of transcribing the new data files onto a magnetic tape and then transferring the data from the tape to the CDC-6500 computer. The files may then be called by KINFIT.

6.b. DA-60. Data to be computer fit was plotted to obtain a hard copy. The plots were digitized using a Science Accessories Corporation GP-3 digitizer available at the Physiology department. The digitized data were then punched onto computer cards in KINFIT acceptable format and run on the CDC-6500 computer.

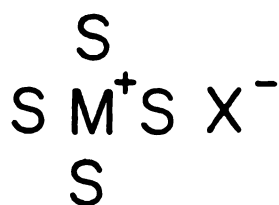
CHAPTER 3
MISCELLANEOUS

A. ION-PAIRING IN TETRAHYDROFURAN SOLUTIONS

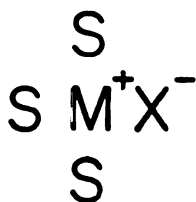
INTRODUCTION

It is reasonable to assume that the observation of an anion influence on the complexation kinetics of sodium ion with 18C6 in tetrahydrofuran, as discussed in Chapter 4, is due to differences in ionic association of the sodium salts and of their complexes; especially since THF has a low dielectric constant ($D = 7.6$). The salt which exhibits slow exchange at room temperature (NaBPh_4) has a large, "soft", bulky anion while the fast exchange salts (NaSCN , NaClO_4 , and NaI) have small, "hard" counterions.

Previous workers (50-55), using conductance measurements, have concluded that in tetrahydrofuran solutions, NaBPh_4 exists primarily in the form of solvent separated ion-pairs (Figure 2). Recently, Chabanel *et al.* (56), using infrared spectroscopy, have concluded that NaSCN exists in the form of contact ion-pairs as well as higher ionic aggregates in THF (Figure 2). Greenberg and coworkers (50), using sodium-23 nmr, observed a concentration independent chemical shift in THF when BPh_4^- was the counterion. However, SCN^- , I^- , and ClO_4^- all influenced the sodium-23 chemical shift. Thus, contact ion-pairing is significant for the fast exchange anions but not for BPh_4^- ion. However, no known studies have been published concerning the ion-pairing of complexed sodium salts in THF.



Solvent-separated



Contact

Figure 2. Types of ion pairs in solution. Note: most experimental techniques can discern only those solvent-separated ion pairs which are separated by a single solvent molecule.

RESULTS AND DISCUSSION

1. Conductance Measurements

The equivalent conductances of 0.1 M sodium salt solutions and of their complexes with 18C6 (when soluble at this concentration) were determined and are listed in Table 9. Also listed is the conductance of 0.1 M NaAlEt₄ in THF reported by Day and coworkers (57). The results for the uncomplexed sodium salt solutions will be considered first.

The conductances of the NaBPh₄ and the NaAlEt₄ solutions are two orders of magnitude greater than those of the "fast" exchange salts. As mentioned above, NaBPh₄ is believed to be predominantly in the form of solvent separated ion-pairs whereas NaSCN, NaI, and NaClO₄ are presumed to form contact ion-pairs and higher ionic aggregates in THF. The conductance data seem to agree with these conclusions since highly associated salts would be poor conductors. Day and coworkers (58) have concluded that NaAlEt₄ exists primarily in the form of solvent separated ion-pairs in THF. The conductance data also suggests that this salt more closely resembles NaBPh₄ (i.e., solvent separated ion-pairs), than the other salts in tetrahydrofuran.

The conductance of the complexed NaBPh₄ salt solution has a slightly lower conductance than the pure salt solution. If strong contact ion-pairing is minimal, this would be the expected behavior since the mobility of the sodium

Table 9. Equivalent Conductances of Various Tetrahydrofuran Solutions at 25°C.

Solution	Λ (mho·cm ² ·equiv. ⁻¹)				
	398 Hz	629 Hz	971 Hz	1942 Hz	3876 Hz
0.09999 <u>M</u> NaBPh ₄	20.98	20.86	20.75	20.64	20.44
0.1 <u>M</u> NaAlEt ₄	-----	-----	-----	-----	24.00 ^(a)
0.1004 <u>M</u> NaSCN	0.1365	0.1430	0.1420	0.1414	0.1381
0.09979 <u>M</u> NaClO ₄	0.4263	0.4465	0.4436	-----	-----
0.1001 <u>M</u> NaI	0.2203	0.2187	0.2169	0.2151	-----
0.1001 <u>M</u> NaBPh ₄ +					
0.1108 <u>M</u> 18C6	15.04	15.00	14.92	14.83	14.68
0.09990 <u>M</u> NaSCN +					
0.1123 <u>M</u> 18C6	1.942	2.035	2.022	2.017	1.968

^aReference 58; @3000 Hz.

ion would be reduced when complexed. Thus, the NaBPh_4 -18C6 complex exists primarily in the form of a crown separated ion-pair.

When NaSCN is complexed by 18C6 the conductance actually increases as compared to the solution of pure NaSCN. It is likely that this is due to the breakup of higher ionic aggregates which are found in the uncomplexed NaSCN solution. The conductance of the complexed NaSCN solution is still one order of magnitude lower than that of the complexed NaBPh_4 solution. Mobility considerations would argue in favor of the complexed NaBPh_4 having the lower conductivity if ion-pairing is negligible since BPh_4^- is the larger counterion. Thus, the complexed NaSCN must be contact ion-paired to some extent.

2. Infrared Studies

The room temperature infrared spectra of the C-N stretching region of the SCN^- ion for a 0.1 M NaSCN solution and of its complex with 18C6 in THF are shown in Figure 3. The spectrum of the uncomplexed salt agrees well with that reported by Chabanel et al. (56). Their band assignments are those listed. It is important to note the absence of a band at 2052 cm^{-1} which would correspond to "free" SCN^- ion (56,59,60).

Upon complexation with 18C6 a single band at 2058 cm^{-1} remains. This band was observed in the pure salt solution

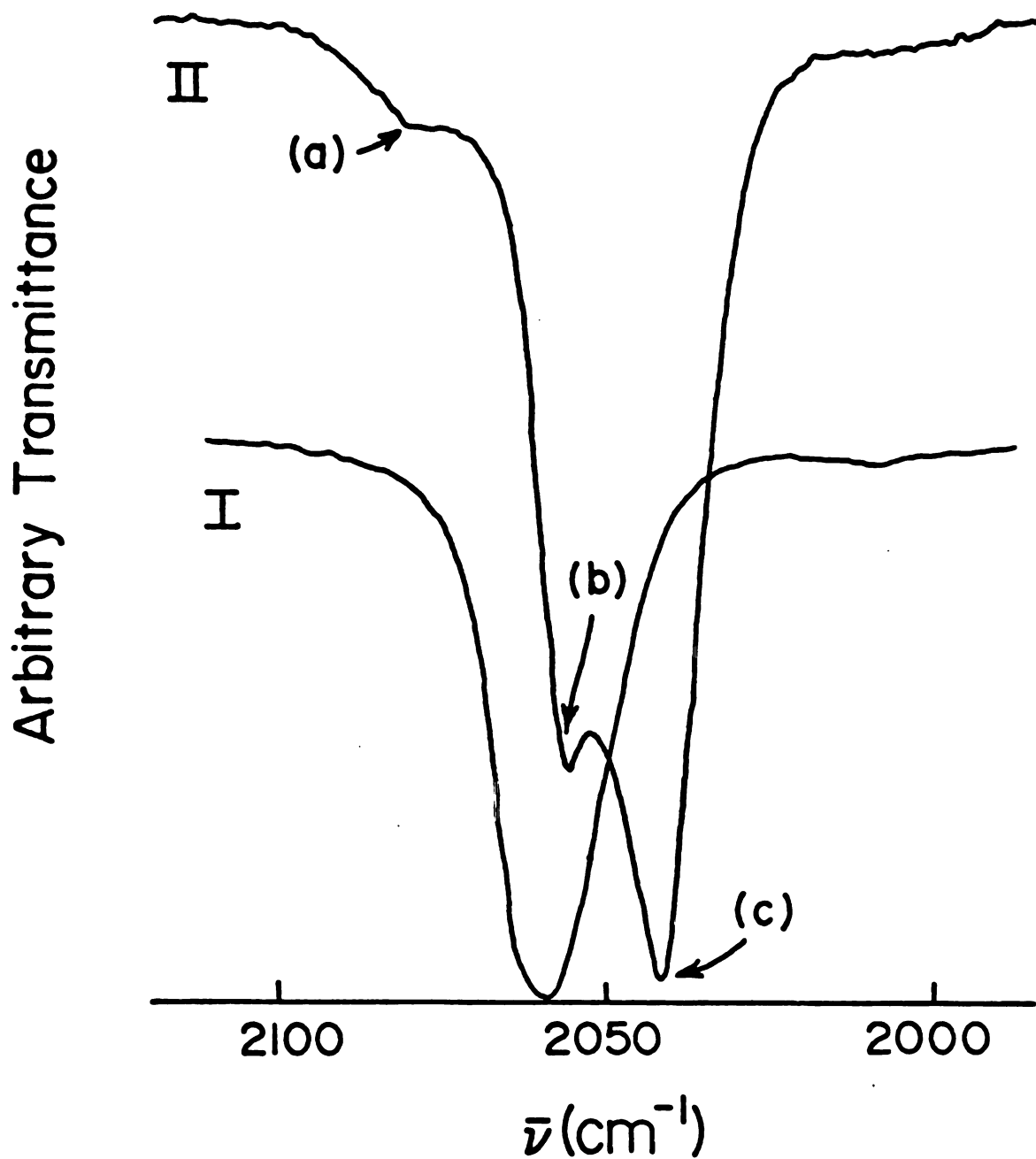


Figure 3. Room temperature infrared spectra of tetrahydrofuran solutions containing NaSCN. I) 0.126 M NaSCN + 0.140 M 18C6: Spectrum of $\text{Na}^+ \cdot 18\text{C}6 \cdot \text{NCS}^-$. II) 0.074 M NaSCN, (a) $\text{Na}^+ \cdot \text{NCS}^- \cdot \text{Na}^+$; (b) $\text{Na}^+ \cdot \text{NCS}^-$; (c) $(\text{Na}^+ \cdot \text{NCS}^-)_2$. Assignments from Reference 56.

and corresponds to the contact ion-paired SCN^- ion. Thus, the complexed NaSCN is contact ion-paired. No free SCN^- band is observed for this solution. As expected from the conductance results, the complexation of the sodium ion has eliminated the higher ionic aggregates found in the pure salt solution. Thus, the conductance and infrared results complement each other.

3. NaAlEt_4 -18C6 Exchange in THF

The observation of similar ionic states for NaBPh_4 and NaAlEt_4 in THF solutions suggests that the system NaAlEt_4 -18C6 may also exhibit slow exchange at room temperature on the sodium-23 nmr timescale in tetrahydrofuran. Approximately a 2:1 mole ratio of NaAlEt_4 to 18C6 solution was prepared. The room temperature sodium-23 nmr spectrum is shown in Figure 4. As can be seen, this salt also exhibits slow exchange with 18C6 in THF. Thus, BPh_4^- is not unusual in being the only anion to exhibit slow exchange at room temperature. Furthermore, the belief is strengthened that differences in ionic association are responsible for the anion influence on the sodium ion-18C6 exchange rate.

CONCLUSIONS

In summary, the slow exchange salts and their complexes with 18C6 form predominantly solvent separated (or crown

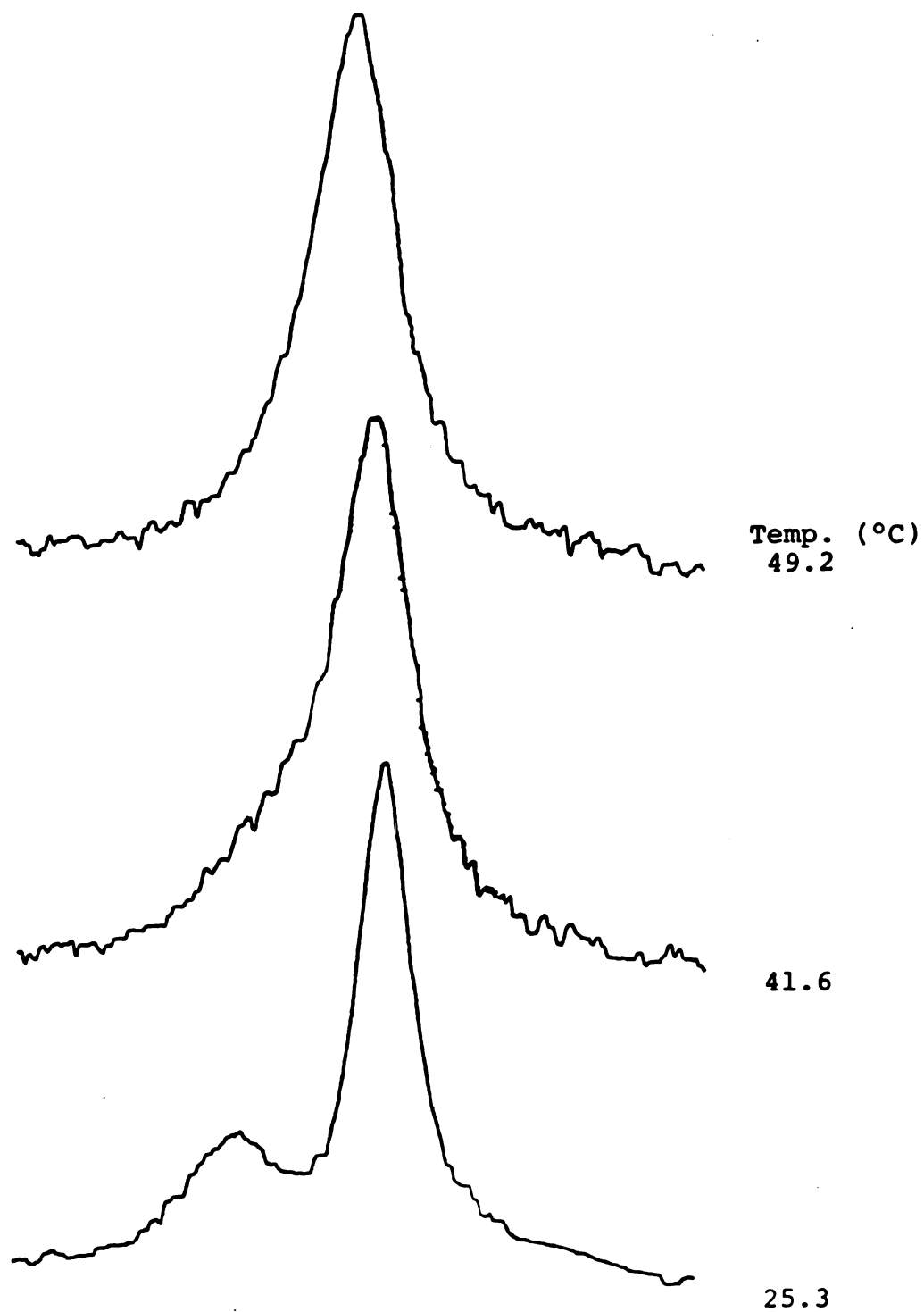


Figure 4. Sodium-23 nmr of a solution containing $[\text{NaAlEt}_4]/[\text{18C6}] \approx 1.9$ in THF at several temperatures.

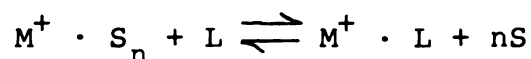
separated) ion-pairs in tetrahydrofuran solutions. The fast exchange salts and their complexes with 18C6 form predominantly contact ion-pairs or higher ionic aggregates.

3B. ISOSOLVATION STUDIES

INTRODUCTION

The role of the solvent has long been recognized to be important in influencing solution equilibria, ionic interactions, reaction kinetics, etc. For example, the stability constant of a complex can change by several orders of magnitude simply by replacing one solvent medium by another.

In a "simple" reaction of a solvated metal ion forming a complex with a ligand the solvent may be viewed as a competing ligand. Thus, the reaction should be written:



where M^+ is the metal ion, L is the ligand, and there are n solvent molecules, S , solvating the metal ion. It is reasonable to assume that the strength of the solvent-ion interactions are important in determining the above equilibrium (solvent interaction with the ligand can also be important).

The need to compare solvating abilities of a given series of solvents has produced several solvent rating systems including the Gutmann donor number scale (20). This "donicity" scale has been found to correlate quite remarkably with the infinite dilution sodium-23 nmr chemical shifts in the solvents (61).

The concept of preferential solvation of ions in solvent mixtures is an additional technique which has been used to compare relative solvating abilities of solvents. Several reviews (62,63) on the topic currently exist and therefore, only the general concept and assumptions will be presented here.

Frankel et al. (64) studied $\text{Co}(\text{acac})_3$ solvation in chloroform- CCl_4 mixtures by following the cobalt-59 chemical shift as the solvent composition was varied. They proposed that a nonlinear relationship between this parameter vs. solvent composition is an indication of preferential solvation. The "isosolvation point" was defined as the composition at which the chemical shift of the solute lies midway between the values in the pure solvents. It was postulated that at this composition the contributions from the two solvents to the solvation sphere of the ion are equivalent. If the two solvents have unequal solvating abilities then the solvent with the lower composition at the isosolvation point is the stronger solvator.

Popov et al. (42,65) have studied the Na^+ ion preferential solvation in a variety of solvent mixtures by ^{23}Na nmr. In general, the solvent which showed preferential solvation for sodium ion in a mixture had the higher Gutmann donor number. Among the more interesting results, however, it was concluded that the Na^+ ion is preferentially solvated by dimethylsulfoxide (DMSO) in mixtures of DMSO and

pyridine. This was unexpected since pyridine has a higher Gutmann donor number than DMSO. The phenomenon was explained as due to the destruction of the associated structure of DMSO by the addition of pyridine which thus enhanced its solvating ability (66). The authors, therefore, cautioned that the properties of solvents in a solvent mixture may be quite unexpected considering those of the neat solvents.

In summary, the study of mixed solvent systems can be very useful in the comparison of relative solvating abilities of a given pair of solvents. In addition, such studies may uncover those solvent mixtures which exhibit unexpected properties as compared to the pure solvents. We have used sodium-23 nmr to study the preferential solvation of sodium ion for the salts NaBPh_4 and NaClO_4 in the systems methanol-tetrahydrofuran and propylene carbonate-tetrahydrofuran.

RESULTS AND DISCUSSION

The sodium-23 nmr chemical shifts as a function of solvent composition have been determined for 0.1 M salt solutions of NaBPh_4 and of NaClO_4 in PC-THF and in MeOH-THF mixtures. The results are tabulated in Tables 10 and 11. The data are shown graphically in Figures 5 and 6.

The "isosolvation point", defined on page 7, has been determined for all systems with the exception of NaBPh_4 in MeOH-THF mixtures (NaBPh_4 is not sufficiently soluble

Table 10. Sodium-23 Chemical Shift vs. Composition of THF/PC Binary Mixtures at 25°C.

χ_{THF}	$\delta_{\text{Na}^+}^{(a)}$	
	$\text{NaBPh}_4^{(b,c)}$	$\text{NaClO}_4^{(b,d)}$
1.000	-7.61 (± 0.10)	-8.39 (± 0.10)
0.793	-8.04	-8.26
0.663	-8.13	-8.33
0.525	-8.24	-8.35
0.380	-8.38	-8.52
0.292	-8.54	-8.68
0.195	-8.80	-8.86
0.104	-9.07	-9.09
0.000	-9.66	-9.58

^aAll sodium-23 chemical shifts in this and following tables are referenced to infinitely dilute aqueous Na^+ .

^b0.1 M in salt.

^cIsosolvation point $\cong 0.23 \chi_{\text{THF}}$.

^dIsosolvation point $\cong 0.15 \chi_{\text{THF}}$.

Table 11. Sodium-23 Chemical Shifts vs. Composition of THF/MeOH Binary Mixtures at 25°C.

χ_{THF}	δ_{Na^+}	
	$\text{NaBPh}_4^{(a)}$	$\text{NaClO}_4^{(a,c)}$
1.000	-7.61 (± 0.05)	-8.39 (± 0.05)
0.897	-6.58	-7.50
0.808	-5.99	-6.99
0.702	-5.57	-6.46
0.597	-5.19	-5.97
0.489	-4.85	-5.55
0.394	-4.59	-5.18
0.320	-4.47	-4.93
0.198	-3.46	-4.52
0.0997	(b)	-4.19
0.000	(b)	-3.87

^a0.1 M in salt.

^bInsoluble.

^cIsosolvation point $\cong 0.63 \chi_{\text{THF}}$.

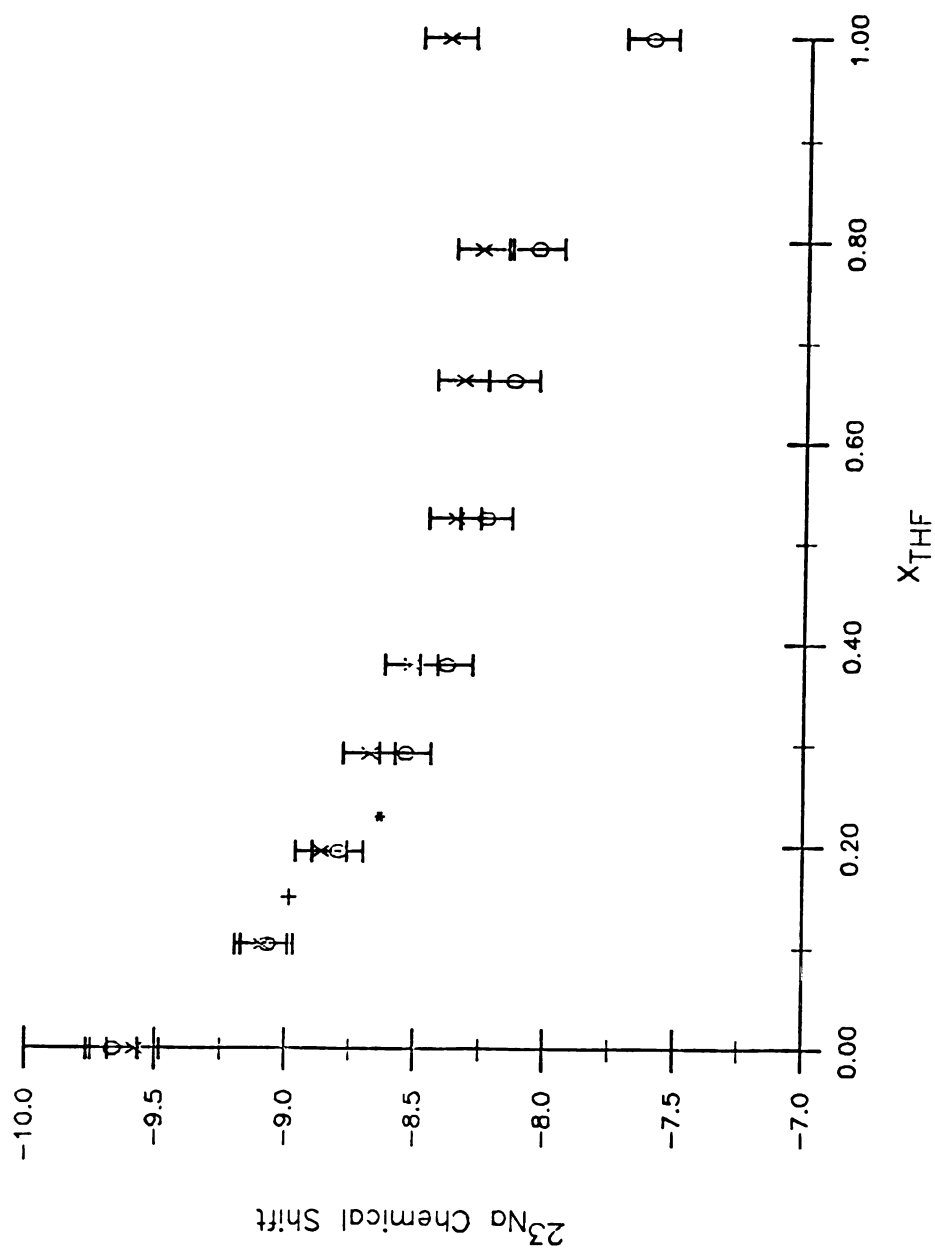


Figure 5. Sodium-23 chemical shift vs. composition of THF/PC mixtures. (o) 0.1 M NaBPh_4 ; (x) 0.1 M NaClO_4 ; (*) (+) isosolvation points.

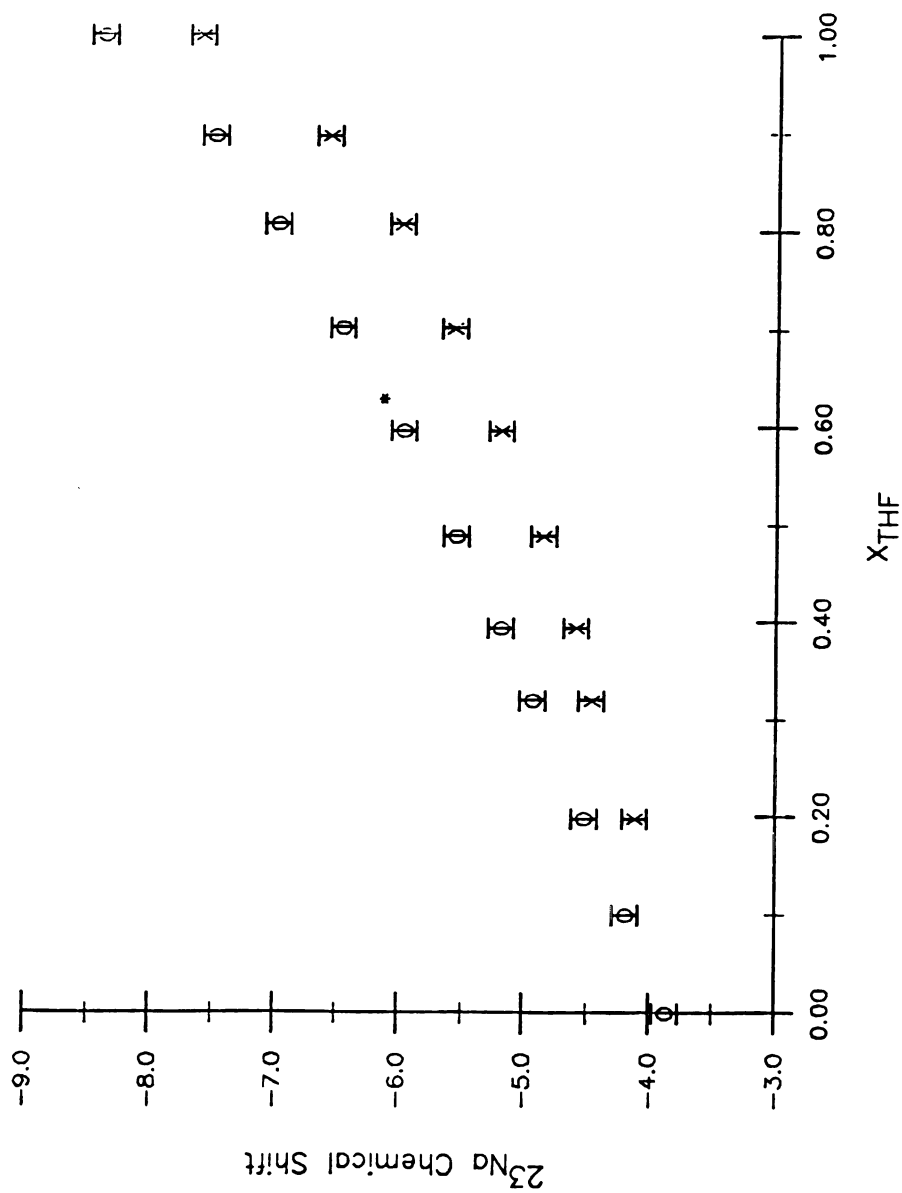


Figure 6. Sodium-23 chemical shift vs. composition of THF/MeOH mixtures. (o) 0.1 M NaClO_4 ; (x) 0.1 M NaBPh_4 ; (*) isosolvation point.

in methanol). The isosolvation point values are listed in Tables 10 and 11.

Differences in the isosolvation points of NaClO_4 and NaBPh_4 in PC-THF mixtures are due to the interactions of the anion with sodium ion, i.e., ionic association. Isosolvation theory assumes no interaction between ions, only solvent-ion interactions. It was shown earlier in this chapter that NaClO_4 strongly forms ion-pairs in THF while NaBPh_4 does not. This difference in ionic interactions is reflected by the difference in ^{23}Na chemical shifts of the two salts in pure tetrahydrofuran. In neat propylene carbonate the chemical shift of the sodium ion is independent of the anion. Previous workers have reported (67) that NaBPh_4 does not form contact ion-pairs in propylene carbonate. It should be noted, however, that the isosolvation curve for NaBPh_4 does not display the usual behavior. In fact, the NaBPh_4 data exhibit an S-shaped curve with varying solvent composition. Thus, there may be ionic influences in the solvent mixtures containing this salt. Nonetheless, the isosolvation composition (low THF mole fraction) is in agreement with the higher Gutmann donor number of THF.

In MeOH-THF mixtures, the data are more difficult to interpret. While NaClO_4 is strongly associated in THF, the chemical shift of this salt parallels that of NaBPh_4 as the composition is varied. This parallelism has been reported

by Popov and coworkers (61) in neat solvents. The only conclusions one may derive for this system is that of an approximate isosolvation point using the NaClO_4 data while recognizing that the anion has an influence. The value thus obtained is again in agreement with the higher donicity of MeOH.

In conclusion, the isosolvation points have been determined by sodium-23 nmr for PC-THF and for MeOH-THF mixtures. In all systems, the solvent with the higher Gutmann donor number had the lower composition at the isosolvation point.

CHAPTER 4

KINETICS OF COMPLEXATION OF SODIUM ION WITH 18-Crown-6 IN NONAQUEOUS SOLVENTS

A. Introduction

The observation by Lin and Popov (31) of an anion and solvent influence on the kinetics of complexation of sodium ion with 18C6 in tetrahydrofuran has remained unexplained. The authors observed slow exchange on the sodium-23 nmr timescale at room temperature for the system $\text{NaBPh}_4 \cdot 18\text{C}6$ in THF when the sodium ion concentration was greater than that of the crown ether. However, fast exchange was observed when ClO_4^- or I^- were the counterions. This is the first known observation of a slow exchange at room temperature for an alkali metal ion-crown ether system. In addition, this is the first known observation of an anion influence on the kinetics of complexation of sodium ion with a crown ether. The kinetic parameters for these systems were not determined in the above investigation.

It is the purpose of the work presented in this chapter to investigate both the anion and solvent influences on the kinetics of complexation of sodium ion with 18C6.

B. Choice of Solvents and Salts


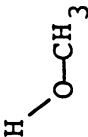
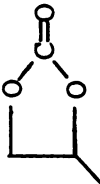
Shchori and coworkers (25) found an Arrhenius activation energy of $\sim 12.5 \text{ kcal} \cdot \text{mol}^{-1}$ for the decomplexation step of $\text{Na}^+ \cdot \text{DB18C}6$ in MeOH, DMF, and DME solutions. They

therefore concluded that the major barrier to decomplexation is the rearrangement of the complex prior to release of the ion. However, the three solvents in which their studies were done have approximately the same donor abilities ($DN_{DMF}=26.6$, $DN_{MeOH}=25.7$, $DN_{DME}=24$). Therefore, it was important to examine the complexation kinetics in several solvents of varying donor abilities to test their hypothesis.

Tetrahydrofuran was chosen to investigate the anion influence on the complexation kinetics in this solvent since the low dielectric constant of this solvent obviously favors ion-ion interactions. In addition, THF has a donor number of 20.0 which is lower than those of the solvents studied by Shchori et al. (25). Methanol was selected to compare the complexation kinetics of $Na^+ \cdot 18C6$ with those of the crown ethers DC18C6 and DB18C6 studied by Shchori and co-workers (25) in this solvent. Propylene carbonate was chosen because this solvent has a donor number still lower than that of THF ($DN = 15.0$) but, on the other hand, has a high dielectric constant. We also studied the kinetics in MeOH-THF and PC-THF solvent mixtures to compare the results with those found in the neat solvents. Table 12 lists key solvent properties for the neat solvents studied.

Sodium tetrphenylborate was the primary sodium salt used. As discussed above, this salt is interesting in that it exhibits slow exchange with 18C6 in THF at room temperature. It was also our intent to minimize whenever possible,

Table 12. Selected Properties of Some Solvents at 25°C.

Solvent	Structure	Dielectric Constant	Gutmann Donor Number	Viscosity (cp)	m.p. (°C)
THF		7.6	20.0	0.452	-109.
MeOH		32.7	25.7	0.597	- 94.
PC		65.0	15.0	2.53	- 55.

ionic association effects on the exchange process in all solvents studied. In THF and in PC this salt is known not to form contact ion pairs to any appreciable extent (50-55,67). Therefore, it was used in all solvent systems with the exception of MeOH in which it is not sufficiently soluble.

The choice of a sodium salt which exhibits fast exchange with 18C6 at room temperature in THF was influenced by several factors. It is necessary that both the solvated and complexed sodium salts be sufficiently soluble to do the experiment. Unfortunately, complexed NaClO_4 is not appreciably soluble ($<0.05 \text{ M}$ (68)). It should be noted, however, that the solubility of the complex increases if the salt concentration is greater than that of the crown (68). The complexes with NaI and NaSCN are soluble at reasonable concentrations ($>0.05 \text{ M}$). The NaSCN was selected over the NaI since in the former case it is possible to investigate ionic associations by infrared spectroscopy (see Chapter 3). In addition, this salt and its complex with 18C6 are soluble in MeOH. Since this was the salt used by Shchori et al. (25) in their kinetic investigations, differences in kinetic results will be due solely to the type of crown ether used.

C. Results and Discussion

The kinetics of complexation of sodium ion with 18C6 was studied in six neat or mixed solvents by using a complete ^{23}Na lineshape analysis. The six solvent systems were THF, PC, MeOH, MeOH-THF mixture (40-60 mole %), and PC-THF (20-80 and 60-40 mole %) mixtures.

The complete lineshape analysis requires information concerning chemical shifts and linewidths of the resonances corresponding to the solvated and complexed sodium sites in the absence of exchange. Therefore, this information was obtained and is presented here. In this discussion, site A refers to the solvated site while site B refers to the complexed site of the sodium ion.

1. Measurements in the Absence of Exchange

The spin-spin relaxation times, T_{2A} , and the chemical shift, δ_A , of the solvated sodium sites in each solvent were obtained with solutions containing salt and solvent only. Since the sodium ion complex with 18C6 is very stable, i.e., $K_f > 10^4 \text{ M}^{-1}$ (31,69), in all neat solvents used here and presumably the solvent mixtures as well, solutions in which the crown concentration is greater than the salt concentration have only complexed sodium ions. Thus, these solutions were prepared to obtain T_{2B} and δ_B . The temperature dependence of T_{2A} , T_{2B} , δ_A , and δ_B are given in Tables 13-19.

Table 13. Sodium-23 Chemical Shifts and Relaxation Rates of NaBPh_4 and of its Complex with 18C6 in THF Solutions.^b

T (°C)	M.R. (a) = 0		M.R. (a) = 1.10		
	1/T _{2A} (s ⁻¹)	δ _A (ppm)	T (°C)	1/T _{2B} (s ⁻¹)	δ _B (ppm)
20.1 (±1)	81.1 (±10%)	-7.55 (±0.1)	19.2 (±1)	824. (±10%)	-15.92 (±0.2)
27.5	80.0	-7.55	26.7	597.	-17.16
35.0	77.3	-7.86	34.4	500.	-16.70
45.2	73.8	-7.93	42.1	364.	-16.70
52.0	70.8	-8.09	50.0	298.	-16.63
59.3	69.7	-8.24	57.9	231.	-16.39

^aM.R. = mole ratio $[\text{18C6}]_{\text{total}}/[\text{Na}^+]_{\text{total}}$

^b0.2 M in salt.

Table 14. Sodium-23 Chemical Shifts and Relaxation Rates of NaSCN and of its Complex with 18C6 in THF Solutions.^b

T (°C)	$\frac{\text{M.R. (a)} = 0}{1/T_{2A} (s^{-1})}$		δ_A (ppm)	T (°C)	$\frac{\text{M.R. (a)} = 1.07}{1/T_{2B} (s^{-1})}$		δ_B (ppm)
	$1/T_{2A} (s^{-1})$				$1/T_{2B} (s^{-1})$		
24.6 (±1)	229. (±10%)	-2.82 (±0.2)	24.6 (±1)	841. (±10%)	-12.00 (±0.3)		
14.4	260.	-2.82	14.4	979.	-12.00		
4.7	291.	-2.92	4.7	1193.	-12.20		
-5.1	344.	-2.43	-5.2	1377.	-12.60		
-14.8	390.	-2.94	-14.7	2053.	-12.40		
-24.6	475.	-2.94	-24.7	2555.	-11.80		
-35.3	566.	-2.94	-34.3	3116.	-12.10		

^aM.R. = mole ratio $[18C6]_{\text{total}}/[Na^+]_{\text{total}}$

^b0.05 M in salt.

Table 15. Sodium-23 Chemical Shifts and Relaxation Rates of NaBPh₄ and of its Complex with 18C6 in PC Solutions.^b

T (°C)	$\frac{\text{M.R. (a)} = 0}{1/T_{2A} (s^{-1})}$		δ_A (ppm)	T (°C)	$\frac{\text{M.R. (a)} = 1.18}{1/T_{2B} (s^{-1})}$		δ (ppm)
	$1/T_{2A} (s^{-1})$				$1/T_{2B} (s^{-1})$		
30.2 (±1)	337. (±10%)	-9.25 (±0.2)		39.8 (±1)	360. (±10%)		-15.58 (±0.2)
20.9	398.	-9.10		32.5	417.		-15.69
11.1	515.	-9.04		24.7	517.		-15.79
1.6	643.	-8.89		18.3	619.		-15.99
-7.9	875.	-8.73		8.4	852.		-16.15
-18.2	1293.	-8.57		-2.5	1349.		-16.39
				-11.7	2330.		-16.19

^aM.R. = mole ratio [18C6]_{total}/[Na⁺]_{total}.

^b0.1 M in salt.

Table 16. Sodium-23 Chemical Shifts and Relaxation Rates of NaSCN and of its Complex with 18C6 in MeOH.^b

T (°C)	$\frac{\text{M.R. (a)} = 0}{1/T_{2A} (s^{-1})}$		δ_A (ppm)	T (°C)	$\frac{\text{M.R. (a)} = 1.16}{1/T_{2B} (s^{-1})}$		δ_B (ppm)
	$1/T_{2A} (s^{-1})$				$1/T_{2B} (s^{-1})$		
31.6 (± 1)	70.4 ($\pm 10\%$)	-3.54 (± 0.1)		33.9 (± 1)	570. ($\pm 10\%$)		-14.12 (± 0.2)
25.3	74.8	-3.43		25.2	701.		-14.11
18.7	83.9	-3.33		13.9	905.		-14.35
7.5	97.1	-3.16		4.0	1165.		-14.46
-3.8	112.5	-2.98		-5.9	1571.		-14.63
-13.3	131.6	-2.80		-15.4	2040.		-14.42
-24.2	160.2	-2.61					

^a M.R. = mole ratio $[18C6]_{\text{total}}/[Na^+]_{\text{total}}$.

^b 0.1 M in salt.

Table 17. Sodium-23 Chemical Shifts and Relaxation Rates of NaBPh_4 and of its Complex with 18C6 in a 40-60 mole % MeOH-THF Mixture.^b

T (°C)	$\frac{\text{M.R. (a)} = 0}{\text{1/T}_{2A} \text{ (s}^{-1}\text{)}}$		δ_A (ppm)	T (°C)	$\frac{\text{M.R. (a)} = 1.05}{\text{1/T}_{2B} \text{ (s}^{-1}\text{)}}$		δ_B (ppm)
	1/T _{2A} (s ⁻¹)				1/T _{2B} (s ⁻¹)		
40.6 (±1)	114. (±10%)		-5.45 (±0.2)	40.6 (±1)	473. (±10%)		-15.16 (±0.3)
33.0	121.		-5.36	32.9	618.		-15.40
25.3	127.		-5.24	25.4	696.		-15.49
17.8	133.		-5.16	17.8	778.		-15.41
9.4	144.		-5.10	8.4	945.		-16.01
0.3	160.		-5.02	-0.4	1105.		-15.67
-9.7	172.		-4.94	-9.6	1374.		-15.62

^aM.R. = mole ratio $[\text{18C6}]_{\text{total}}/[\text{Na}^+]_{\text{total}}$.

^b0.1 M in salt.

Table 18. Sodium-23 Chemical Shifts and Relaxation Rates of NaBPh₄ and of its Complex with 18C6 in a 80-20 mole % THF-PC Mixture.^b

T (°C)	M.R. (a) = 0		M.R. (a) = 1.19		
	1/T _{2A} (s ⁻¹)	δ _A (ppm)	T (°C)	1/T _{2B} (s ⁻¹)	δ _B (ppm)
40.2 (±1)	110. (±10%)	-8.21 (±0.2)	40.0 (±1)	372. (±10%)	-16.6 (±0.2)
32.8	115.	-8.12	32.5	479.	-16.7
25.4	122.	-8.03	24.8	551.	-16.6
16.4	128.	-7.96	16.4	674.	-16.7
7.0	142.	-7.86	7.0	912.	-16.8
-2.4	160.	-7.76	-2.4	1249.	-16.8
-10.6	177.	-7.66	-10.5	1443.	-16.6

^aM.R. = mole ratio $[18C6]_{\text{total}}/[Na^+]_{\text{total}}$.

^b0.1 M in salt.

Table 19. Sodium-23 Chemical Shifts and Relaxation Rates of NaBPh₄ and of its Complex with 18C6 in a 60-40 mole % PC-THF Mixture.^b

T (°C)	$\frac{\text{M.R. (a)} = 0}{1/T_{2A} (s^{-1})}$		δ_A (ppm)	T (°C)	$\frac{\text{M.R. (a)} = 1.15}{1/T_{2B} (s^{-1})}$		δ_B (ppm)
	179. (±10%)	199.			604. (±10%)	803.	
25.3	179. (±10%)		-8.31 (±0.2)	25.0 (±1)	604. (±10%)		-16.76 (±0.2)
15.6		199.	-8.16	14.6		803.	-16.85
5.3		229.	-8.05	5.2		1117.	-17.04
-5.0		272.	-7.90	-4.2		1516.	-16.97
-14.3		328.	-7.78	-14.3		2292.	-16.71
-24.9		432.	-7.65				

^aM.R. = mole ratio $[18C6]_{\text{total}}/[Na^+]_{\text{total}}$.

^b0.1 M in salt.

Figure 7 shows plots of $\log(1/T_2)$ vs. inverse temperature for NaBPh_4 , NaSCN , and their complexes with 18C6 in THF. Figure 8 shows such plots for NaBPh_4 and its complex with 18C6 in PC and for NaSCN and its complex in MeOH. Figures 9 and 10 show the results obtained in the mixed solvents MeOH-THF (40-60 mole %), PC-THF (20-80 mole%), and PC-THF (60-40 mole %).

Sodium-23 nucleus has a spin of $3/2$ and thus, has a quadrupole moment. The dominant relaxation mechanism is through quadrupolar interaction modulated either by diffusion of solvent molecules in and out of the solvation sphere of the Na^+ ion or by rotational diffusion of the complex. The quadrupolar relaxation rate may be written as (70):

$$\frac{1}{T_1} = \frac{1}{T_2} = \frac{3}{40} \frac{2I+3}{I^2(2I+1)} \left(1 + \frac{\xi^2}{3}\right) \left(\frac{eQ}{h} \frac{\partial^2 V}{\partial z'^2}\right)^2 \tau_c$$

where $1/T_1$ is the spin-lattice relaxation rate, $1/T_2$ is the spin-spin relaxation rate, I is the spin of the nucleus, ξ is the asymmetry parameter, Q is the quadrupole moment of the nucleus, $\partial^2 V / \partial z'^2$ is the z component of the electric field gradient at the nucleus, and τ_c is the correlation time which characterizes the fluctuations of the field gradient. For a simple reorientation process the variation of the correlation time with temperature may be expressed by (71):

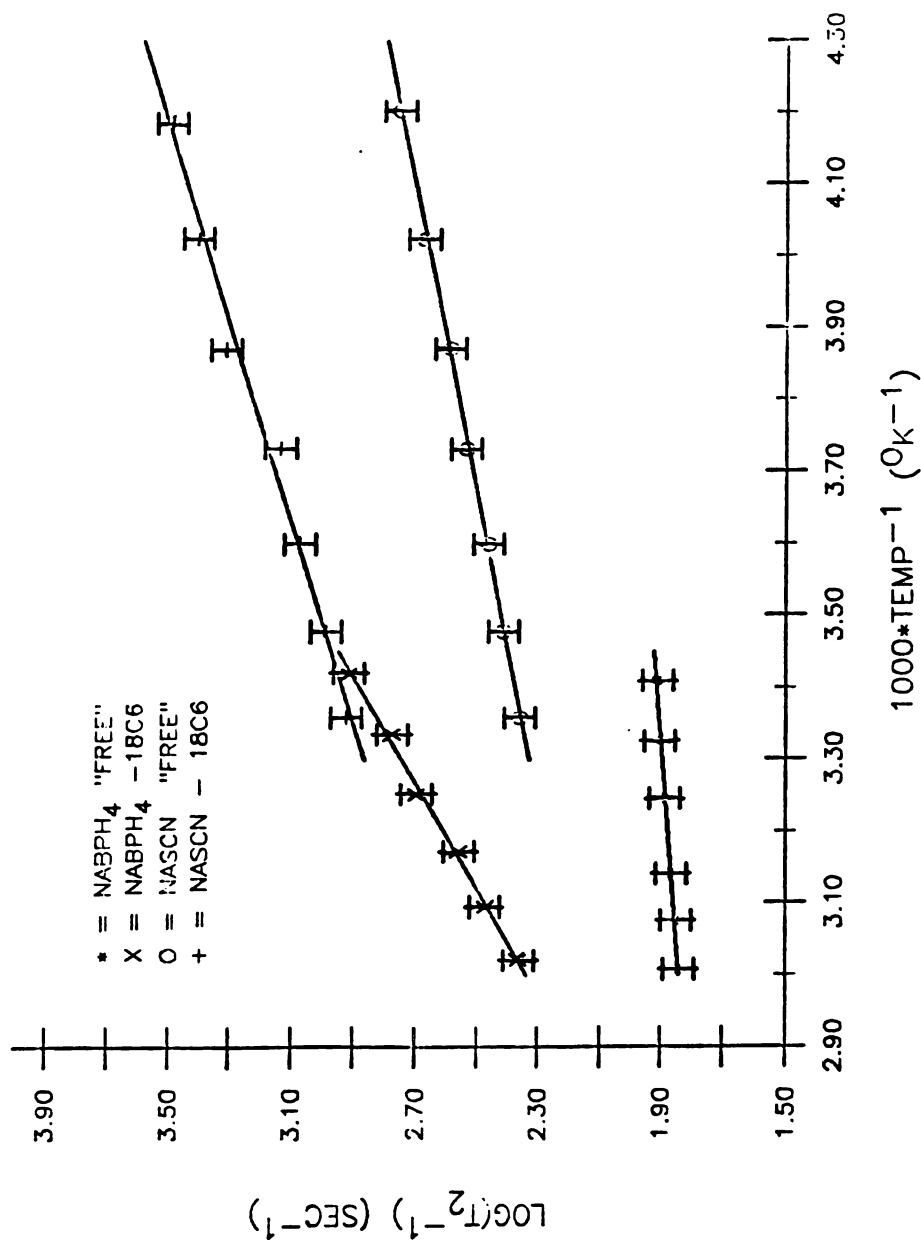


Figure 7. Semilog plots of $1/T_2$ vs. reciprocal temperatures for tetrahydrofuran solutions containing solvated and 18C6 complexed Na^+ ion.

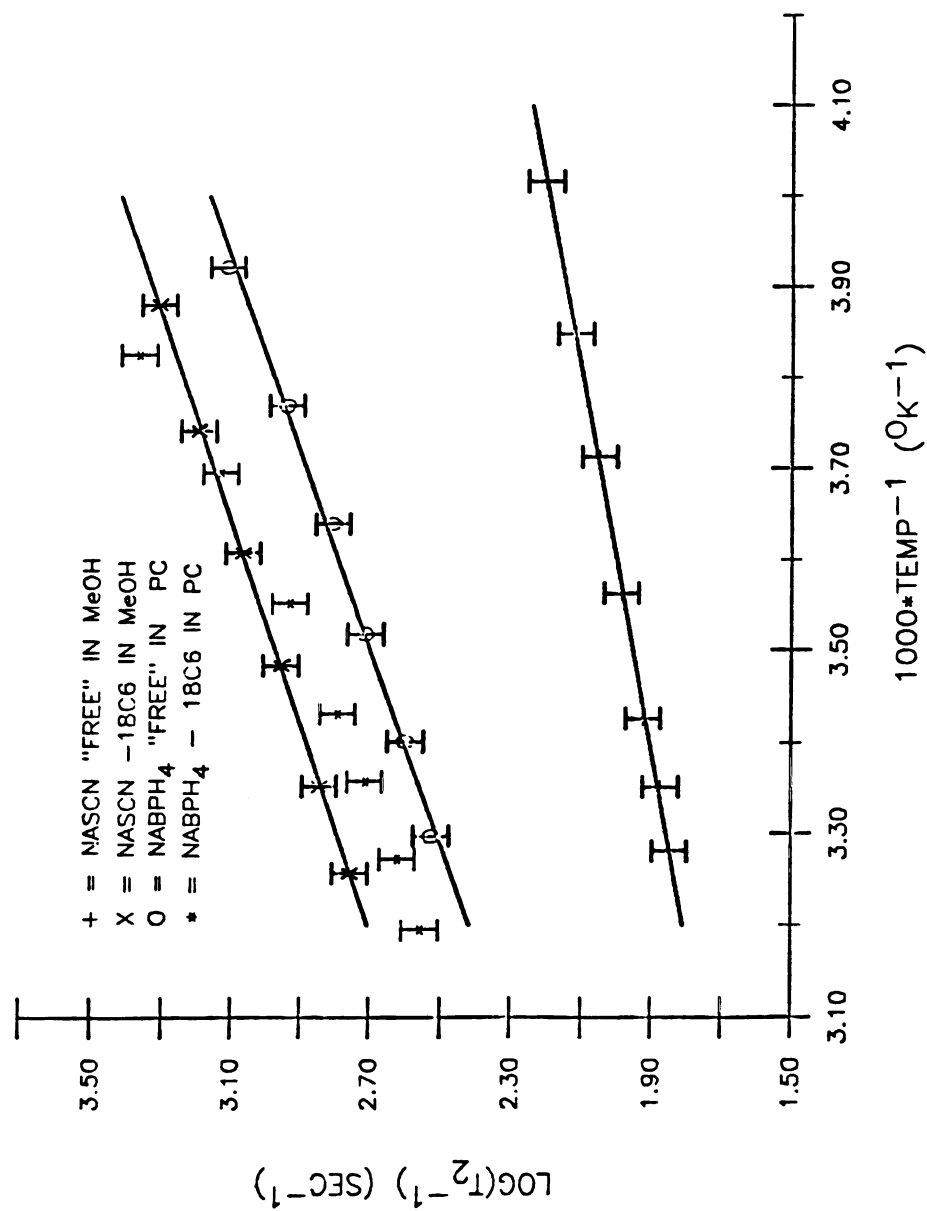


Figure 8. Semilog plots of $1/T_2$ vs. reciprocal temperatures for solutions containing solvated and 18C6 complexed Na^+ ion.

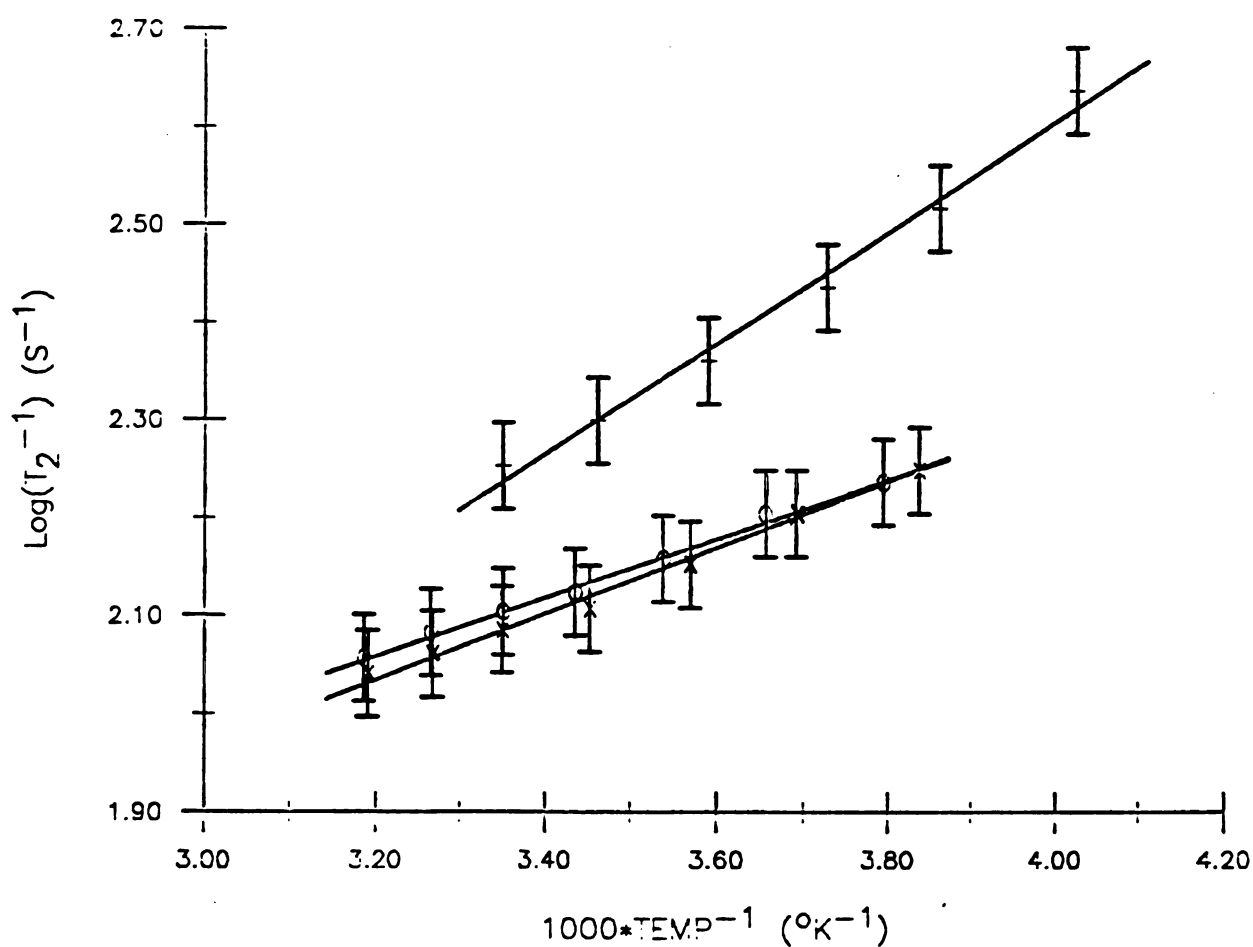


Figure 9. Semilog plots of $1/T_2$ vs. reciprocal temperatures for solutions containing solvated Na^+ ion. (x) 0.1 M NaBPh₄ in a 20-80 mole % PC-THF mixture; (o) 0.1 M NaBPh₄ in a 40-60 mole % MeOH-THF mixture; (+) 0.1 M NaBPh₄ in a 60-40 mole % PC-THF mixture.

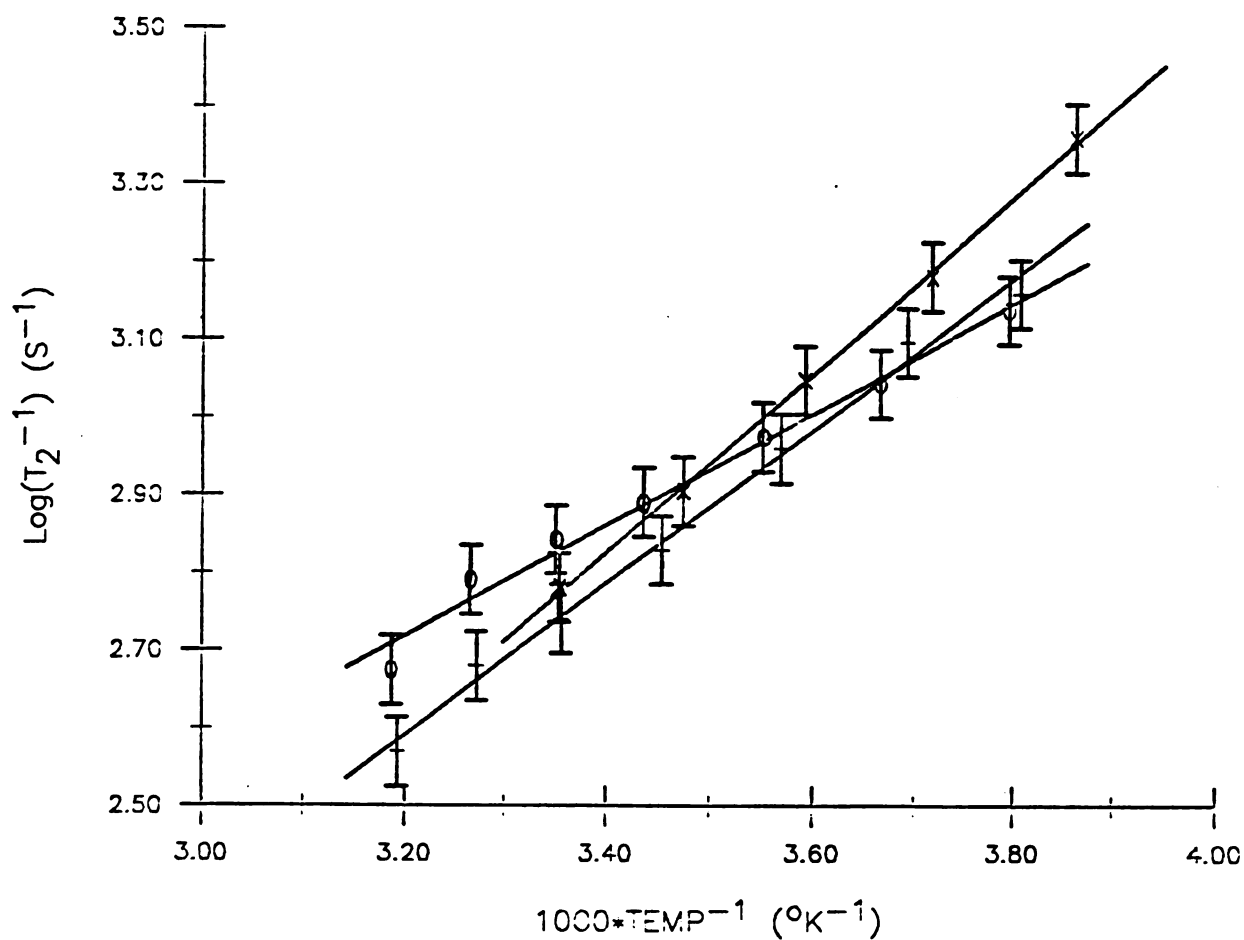


Figure 10. Semilog plots of $1/T_2$ vs. reciprocal temperatures for solutions containing 18C6 complexed Na^+ ion. (x) 0.1 M NaBPh₄ in a 60-40 mole % PC-THF mixture; (+) 0.1 M NaBPh₄ in a 20-80 mole % PC-THF mixture; (o) 0.1 M NaBPh₄ in a 40-60 MeOH-THF mixture.

$$1/T_2 \propto \tau_c = A' \exp(E_r/RT)$$

where E_r is an activation energy for solvent reorientation and A' is a constant. Debye's relationship $\tau_c = 4\pi\xi a^3/3kT$ (ξ = viscosity), although it has been found to yield unreasonably large values for solvated and complexed species (72,73), is still useful in that it predicts a viscosity dependence of the correlation time. The relaxation time varies exponentially as a function of temperature provided that the nuclear quadrupole coupling constant (NQCC) $((eQ/h)(\partial^2 V/\partial Z'^2))$ remains constant over a given temperature range. As may be seen in Figures 7-10, this behavior has been observed in all systems studied here with the exception of $\text{NaBPh}_4 \cdot 18\text{C}_6$ in PC. Where such linear behavior has been observed the relaxation rates have been fitted to the following equation:

$$\frac{1}{T_2} = \left(\frac{1}{T_2}\right)_{298.15} \exp\left[\left(\frac{E_r}{R}\right)\left(\frac{1}{T} - \frac{1}{298.15}\right)\right]$$

where $\left(\frac{1}{T_2}\right)_{298.15}$ is the relaxation rate at 298.15°K, T is the absolute temperature, E_r is the activation energy, and R is the gas constant. The values obtained for $\left(\frac{1}{T_2}\right)_{298.15}$ and E_r from such fits are reported, along with chemical shifts at 25°C, in Tables 20 and 21.

The results for 0.2 M NaBPh_4 solution in THF agree quite well with those of Ceraso (74) for a 0.4 M NaBPh_4 solution

Table 20. Sodium-23 Results for Solvated Na⁺ in Selected Solvents.^a

Solution	$\left(\frac{1}{T_2}\right)_{298}$ (s ⁻¹)	E _r (kcal·mol ⁻¹)	δ (ppm)
NaBPh ₄ in THF ^(b)	80.2 (±10%)	0.815 (±10%)	-7.55 (±0.1)
NaBPh ₄ in THF ^(c)	96.9	0.86	-7.43
NaSCN in THF ^(d)	226.	2.14	-2.82 (±0.2)
NaSCN in MeOH	76.2	2.21	-3.43 (±0.1)
NaBPh ₄ in PC	365.	4.26	-9.18 (±0.2)
NaBPh ₄ in MeOH-THF (40-60%)	127.	1.37	-5.24 (±0.2)
NaBPh ₄ in PC-THF (20-80%)	122.	1.54	-8.03 (±0.2)
NaBPh ₄ in PC-THF (60-40%)	173.	2.58	-8.31 (±0.2)

^a0.1 M in salt.^b0.2 M in salt.^cReference 7, 0.4 M in salt.^d0.05 M in salt.

Table 21. Sodium-23 Results for Complexed Na^+ in Selected Solvents.^a

Solution	$\left(\frac{1}{T_2}\right)_{298}$ (s^{-1})	E_r ($\text{kcal}\cdot\text{mol}^{-1}$)	δ (ppm)
$\text{NaBPh}_4\cdot 18\text{C}6$ in THF^b	660. ($\pm 10\%$)	6.22 ($\pm 10\%$)	-17.0 (± 0.2)
$\text{NaSCN}\cdot 18\text{C}6$ in THF^c	804.	3.30	-12.0 (± 0.3)
$\text{NaSCN}\cdot 18\text{C}6$ in MeOH	698.	4.08	-14.1 (± 0.2)
$\text{NaBPh}_4\cdot 18\text{C}6$ in PC	517.	~ 4.9	-15.8 (± 0.2)
$\text{NaBPh}_4\cdot 18\text{C}6$ in MeOH-THF (40-60%)	674.	3.26	-15.5 (± 0.3)
$\text{NaBPh}_4\cdot 18\text{C}6$ in PC-THF (20-80%)	552.	4.48	-16.6 (± 0.2)
$\text{NaBPh}_4\cdot 18\text{C}6$ in PC-THF (60-40%)	594.	5.21	-16.8 (± 0.2)

^a0.1 M in salt.^b0.2 M in salt.^c0.05 M in salt.

(see Table 20). The observation of a somewhat larger relaxation rate by Ceraso may be simply due to the increased viscosity of the more concentrated solution.

The difference in the results for THF solutions containing NaSCN and NaBPh₄ are quite striking. As discussed in Chapter 3, these differences are the result of ion pairing differences of the two salts. The relaxation rate of a quadrupolar nucleus is very sensitive to the symmetry of the environment around the nucleus. Contact ion pairing which occurs for NaSCN in THF (56) distorts the symmetry of the ion and thus increases the relaxation rate. Sodium tetraphenylborate does not form contact ion pairs to an appreciable extent (50-55) and therefore, a slower relaxation rate is observed. Ion pairing also influences the ²³Na chemical shift (50). The effect of ionic association on the activation energy for solvent reorientation, although more difficult to interpret, must be recognized.

The relaxation rate for site A in PC solutions is much larger than in THF, MeOH, or the MeOH-THF mixture. Other workers (67) have concluded that NaBPh₄ does not form contact ion pairs in PC. Therefore, this increase in the relaxation rate is most likely due to the much larger viscosity of PC as compared to MeOH and THF (Table 12).

It is interesting to note that the value of Er for the MeOH-THF mixture falls exactly where one would expect if a linear relationship occurs between solvent composition

and solvent reorientation energy, i.e., $E_{\text{mixture}} = (0.6)(E_{\text{THF}}) + (0.4)(E_{\text{MeOH}}) = 1.37 \text{ kcal}\cdot\text{mol}^{-1}$. The inverse relaxation time is larger in this mixture than in the pure solvents. This is likely due to the fact that both types of solvents molecules enter into the primary solvation shell of the ion thus distorting the symmetry around it. This distortion may also be causing the increase in the observed relaxation rates in the PC-THF mixtures but it is difficult to separate this effect from that of increased viscosity upon addition of PC.

The complexation of the sodium ion by a planar macrocyclic ligand, such as 18C6, also distorts the symmetry around the ion, thus increasing its relaxation rate. This effect can be seen in Table 21. Upon complexation of NaBPh_4 by 18C6 in THF the inverse relaxation time increases by a factor of eight. The differences in relaxation rates, chemical shifts, and activation energies between complexed NaBPh_4 and complexed NaSCN in THF solutions are due to the fact that complexed NaSCN is contact ion paired while complexed NaBPh_4 forms crown separated ion pairs (Chapter 3).

Of particular interest are the results observed in the solvent mixture as compared to those of the pure solvents. In the series neat THF---(60-40 mole % THF-MeOH)---neat MeOH the inverse relaxation time of the complexed ion increases while the activation energies go through a minimum. In the series neat THF---(80-20 mole % THF-PC)---(40-60 mole %

THF-PC)---neat PC the inverse relaxation times of the complex decrease while the activation energies also go through a minimum. The decrease in relaxation rates is unexpected considering viscosity influences only. No explanations for these observed trends are known at this time.

2. Fourier Transform NMR Exchange Equations

The theoretical description of the effects of chemical exchange between sites A and B on the nmr lineshape has been given by Gutowsky et al. (75) and by Woessner (76). Ceraso and Dye (77) have modified the lineshape equations to include some instrumental corrections. These equations have the form:

$$G(\omega) = K[I \cos(\theta_0 + \theta') - R \sin(\theta_0 + \theta')] + C$$

$$I = \frac{SU + TV}{S^2 + T^2} ; \quad R = \frac{UT - SV}{S^2 + T^2}$$

$$S = \frac{P_A}{T_{2A}} + \frac{P_B}{T_{2B}} + \frac{\tau}{T_{2A}T_{2B}} - \tau(\omega_A + \Delta - \omega)(\omega_B + \Delta - \omega)$$

$$U = 1 + \tau\left(\frac{P_B}{T_{2A}} + \frac{P_A}{T_{2B}}\right)$$

$$T = P_A\omega_A + P_B\omega_B + \Delta - \omega + \tau\left(\frac{\omega_A + \Delta - \omega}{T_{2B}} + \frac{\omega_B + \Delta - \omega}{T_{2A}}\right)$$

$$V = \tau(P_B \omega_A + P_A \omega_B + \Delta - \omega)$$

$$\tau = \frac{\tau_A \tau_B}{\tau_A + \tau_B}$$

$$P_A = \frac{\tau_B}{\tau_A + \tau_B} \quad ; \quad P_B = \frac{\tau_A}{\tau_A + \tau_B}$$

$$\alpha_A = \frac{1}{T_{2A}} - i(\omega_A - \omega)$$

$$\alpha_B = \frac{1}{T_{2B}} - i(\omega_B - \omega)$$

where $G(\omega)$ describes the lineshape as a function of frequency, ω , τ_A and τ_B are the mean lifetimes for sites A and B, ω_A and ω_B are the resonance frequencies for these sites in the absence of exchange, T_{2A} and T_{2B} are the relaxation times in the absence of exchange, $P_A = 1 - P_B$ is the relative population of site A, θ_0 is the zero order phase correction, θ' is the first order phase correction, K is the intensity, C is the baseline height, and Δ is a frequency adjustment.

The nonlinear least squares program KINFIT (49) was used to fit the nmr spectra to the equations of Ceraso and Dye (77). While the authors chose to fix the value of the first order phase correction, θ' , we chose to adjust this parameter visually before the data transfer process, thus eliminating the need to include it in the fit.

Therefore, five parameters are required for the adjustment by KINFIT in order to fit the experimental data. These parameters are the intensity, K , baseline, C , zero order phase correction, θ_0 , frequency shift, Δ , and the exchange time, τ . Values for T_{2A} , T_{2B} , ω_A , and ω_B were known from the measurements of the nonexchanging systems described previously and are entered as constants. Because the formation constants of the $\text{Na}^+\cdot 18\text{C}6$ complex are large in all systems studied ($K_f > 10^4 \text{ M}^{-1}$ (31,69)) all crown in solution was complexed with the cation. Therefore, P_A and P_B are known from solution preparation and are also entered as constants.

Unfortunately, less than satisfactory results were obtained for the fits of experimental data. It was noticed that the severity of the problem increased with increasing experimental delay time. The delay time is the period of time which elapses between the application of a pulse to the nuclei and the collection of the FID. This influence on the quality of the fit may be seen in Figure 11.

The problem arises from the fact that the relaxation rates of the two species undergoing exchange are very different. In this particular example, $\text{NaBPh}_4\text{-}18\text{C}6$ in THF at 25°C , the ratio of $T_{2A}/T_{2B} \sim 8$. Figure 12 shows the sum of two free induction decays with different relaxation rates. The first point of the FID determines the relative areas of the two resonances in the Fourier transformed

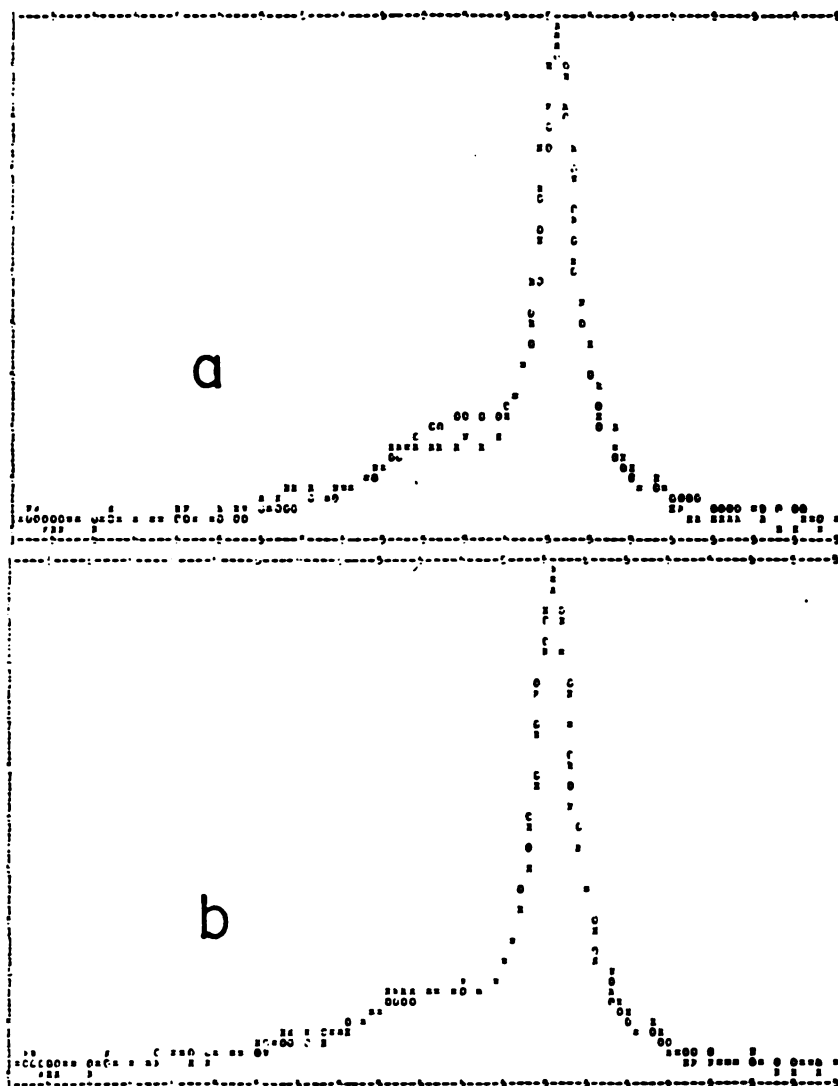


Figure 11. Computer fits of a sodium-23 nmr spectrum of a solution containing 0.2 M NaBPh₄ and 0.1 M 18C6 in THF at 25°C and a delay time of 800 μ s. (x) experimental point; (o) calculated point; (=) no difference between calculated and experimental points within plot accuracy. (a) no delay time correction; (b) with delay time correction.

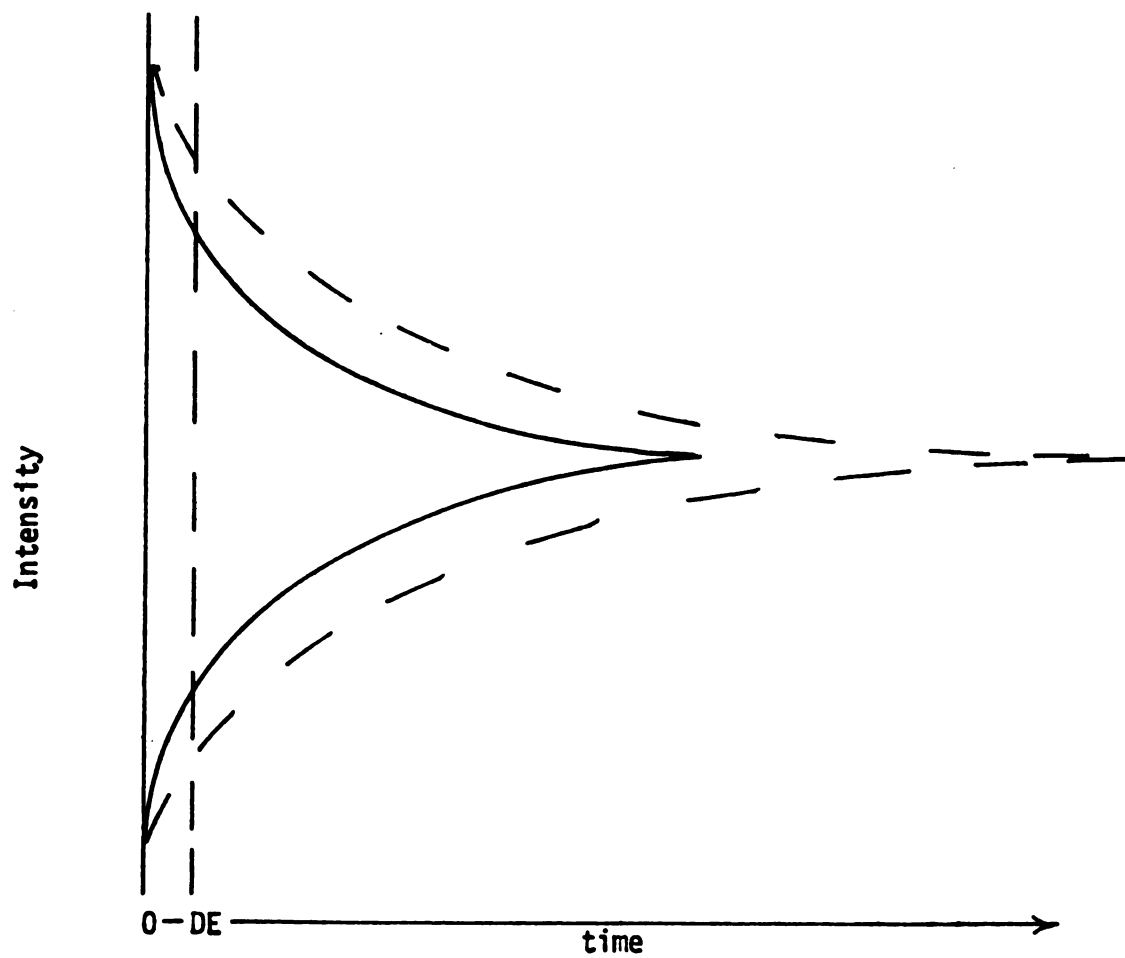


Figure 12. Free induction decays with different relaxation times.

spectrum. If no delay time is used, the ratio of areas in the transformed spectrum would be the one expected from solution preparation. Experimentally, a delay time is required due to the fact that the applied pulse does not fall instantly to zero. As may be seen in Figure 12, during the delay time period the resonance which has a faster relaxation rate decays a greater extent than the one with a slower relaxation rate. Since the first point of the FID is now at the end of the delay time, the apparent relative areas of the two resonances in the transformed spectrum are different from those expected on the basis of solution preparation. The relative area of the broader resonance is less than the predicted one due to the use of the delay time.

The nmr lineshape equations modified to include chemical exchange, therefore, have been modified to include effects of the experimental delay time as well as the use of exponential linebroadening which is applied to increase the signal/noise ratio. The derivation is given in Appendix B. The modified equations have the form:

$$G(\omega) = K\{I\cos[\theta_0 - (\omega_A + \Delta - \omega)DE] - R\sin[\theta_0 - (\omega_A + \Delta - \omega)DE]\} + C$$

$$I = \text{AIMAG}(XS) \quad ; \quad R = \text{REAL}(XS)$$

$$XS = \frac{C_1 \exp[(\Lambda_1 - LB)DE]}{\Lambda_1 - LB} - \frac{C_2 \exp[(\Lambda_2 - LB)DE]}{\Lambda_2 - LB}$$

$$C_1 = \frac{i(\Lambda_2 + P_A \alpha_A + P_B \alpha_B)}{(\Lambda_2 - \Lambda_1)}$$

$$C_2 = \frac{i(\Lambda_1 + P_A \alpha_A + P_B \alpha_B)}{(\Lambda_1 - \Lambda_2)}$$

$$\Lambda_1, \Lambda_2 = [-(\alpha_A + \alpha_B + \tau)^{-1} \pm \{(\alpha_A - \alpha_B + \frac{P_B}{\tau} - \frac{P_A}{\tau})^2 + \frac{4P_A P_B}{\tau^2}\}^{1/2}]/2$$

$$\alpha_A = T_{2A}^{-1} + i(\omega_A - \omega)$$

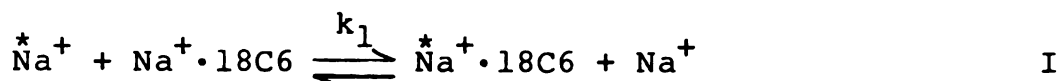
$$\alpha_B = T_{2B}^{-1} + i(\omega_B - \omega)$$

where DE is the delay time, AIMAG(XS) and REAL(XS) are the imaginary and real parts of XS, respectively, and all other symbols have their previously defined meanings. The application of these equations to the example illustrated in Figure 11a is shown in Figure 11b. As may be seen, the fit is much more satisfactory.

Thus, these new equations have been used in all fits of kinetic data. It should be noted that the use of an experimental delay time in any nmr experiment will affect the relative areas of the resonances being observed regardless of whether or not they undergo exchange. The correction for the delay time effect in these instances is similar to that described in Appendix B and has been done for the Lorentzian lineshape case by Szczygiel (8).

3. Mechanisms of Exchange

There are two mechanisms possible for the exchange of Na^+ ion between solvated and complexed sites as proposed by Shchori et al. (10). These are the bimolecular process (I) and the dissociative process (II).



The relaxation time for site i is given by

$$\frac{1}{\tau_A} = \frac{\text{rate of removal from site i}}{\text{number of molecules in site i}}$$

Considering mechanisms I and II, then,

$$\frac{1}{\tau_A} = \frac{1}{[\text{Na}^+]} (2 k_1 [\text{Na}^+][\text{Na}^+ \cdot 18\text{C6}] + k_2 [\text{Na}^+][18\text{C6}])$$

$$\frac{1}{\tau_A} = 2k_1 [\text{Na}^+ \cdot 18\text{C6}] + k_2 [18\text{C6}]$$

Since

$$K_f = \frac{k_2}{k_{-2}} = \frac{[\text{Na}^+ \cdot 18\text{C6}]}{[\text{Na}^+][18\text{C6}]}$$

then

$$k_2[18C6] = k_{-2} \frac{[Na^+ \cdot 18C6]}{[Na^+]}$$

or

$$\frac{1}{\tau_A} = 2k_1[Na^+ \cdot 18C6] + k_{-2} \frac{[Na^+ \cdot 18C6]}{[Na^+]}$$

For the complexed site

$$\frac{1}{\tau_B} = \frac{1}{[Na^+ \cdot 18C6]} (2k_1[Na^+ \cdot 18C6][Na^+] + k_{-2}[Na^+ \cdot 18C6])$$

$$\frac{1}{\tau_B} = 2k_1[Na^+] + k_{-2}$$

Since

$$\frac{1}{\tau} = \frac{1}{\tau_A} + \frac{1}{\tau_B}$$

then

$$\frac{1}{\tau} = 2k_1([Na^+] + [Na^+ \cdot 18C6]) + k_{-2}(1 + \frac{[Na^+ \cdot 18C6]}{[Na^+]})$$

or

$$\frac{1}{\tau} = 2k_1[Na^+]_{total} + k_{-2} \frac{[Na^+]_{total}}{[Na^+]_{free}}$$

The relative contributions of these two mechanisms to the exchange process may be determined at a given temperature

by plotting $1/(\tau[\text{Na}^+]_{\text{total}})$ vs. $1/[\text{Na}^+]_{\text{free}}$ for several different relative free populations of Na^+ ion. The slope will equal k_{-2} , and the intercept will be $2k_1$. Assuming either mechanism to be predominant a plot of $\log(1/\tau)$ vs. inverse absolute temperature will be an Arrhenius type plot since $(1/\tau) \propto k$, and the slope will be proportional to the Arrhenius activation energy. If the mechanism is known the rate constants may be determined. From the Eyring theory

$$k = \frac{k_B T}{h} \exp\left(\frac{-\Delta G^\ddagger}{RT}\right) = \frac{k_B T}{h} \exp\left(\frac{\Delta S^\ddagger}{RT}\right) \exp\left(\frac{-\Delta H^\ddagger}{RT}\right)$$

where T is the temperature, ΔG^\ddagger is the free energy of activation, ΔS^\ddagger and ΔH^\ddagger are the activation entropy and enthalpy respectively, and all other symbols have their usual meanings. Also, in solution, $\Delta H^\ddagger = E_a - RT$. Therefore, all kinetic parameters may easily be determined once the mechanism is known.

4. Results in THF Solutions

The exchange time, τ , was determined at various temperatures at two different free sodium ion populations for the systems $\text{NaBPh}_4 \cdot 18\text{C6}$ and for $\text{NaSCN} \cdot 18\text{C6}$ in THF solutions. Tables 22 and 23 list the τ values for these systems and Figures 13 and 14 are plots of $\log(1/\tau)$ vs. inverse temperature for these systems. Figure 14 shows a plot of

Table 22. Mean Lifetimes as a Function of Temperature
for the System $\text{NaBPh}_4 \cdot 18\text{C6}$ in THF Solutions.^a

P_{Na^+}	Temperature ($^{\circ}\text{C}$)	$\tau \times 10^3$ (s)
0.412	26.0 ($\pm 1.$)	7.10 (0.31) ^b
"	36.7	3.72 (0.13)
"	40.8	2.84 (0.08)
"	45.8	2.02 (0.08)
"	50.6	1.62 (0.07)
"	57.3	1.06 (0.14)
0.735	25.2 (± 1)	16.7 (2.1)
"	30.2	9.82 (0.85)
"	41.6	4.34 (0.27)
"	49.8	2.59 (0.10)
"	54.6	2.45 (0.21)
"	59.6	1.66 (0.15)

^a0.2 M in salt.

^bStandard deviation estimate.

Table 23. Mean Lifetimes as a Function of Temperature for the System NaSCN·18C6 in THF Solutions.^a

P_{Na^+}	Temperature (°K)	$\tau \times 10^4$ (s)
0.475	303.0 (± 1)	0.8933(0.035) ^(b)
"	297.8	1.048 (0.036)
"	293.6	1.047 (0.041)
"	288.0	1.363 (0.063)
"	283.7	1.508 (0.077)
"	278.6	1.493 (0.084)
"	268.3	1.993 (0.140)
"	267.1	2.203 (0.14)
"	278.3	1.526 (0.10)
"	274.1	1.748 (0.11)
"	258.1	2.731 (0.38)
"	264.0	2.707 (0.27)
0.735	309.4	0.9145(0.019)
"	303.8	0.9878(0.020)
"	298.6	1.050 (0.020)
"	293.8	1.210 (0.031)
"	288.2	1.401 (0.045)
"	283.6	1.442 (0.05)

^a0.05 M in salt.

^bStandard deviation estimate.

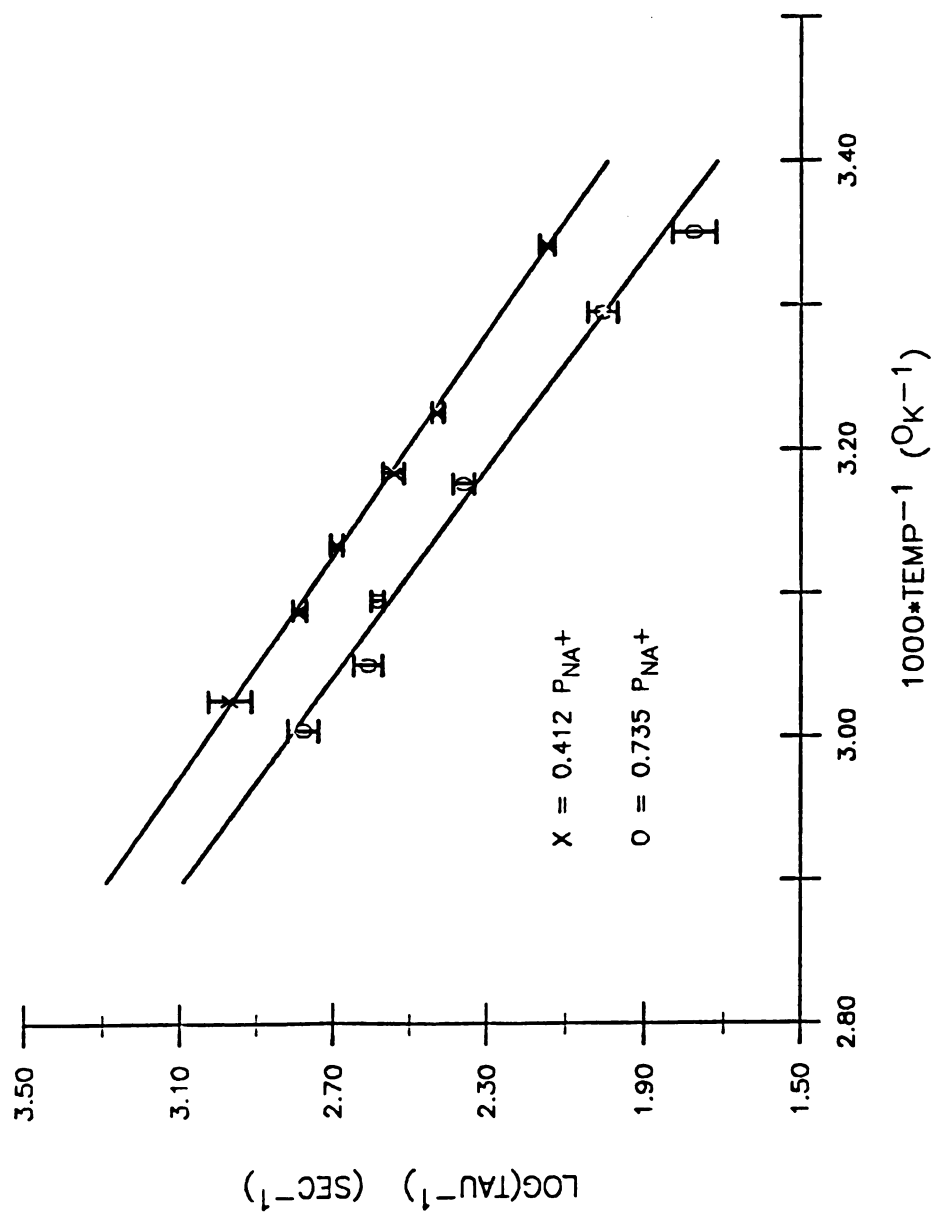


Figure 13. Semilog plots of $1/\tau$ vs. $1/T$ at various $[\text{NaBPh}_4]/[\text{18C6}]$ mole ratios in tetrahydrofuran solutions.

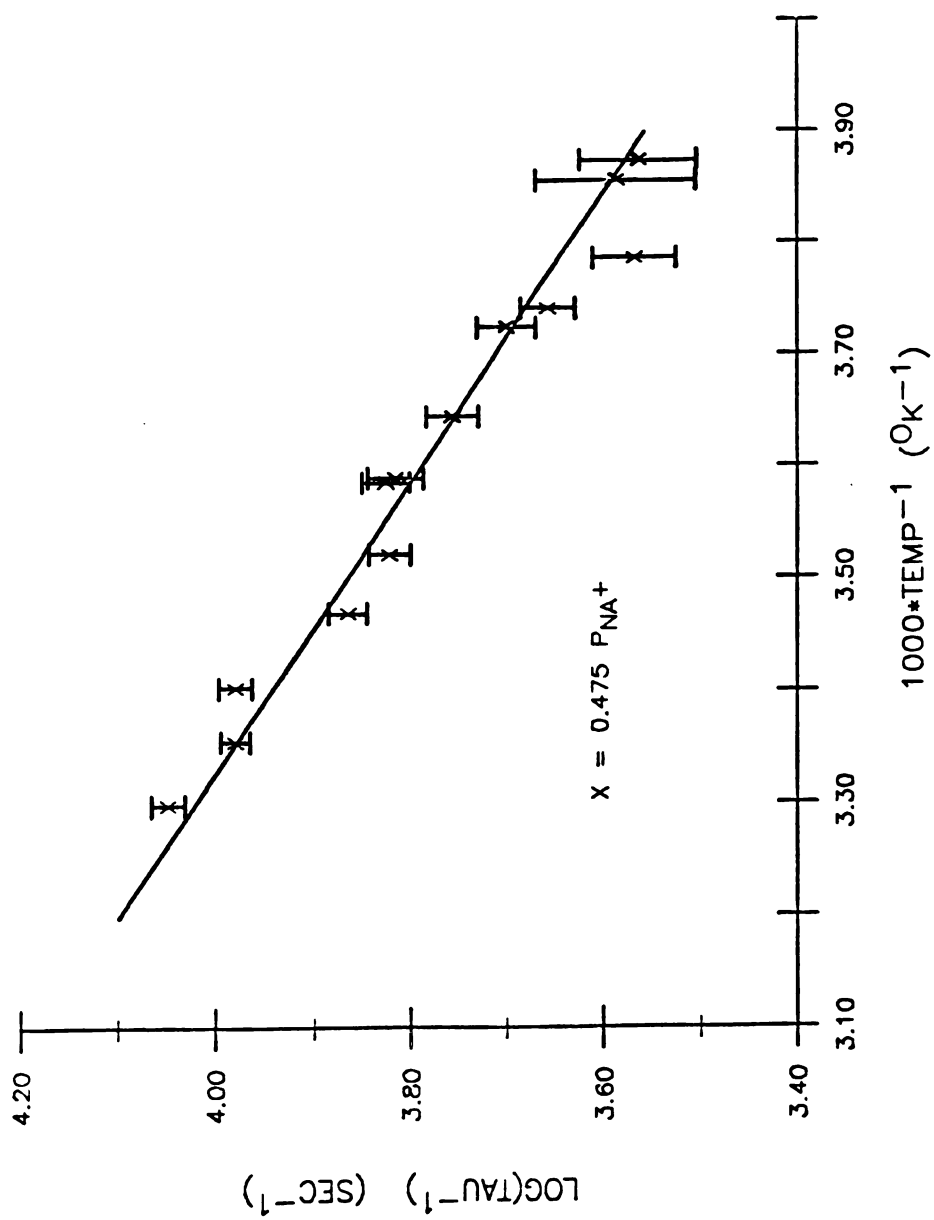


Figure 14. Semilog plot of $1/\tau$ vs $1/T$ for $\text{NaSCN} \cdot 18\text{C6}$ in tetrahydrofuran solutions.

only one relative free NaSCN population since the other is the same within experimental error. The Arrhenius activation energies for these systems are listed in Table 24. The influence of the anion on the magnitude of these values is immediately obvious. Equally striking are the differences in the Arrhenius activation energies for the two salts.

Figures 15 and 16 are plots of $1/(\tau[\text{Na}^+]_{\text{total}})$ vs. $1/[\text{Na}^+]_{\text{free}}$ for the two sodium salts. As may be seen in Figure 15, when BPh_4^- is the counterion the exchange proceeds via the dissociative mechanism (the intercept is zero). This is not unusual in that this mechanism has been shown to occur with analogues of 18C6 in DMF, MeOH, and DME by Shchori and coworkers (10,25). The rate data calculated for this salt are listed in Table 24 and the weighted average values are listed in Table 25. Of particular interest is the large free energy of activation, ΔG_{-2}^\ddagger . This large free energy barrier is responsible for the slow exchange at room temperature in THF solutions.

In Figure 16 we see that the plots have a slope of essentially zero which indicate that with SCN^- as the counterion the primary mechanism of exchange is the bimolecular process. This seems to be the first demonstrated observation of this mechanism for the exchange of sodium ion with a crown ether.

Considering the results concerning ion pairing of the salts and of their complexes with 18C6, as discussed in

Table 24. Kinetic Parameters for the Complexation of Na^+ with 18C6 at 25°C.

Solvent	P_{Na^+}	Anion	$k_d^{(a)}$	$E_a^{(b)}$	$\Delta H_d^\ddagger(b)$	$\Delta S_d^\ddagger(c)$	$\Delta G_d^\ddagger(b)$	Mech. (d)
THF	0.412	BPh_4^-	65.(17.) ^(f)	11.8 (0.3)	11.2 (0.3)	-12.7(1.2)	15.0 (0.2)	II
"	0.735	"	51.(6.)	12.6 (0.9)	11.8 (0.9)	-11.1(3.0)	15.1 (0.1)	II
"	0.475	SCN^-	95600.(4200.) ^(e)	3.54(0.4)	2.94(0.4)	-25.9(1.4)	10.66(0.3)	I
"	0.735	"	91300.(1200.) ^(e)	3.26(0.3)	2.66(0.3)	-26.9(1.0)	10.68(0.001)	I
MeOH	0.413	"	36500.(700.)	9.68(0.3)	9.08(0.3)	- 7.2(1.0)	11.23(0.02)	II
PC	0.505	BPh_4^-	130000.(7000.) ^(e)	4.57(0.5)	3.97(0.5)	-21.7(1.7)	10.48(0.04)	I
0.6X _{THF} , 0.4X _{MeOH}	0.477	"	3560.(90.)	9.84(0.3)	9.24(0.3)	-11.3(1.0)	12.61(0.03)	II
0.8X _{THF} , 0.2X _{PC}	0.283	"	876.(25.)	9.01(0.3)	8.41(0.3)	-16.9(1.0)	13.44(0.02)	II
"	0.415	"	928.(17.)	10.42(0.1)	9.82(0.1)	-12.0(0.4)	13.40(0.01)	II
"	0.646	"	936.(34.)	9.95(0.4)	9.35(0.4)	-13.6(1.4)	13.40(0.02)	II
0.4X _{THF} , 0.6X _{PC}	0.270	"	53600.(3500.) ^(e)	8.64(0.6)	8.04(0.6)	- 7.9(2.0)	11.00(0.04)	I
"	0.406	"	53800.(4000.) ^(e)	9.66(0.6)	9.06(0.6)	- 6.5(2.0)	11.00(0.04)	I
"	0.663	"	42000.(4300.) ^(e)	9.1 (1.1)	8.5 (1.1)	- 8.9(3.7)	11.14(0.06)	I

 a_s^{-1} . $b_{\text{kcal}\cdot\text{mol}^{-1}}$ $c_{\text{e.u.}}$ ^dSee text for description of mechanism.^e $\text{M}^{-1}\text{s}^{-1}$ ^fStandard deviation estimate.

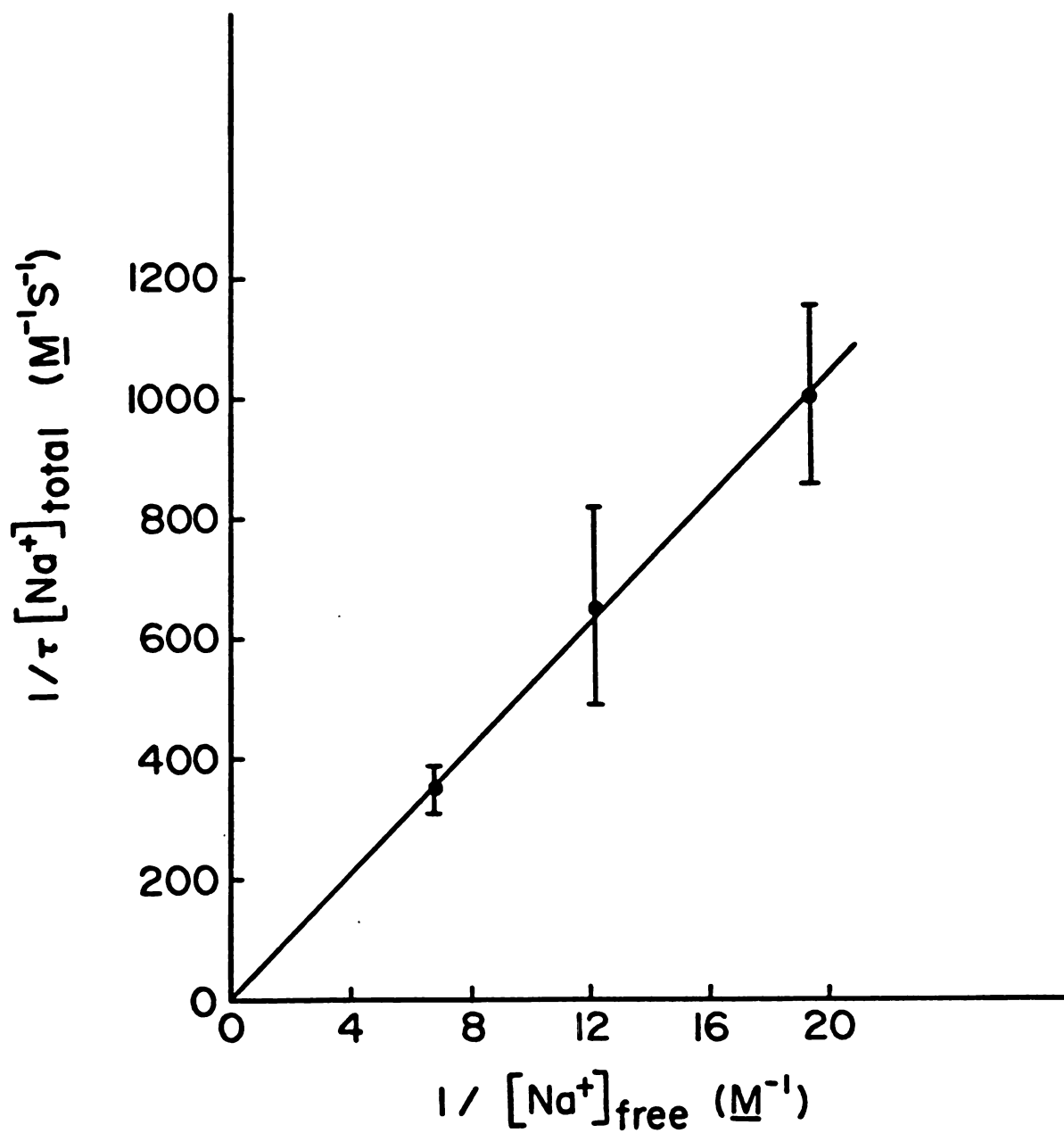


Figure 15. Plot of $1/(\tau[\text{Na}^+]_{\text{total}})$ vs. the inverse of the free sodium ion concentration for $\text{NaBPh}_4 \cdot 18\text{C}6$ in tetrahydrofuran solutions at 25°C .

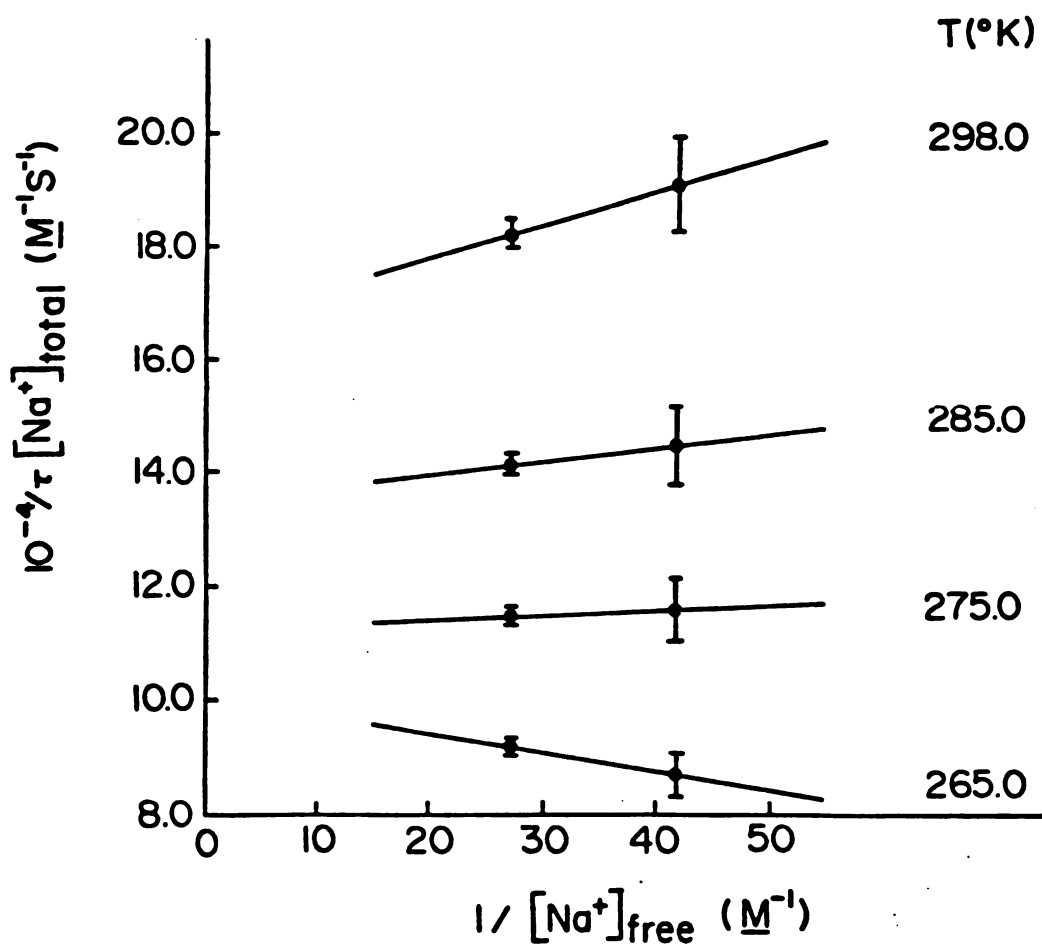


Figure 16. Plots of $1/(\tau[\text{Na}^+]_{\text{total}})$ vs. the inverse of the free sodium ion concentration for NaSCN·18C6 in tetrahydrofuran solutions at several temperatures.

Table 25. Weighted Average List of Kinetic Parameters for Complexation of Na^+ with 18C6 at 25°C.

Solvent	Anion	$k_d^{(a)}$	$E_a^{(b)}$	$\Delta H_d^\ddagger(b)$	$\Delta S_d^\ddagger(c)$	$\Delta G_d^\ddagger(b)$	Mech. ^(d)
THF	BPh_4^-	53.(6.)(g)	11.9 (0.3)	11.3 (0.3)	-12.5 (1.2)	15.1 (0.1)	II
"	SCN^-	91600.(1200.)(e)	3.36(0.3)	2.76(0.3)	-26.6 (0.8)	10.68(0.01)	I
MeOH	"	36500.(700.)	9.68(0.3)	9.08(0.3)	- 7.21(1.0)	11.23(0.02)	II
PC	BPh_4^-	130000.(7000.)(e)	4.57(0.5)	3.97(0.5)	-21.7 (1.7)	10.48(0.04)	I
$0.6X_{\text{THF}}, 0.4X_{\text{MeOH}}$	"	3560.(90.)	9.84(0.3)	9.24(0.3)	-11.3 (1.0)	12.61(0.03)	II
$0.8X_{\text{THF}}, 0.2X_{\text{PC}}$	"	915.(13.)	10.26(0.1)	9.66(0.1)	-12.6 (0.4)	13.41(0.02)	II
$0.4X_{\text{THF}}, 0.6X_{\text{PC}}$	"	50300.(2300.)(e)	9.13(0.4)	8.53(0.4)	- 8.4 (1.4)	11.04(0.03)	I
$\text{H}_2\text{O}^{(f)}$	Cl^-	3.4×10^7	-----	-----	-----	7.18	II

a_s^{-1} .

$b_{\text{kcal} \cdot \text{mol}^{-1}}$

$c_{\text{e.u.}}$

d See text for description of mechanism.

$e_{\text{M}^{-1} \cdot \text{s}^{-1}}$

f Reference 78.

g Standard deviation estimate.

Chapter 3, and these kinetic results we are now able to explain the anion influence on the kinetics of complexation of sodium ion with 18C6 in THF solutions. In the bimolecular exchange process two sodium ions must approach each other in the transition state. The contact ion pairing which exists for NaSCN and for its complex with 18C6 in THF is able to reduce the charge-charge repulsion which occurs between the Na^+ ions in the transition state. Because in THF solutions NaBPh_4 and its complex do not form contact ion pairs, the charge-charge repulsion is not offset and the dissociative mechanism is preferred.

To be more precise, it is the degree of ionic association which determines which mechanism predominates. In THF solutions sodium iodide, perchlorate, and thicyanate all are strongly ion paired. They exhibit fast exchange and in all cases the exchange proceeds by the bimolecular exchange mechanism. Although this hypothesis was not tested for NaI and NaClO_4 , it follows that in the case of NaAlEt_4 the dissociative mechanism should predominate since the degree of ion pairing of this salt is minimal (see Chapter 3). Although the salt used may contain some impurities, two solutions with different mole ratios of $[\text{Na}^+]_{\text{total}}/[\text{18C6}]_{\text{total}}$ were prepared and the ^{23}Na nmr spectra were recorded at 25°C. Since the total salt concentration was not known the value for P_A was also adjusted in the computer fit routine. The results are listed in Table 26.

Table 26. Kinetic Results for the System $\text{NaAlEt}_4 \cdot 18\text{C6}$ in THF Solutions at 25°C.

$\frac{1}{T_{2A}} \text{ (s}^{-1}\text{)}$	$\delta_A \text{ (ppm)}$	$\frac{1}{T_{2B}} \text{ (s}^{-1}\text{)}$	$\delta_B \text{ (ppm)}$	P_A^{Fit}	$\tau \times 10^3 \text{ (s)}$
352. ($\pm 10\%$)	-7.18(0.2)	619($\pm 10\%$)	-15.8(0.3)	0.182 ^(a) (± 0.004)	1.22 (± 0.04)
"	"	"	"	0.338 ^(b) (± 0.005)	2.60 (± 0.11)

^a $P_{\text{Na}^+} = 0.331$ assuming no impurities in salt.

^b $P_{\text{Na}^+} = 0.482$ assuming no impurities in salt.

The mechanism plot is shown in Figure 17. Although the accuracy of the rate data is suspect due to the suspect impurity of the NaAlEt_4 , the conclusion remains that the predominant mechanism is indeed the dissociative one as predicted above. It should be noted that the chemical shift and linewidth of the complexed NaAlEt_4 is the same, within experimental error, as that found for complexed NaBPh_4 . However, the linewidth and chemical shift of the solvated NaAlEt_4 do not agree with those of the solvated NaBPh_4 . This is likely due to impurities which affect the solvated salt but not the complexed cation. More work, however, is needed to clarify this point.

5. Results in Methanol Solutions

Table 27 lists the mean lifetime, τ , as a function of temperature for a solution in which $P_A = 0.413$ for NaSCN and 18C6 in MeOH solution. Figure 18 is the Arrhenius plot of the values. The values for several solutions at various mole ratios of $[\text{Na}^+]_{\text{total}}/[\text{18C6}]_{\text{total}}$, obtained at -5°C , are listed. To determine the exchange mechanism Figure 19 was constructed.

The intercept of the plot in Figure 19 is zero. Therefore, the primary exchange mechanism is the dissociative process as shown by Shchori et al. (25) for DB18C6, DC18C6, and analogues of DB18C6 in MeOH solutions. The kinetic parameters for our system in MeOH are listed in Tables 24,

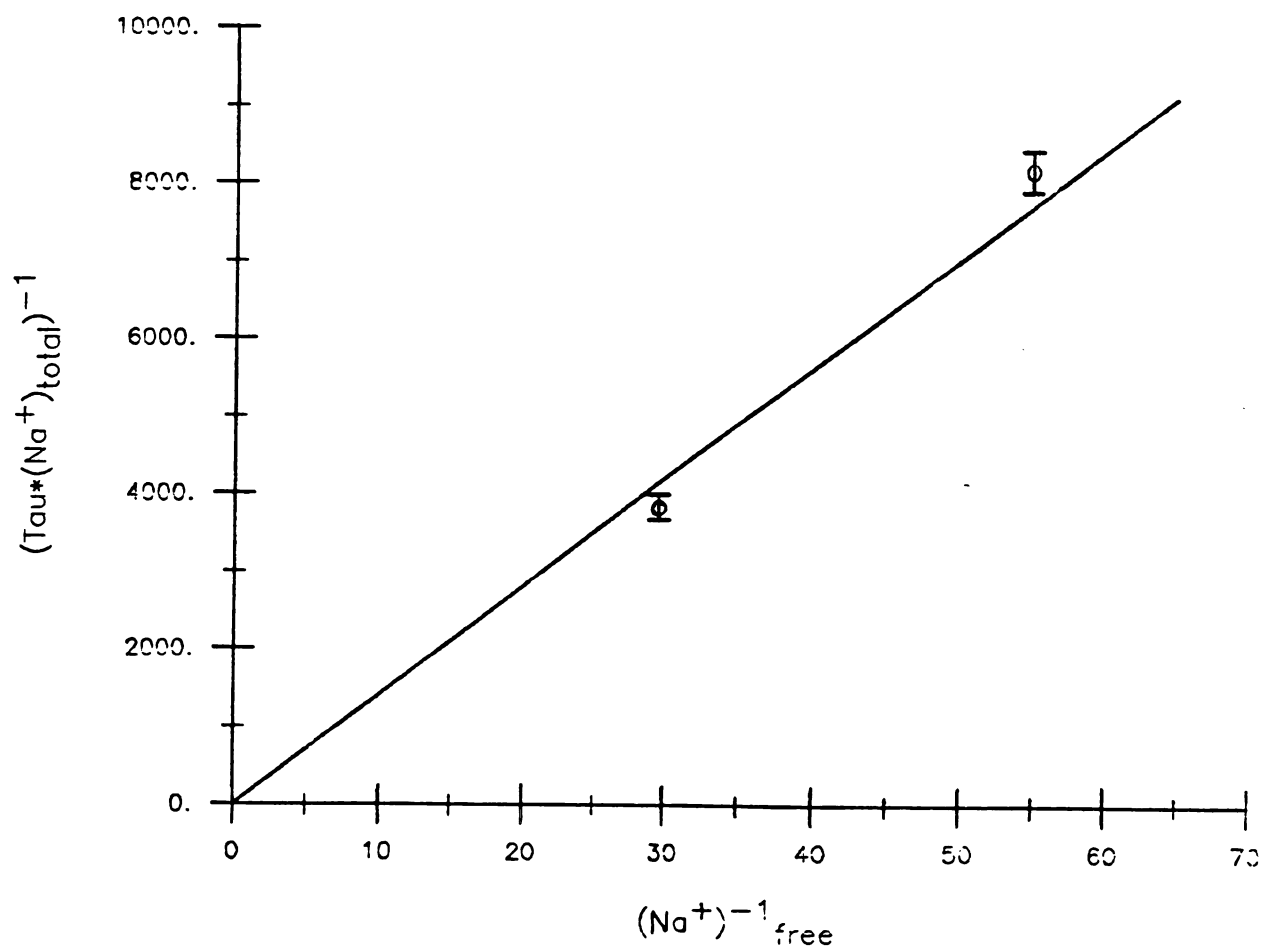


Figure 17. Plot of $1/(\tau[\text{Na}^+]_{\text{total}})$ vs the inverse of the free sodium ion concentration for $\text{NaAlEt}_4 \cdot 18\text{C6}$ in tetrahydrofuran solutions at 25°C .

Table 27. Mean Lifetimes as a Function of Temperature
for the System NaSCN·18C6 in MeOH Solutions.^a

P_{Na^+}	Temperature (°C)	$\tau \times 10^5$ (s)
0.412	31.7 (± 1)	0.831(0.18) ^(b)
"	25.3	1.13 (0.18)
"	18.7	1.36 (0.18)
"	12.0	2.44 (0.19)
"	6.0	3.65 (0.24)
"	0.4	4.83 (0.24)
"	-5.8	7.91 (0.29)
"	-10.4	9.75 (0.27)
"	-15.4	14.6 (0.03)
"	-20.0	20.3 (0.09)
0.352	-4.7	4.02 (0.49)
0.663	-4.7	8.87 (0.30)

^a0.1 M in salt.

^bStandard deviation estimate.

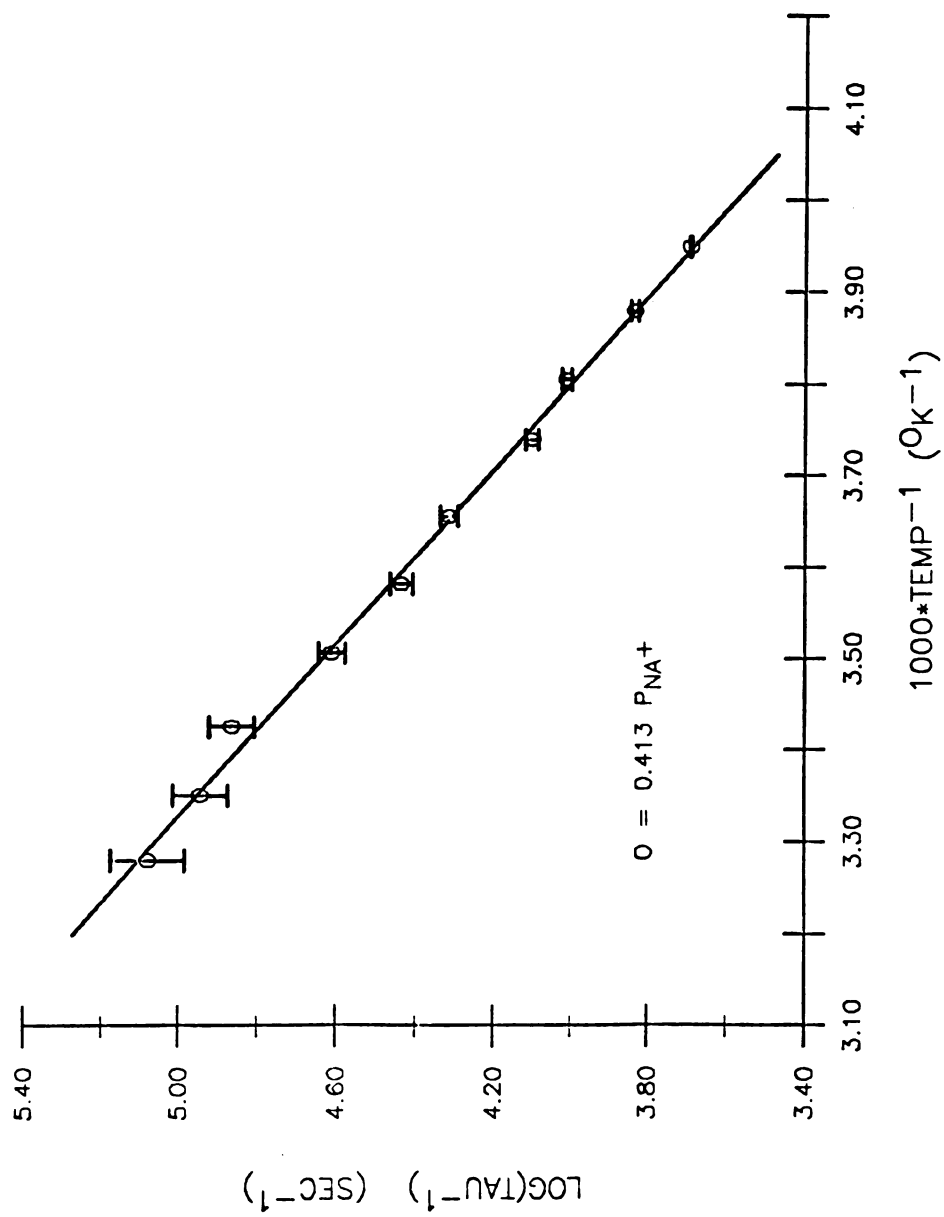


Figure 18. Semilog plot of $1/\tau$ vs. $1/T$ for $\text{NaSCN} \cdot 18\text{C6}$ in methanol solutions.

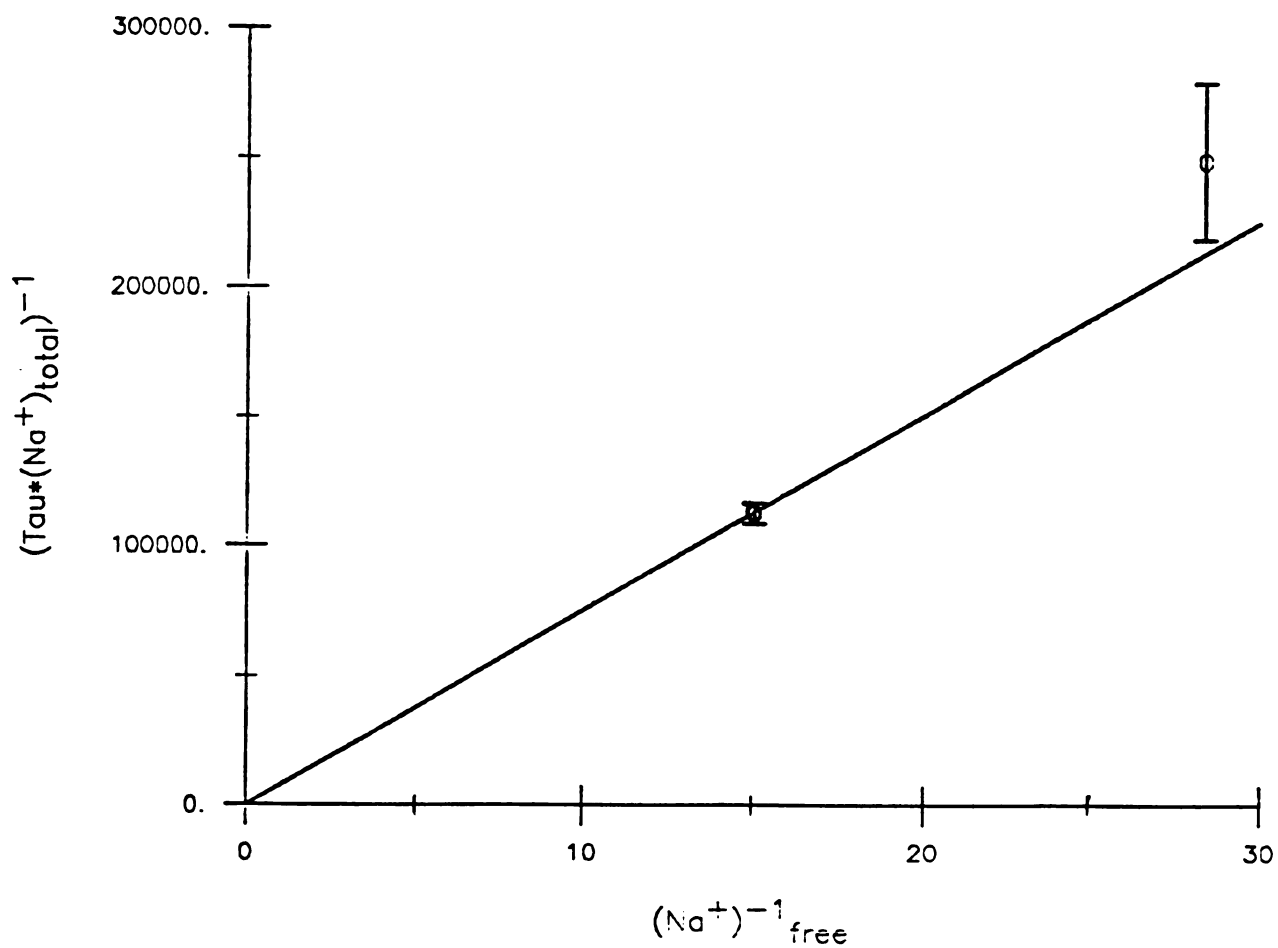


Figure 19. Plot of $1/(\tau[\text{Na}^+]_{\text{total}})$ vs. the inverse of the free sodium ion concentration for NaSCN·18C6 in methanol solutions at -4.7°C .

Table 28. Kinetic Parameters for the Complexation of NaSCN by Several Crown Ethers in MeOH Solutions at 25°C.

Crown	K_f (a)	k_2 (b)	k_{-2} (c)	E_{a-2} (d)	ΔH_{-2}^\ddagger (d)	ΔS_{-2}^\ddagger (e)	ΔG_{-2}^\ddagger (d)	ΔG_2^\ddagger (d)
18C6	21000.	7.6×10^8	3.6×10^4	9.68	9.08	-7.2	11.23	5.3
DC18C6(f)	4800.	2.6×10^8	5.2×10^4	8.3	7.7	-11.1	11.0	6.0
DB18C6(f)	23000.	3.2×10^8	1.4×10^4	11.7	11.1	-2.3	11.8	5.8

^aReference 69.

^b $M^{-1}s^{-1}$.

^c s^{-1} .

^d $kcal \cdot mol^{-1}$

^ee.u.

^fReference 25.

25, and 28 together with those of Shchori and coworkers (25) for comparison.

It is interesting to note that the trend in the magnitude of the formation constants for the 18C6 analogues in MeOH follow the trend in the dissociation rate constants, k_{-2} . If k_2 is diffusion controlled, the value of k_{-2} will determine the magnitude of the formation constant. In addition, the Arrhenius activation energies, E_a , and the enthalpies of activation, ΔH_{-2}^\ddagger , for the dissociation step, follow this same trend. However, the entropies of activation, ΔS_{-2}^\ddagger , for the dissociative mechanism follow the reverse trend and thus, the free energies of activation, ΔG_{-2}^\ddagger , are all essentially the same.

One explanation for these trends may lie in the differences in the flexibility of the crown ethers. The flexibility of these crowns most likely follows the order DB18C6 < 18C6 \leq DC18C6 where DB18C6 is the least flexible. Shchori and coworkers (25) have postulated that the main contribution to the Arrhenius activation energy (and thus, ΔH_{-2}^\ddagger) may be due to a change in the crown conformation. If this is true, it is reasonable to expect that the more flexible crown has a lower E_a and the more rigid crown has a larger E_a . This is the observed trend. In addition, if the transition states are similar, regardless of the crown ether, it is also reasonable to conclude that the more flexible crown will lose the most entropy in going to

the transition state. This is also the observed trend.

The forward rate constants and free energies of activation for DB18C6 and for DC18C6 are essentially the same. However, the forward rate constant for 18C6 is more than twice as large as for the other two crowns while the free energy of activation for the forward step is roughly ~ 0.5 kcal \cdot mol $^{-1}$ lower. The greater flexibility of 18C6 over that of DB18C6 would explain this observation. The more flexible crown ether will be able to encapsulate the ion faster.

The forward rate constant and ΔG_2^\ddagger for DC18C6 do not follow the trends described above. The rate constant is lower and the free energy barrier is higher than those of the comparably flexible crown 18C6. Assuming that the above assumptions are indeed correct, one possible explanation for this observation may lie in the structural differences of DC18C6 as compared to 18C6. The DC18C6 molecule (isomer B) has cyclohexyl rings above and below the plane of the crown cavity. These rings may result in a steric hindrance for the incoming Na $^+$ ion, thus slowing the forward rate. Further studies are needed to elucidate these effects.

6. Results in PC Solutions

Table 29 lists the τ values, at various temperatures, for the system NaBPh $_4$ \cdot 18C6 in PC solutions. Figure 20 is

Table 29. Mean Lifetimes as a Function of Temperature
for the System $\text{NaBPh}_4 \cdot 18\text{C6}$ in PC Solutions.^a

P_{Na^+}	Temperature ($^{\circ}\text{C}$)	$\tau \times 10^5$ (s)
0.505	30.5 (± 1)	3.05 (0.37) ^(b)
"	25.3	4.61 (0.40)
"	20.8	4.36 (0.37)
"	15.3	4.76 (0.38)
"	10.9	5.61 (0.39)
"	5.8	5.98 (0.36)
"	0.5	7.94 (0.49)
"	-4.6	9.86 (0.70)
"	-9.1	10.1 (0.90)
0.341	-4.6	9.9 (1.1)
0.729	-4.7	7.31 (0.86)

^a0.1 M in salt.

^bStandard deviation estimate.

an Arrhenius plot for this system. The mechanism is determined from the plot shown in Figure 21. As may be deduced from Figure 21, the predominant mechanism of exchange is the bimolecular process. The kinetic results from the PC solutions are listed in Tables 24 and 25.

It has been reported (67) that NaBPh_4 does not form contact ion pairs in PC solutions. Thus, contact ion pairing does not offset the charge-charge repulsion of the sodium ions in the transition state in this system. Apparently, the high dielectric constant of PC ($D = 65.0$) is able to reduce this charge-charge repulsion and allow the bimolecular process to be favored. If this explanation is correct, then it remains to be explained why the exchange proceeds via the dissociative process in DMF (10,25) and in aqueous (78) solutions, both solvents having high dielectric constants of 36.7 and 78.5 respectively.

7. Comparison of Results in Neat Solvents

Whenever the dissociative process is predominant, there is a large solvent influence on the kinetic parameters for the complexation of sodium ion with 18C6, as may be seen in Table 25. The free energy of activation, ΔG_{-2}^\ddagger , varies from $15.1 \text{ kcal}\cdot\text{mol}^{-1}$ in THF to $7.2 \text{ kcal}\cdot\text{mol}^{-1}$ in aqueous solutions. Other kinetic parameters (E_a , ΔH_{-2}^\ddagger , ΔS_{-2}^\ddagger , and k_{-2}) show equally impressive solvent dependence.

However, in those systems in which the bimolecular

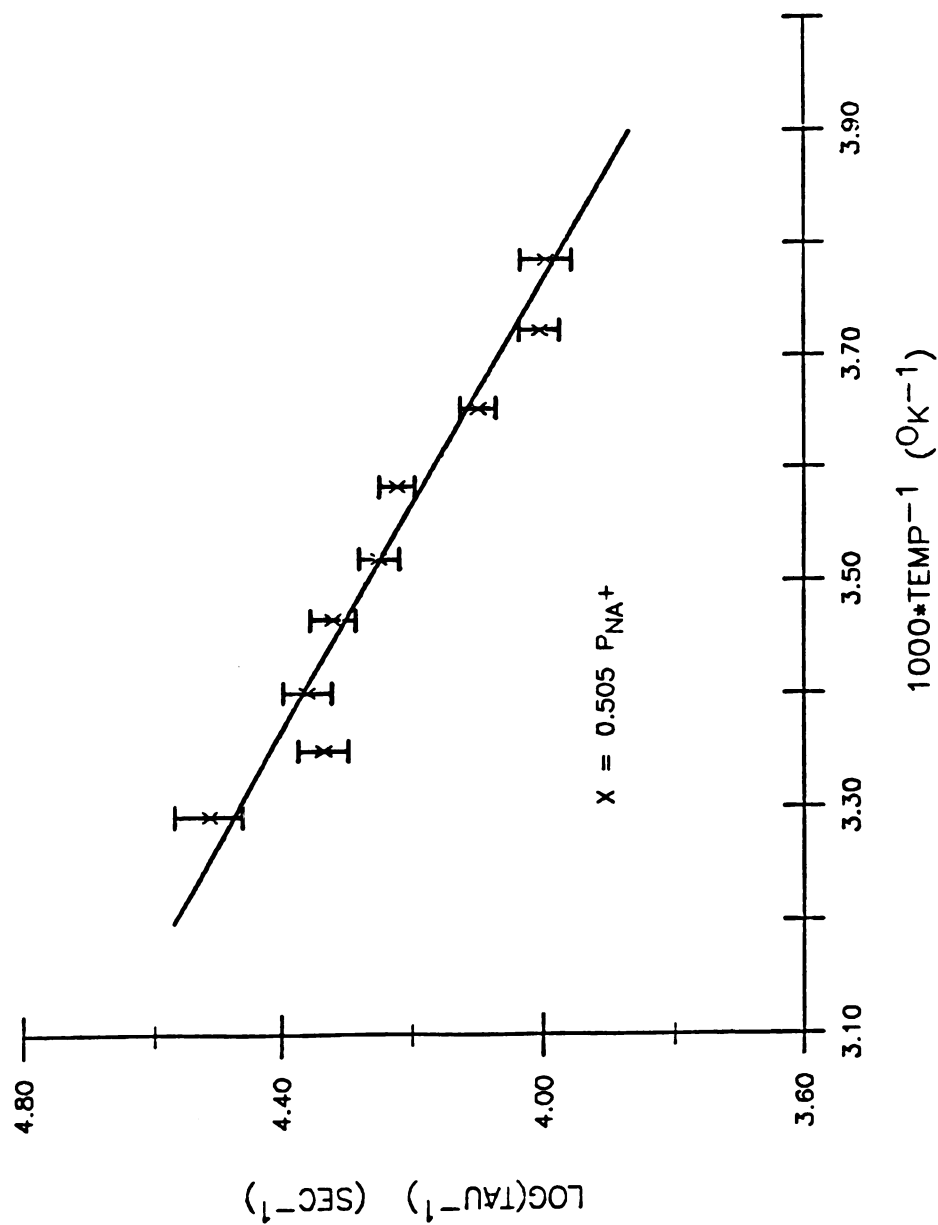


Figure 20. Semilog plot of $1/(\tau[\text{Na}^+]_{\text{total}})$ vs. $1/T$ for $\text{NaBPh}_4 \cdot 18\text{C}6$ in propylene carbonate solutions.

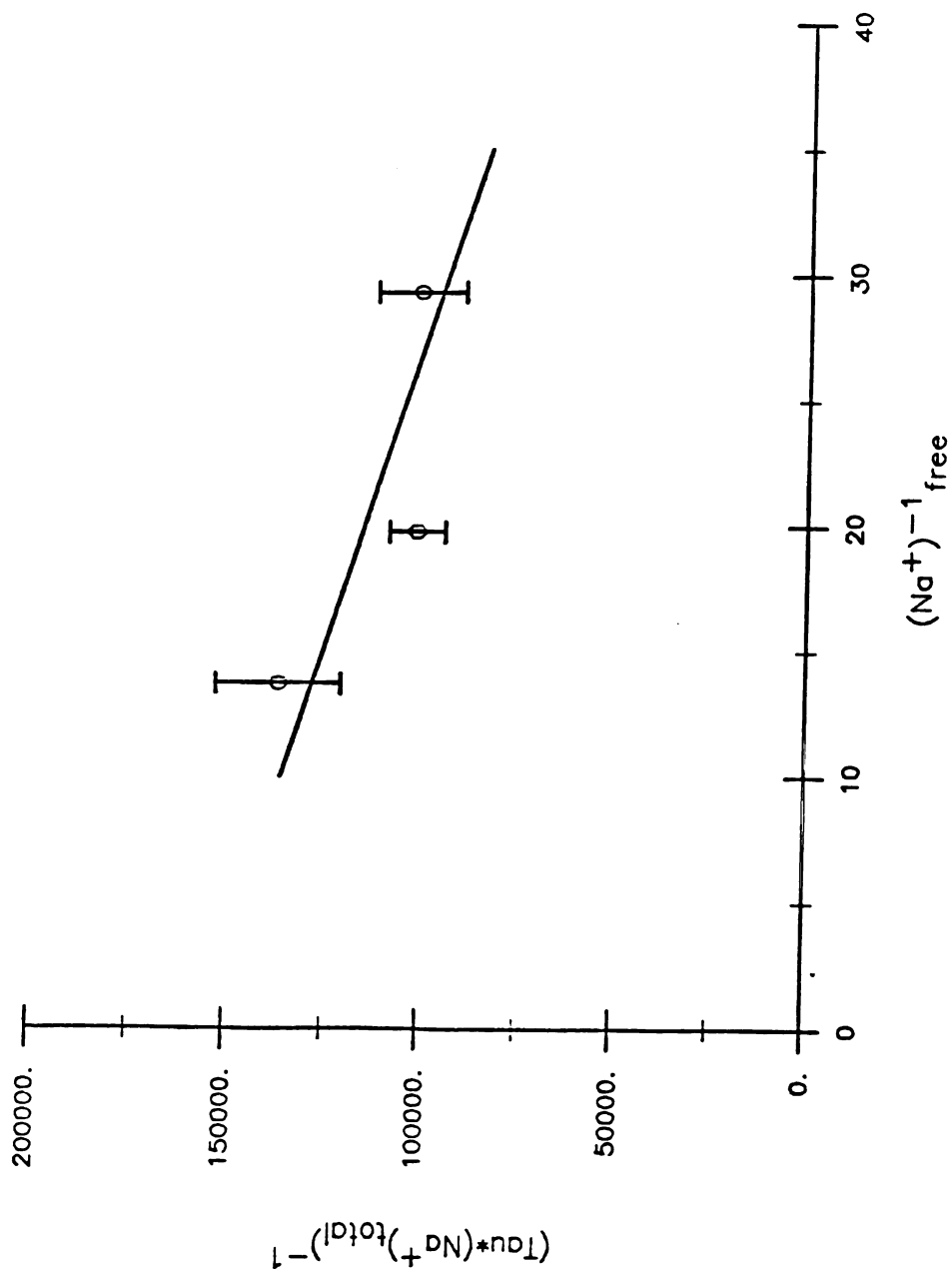
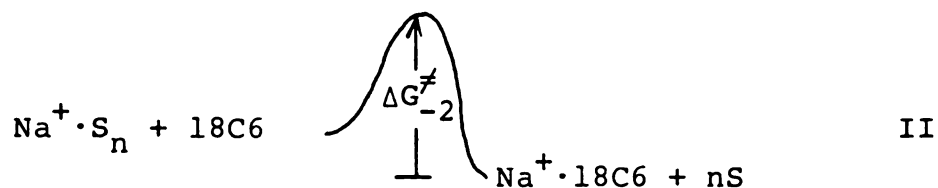


Figure 21. Plot of $1/(\tau[\text{Na}^+]_{\text{total}})^{-1}$ vs. the inverse of the free sodium ion concentration for $\text{NaBPh}_4 \cdot 18\text{C}_6$ in propylene carbonate solutions of -4.7°C .

exchange mechanism is predominant, the free energies of activation are essentially solvent independent. In both cases the free energies of activation are $\sim 10.7 \text{ kcal} \cdot \text{mol}^{-1}$. There are differences in their activation energies and enthalpies. Schmidt and Popov (27) have also found that when the bimolecular mechanism predominates for K^+ ion complexation with 18C6 in most solvents studied the free energies of activation are very similar. They found, however, a large dependence of E_a on the solvent system. The activation entropy compensates this change in activation energy to give essentially the same free energy of activation regardless of solvent. The results are rationalized in terms of the solvation of K^+ ion in the transition state. Large ΔH_1^\ddagger values are assumed to indicate weak solvation in the transition state. Since the solvation is weak, the ions cannot approach each other closely due to charge-charge repulsion. Therefore, ΔS_1^\ddagger is more positive in weak solvating solvents since the crown has more room to "breathe". In better solvating solvents, the ions may approach each other more closely in the transition state with the result of a lower activation energy and higher activation entropy. The same conclusions may indeed apply to our results. It is difficult, however, to say that the Na^+ ion is more strongly solvated in the transition state of the system $\text{NaSCN} \cdot 18\text{C6}$ in THF solutions as compared to the PC results due to the strong ion pairing that occurs in THF solutions.

Cox and coworkers (79) observed a linear relationship between $\log(k_{-2})$ and the Gutmann donor number of the solvent for K^+ -cryptate dissociation. Sodium-23 chemical shifts were found to be even more correlated with the donor number than ^{39}K chemical shifts (61,80). Therefore, a plot of $\log(k_{-2})$ vs. solvent donor number was prepared for those systems in which the predominant mechanism of exchange is the dissociative one. Such a plot is shown in Figure 22. As may be seen the correlation is very good. Since $\log(k_{-2}) \propto \Delta G_{-2}^\ddagger$ according to the transition state theory, a plot of ΔG_{-2}^\ddagger vs. donor number was also expected to correlate well and is shown in Figure 23. The correlation between ΔG_{-2}^\ddagger and solvent donor number may be explained as follows:

The free energy profile for the reactions may be expressed as shown below:



where S = solvent

In the dissociative mechanism, there is a net change in the number of solvent molecules in going from reactants to

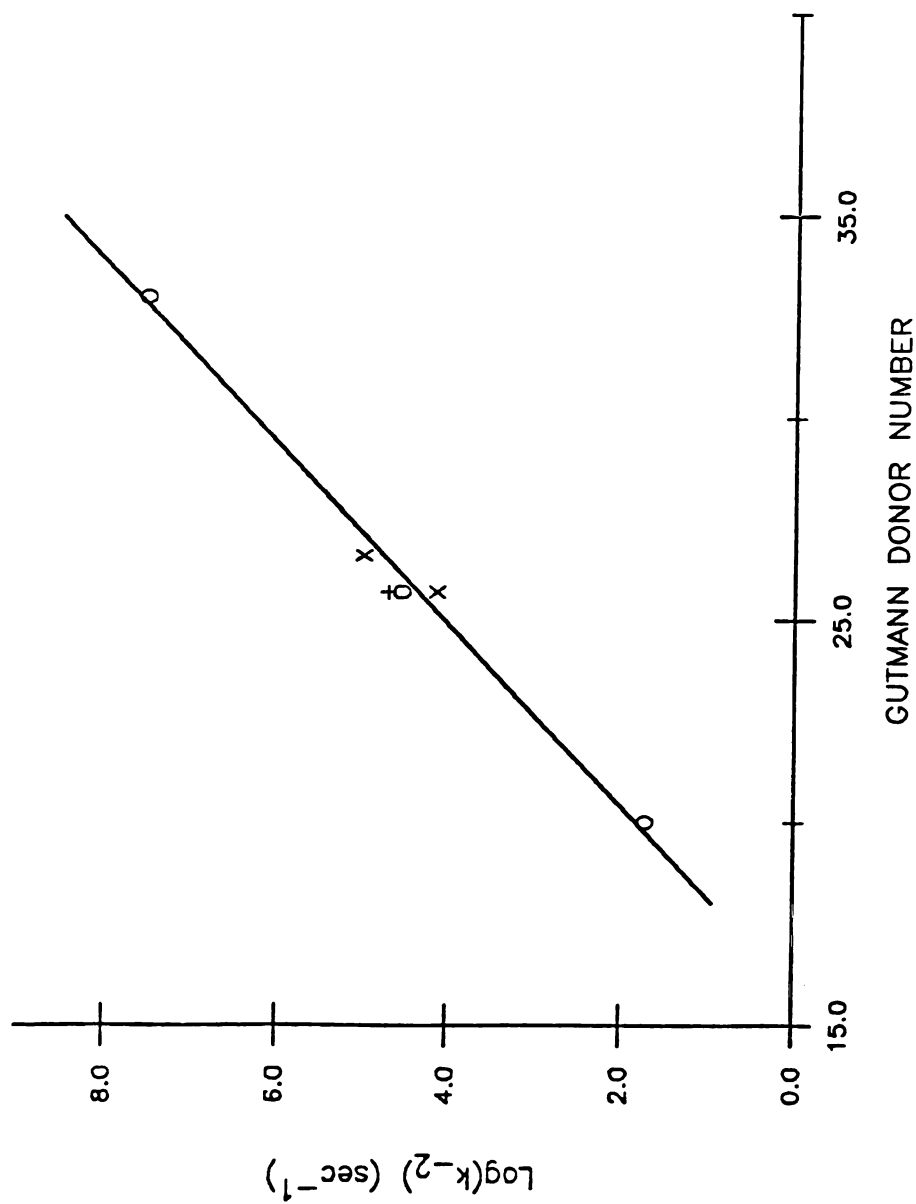


Figure 22. Semilog plot of k_{-2} vs Gutmann donor number for Na^+ -crown in various solvents. (o) 18C6; (x) DB18C6; (+) DC18C6 (References 10, 25, 78).

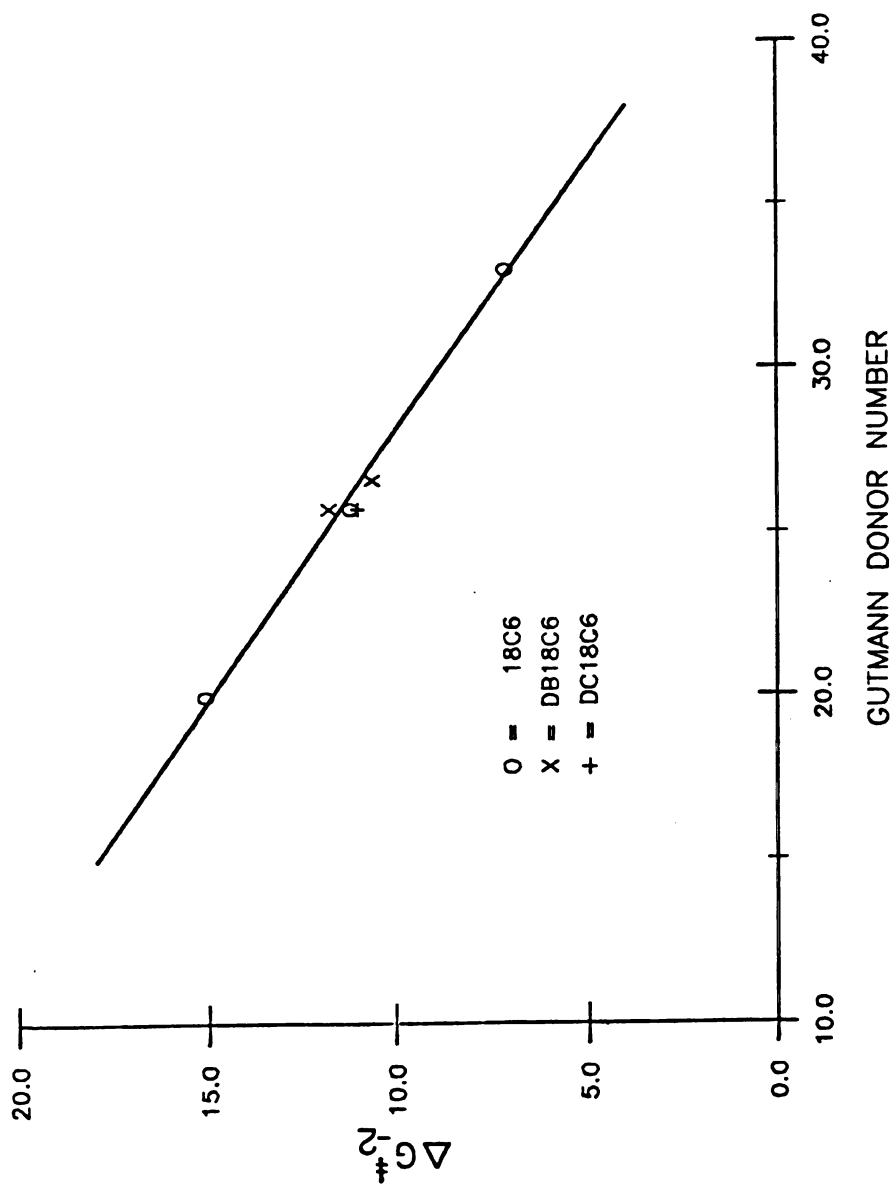
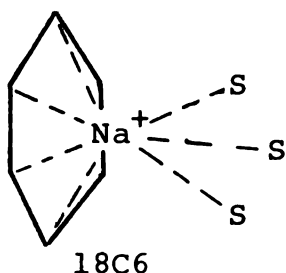


Figure 23. Plot of ΔG^\ddagger_2 vs. Gutmann donor number for Na^+ crown in various solvents. (○) 18C6; (×) DB18C6; (+) DC18C6 (References 10, 25, 78).

products. However, there is no net change in solvent molecules in the bimolecular exchange process. Thus, when the dissociative mechanism occurs, one must consider the solvent as an active participant. Certainly, the solvating ability of the solvent must influence ΔG_{-2}^\ddagger since in the transition state of the dissociative mechanism we have:



A strongly solvating solvent (high donor number) will compete better with the crown ether and thus, reduce ΔG_{-2}^\ddagger .

In contrast, one would not expect the solvent to have a large influence on the free energy barrier when the bimolecular exchange mechanism is predominant. This is what has been observed by Schmidt and Popov (27) and by ourselves. Although the solvent does not appear to influence ΔG_1^\ddagger , there is certainly a solvent dependence of ΔH_1^\ddagger and of ΔS_1^\ddagger as discussed above.

Although one would not expect such good correlation between ΔG_{-2}^\ddagger and donor number in all solvents, the trend does allow us to make reasonable conclusions concerning these systems.

According to Figure 23, if the dissociative mechanism were to occur in PC solutions, the free energy barrier would be $\sim 18 \text{ kcal} \cdot \text{mol}^{-1}$ (DN = 15.). This would be the largest ΔG_{-2}^{\ddagger} value observed for a crown ether-alkali metal ion complex. The high dielectric constant tends to favor the bimolecular process, thus bypassing the need to proceed through such a high free energy barrier.

Water has a much higher donor number (DN = 33.) and thus, a lower ΔG_{-2}^{\ddagger} for the dissociative process. Therefore, the predominant mechanism is the dissociative process in this solvent even though the high dielectric constant of water will support the bimolecular exchange mechanism.

If we assume that ion pairing is negligible, predictions concerning the predominant mechanism in a given solvent may be made on the basis of the trends discussed above. The predominant mechanism will be the dissociative one in solvents which have both high donor numbers and high dielectric constants. The predominant mechanism will be the bimolecular process in solvents which have low donor numbers but high dielectric constants. In solutions of either low donor number and low dielectric or high donor number and low dielectric constant the mechanism will likely be determined by whether or not ion pairing occurs. Tetrahydrofuran solutions with either NaBPh_4 or NaSCN salts exchanging with 18C6 are examples of this last case.

8. Results in MeOH-THF Mixture

Table 30 lists the mean lifetime values as a function of temperature in a mixture containing 60-40 mole % THF-MeOH. The Arrhenius plot for this system is shown in Figure 24. As may be seen in Figure 25, the predominant exchange mechanism is the dissociative process. This was also the mechanism observed in both neat solvents of which the mixture is composed.

All kinetic parameters for exchange in this mixture lie between those found in the neat solvents. However, the activation energy is closer to that found in neat MeOH solutions while the activation entropy is nearer to the value found in neat THF solutions.

The composition of the MeOH-THF mixture is that which occurs at the isosolvation point (Chapter 3). Since the sodium-23 chemical shift has been found to correlate well with the Gutmann donor number of the solvent (61), it is reasonable to predict that the donor number for this mixture lies midway between the donor numbers of the neat solvents. Thus, the approximate donor number of this MeOH-THF mixture is $(1/2)(DN_{\text{THF}} + DN_{\text{MeOH}}) = 22.8$. Figure 26 is a plot of ΔG_{-2}^\ddagger vs. donor number, as shown in Figure 23, but with the result for the MeOH-THF mixture included. The correlation remains quite good.

This result suggests two important points. First, it strengthens the belief that ΔG_{-2}^\ddagger is very dependent on the

Table 30. Mean Lifetimes as a Function of Temperature for the System $\text{NaBPh}_4 \cdot 18\text{C6}$ in a 60-40 Mole % THF-MeOH Mixture.^a

P_{Na^+}	T (°C)	$\tau \times 10^4$ (s)
0.477	31.8 (± 1)	0.948(0.027) ^(b)
"	25.3	1.24 (0.07)
"	19.7	1.91 (0.04)
"	14.0	2.42 (0.01)
"	9.4	3.23 (0.09)
"	4.0	4.84 (0.13)
"	-0.4	6.42 (0.095)
"	-5.9	9.15 (0.18)
0.744	25.3	2.61 (0.20)

^a0.1 M in salt.

^bStandard deviation estimate.

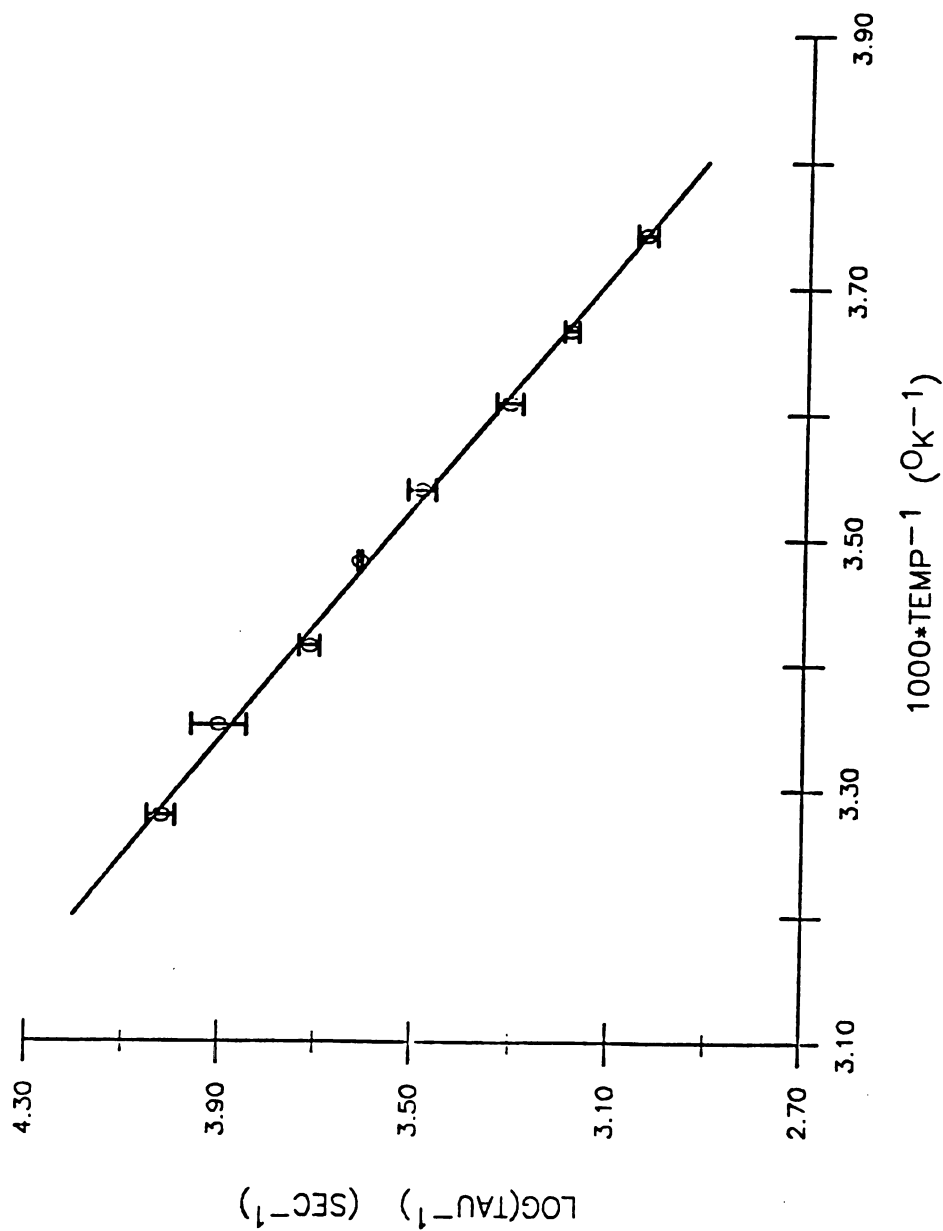


Figure 24. Semilog plot of $1/\tau$ vs. $1/T$ for $[\text{NaBPh}_4]/[\text{18C6}] = 1.91$ in a 40-60 mole % MeOH-THF mixture.

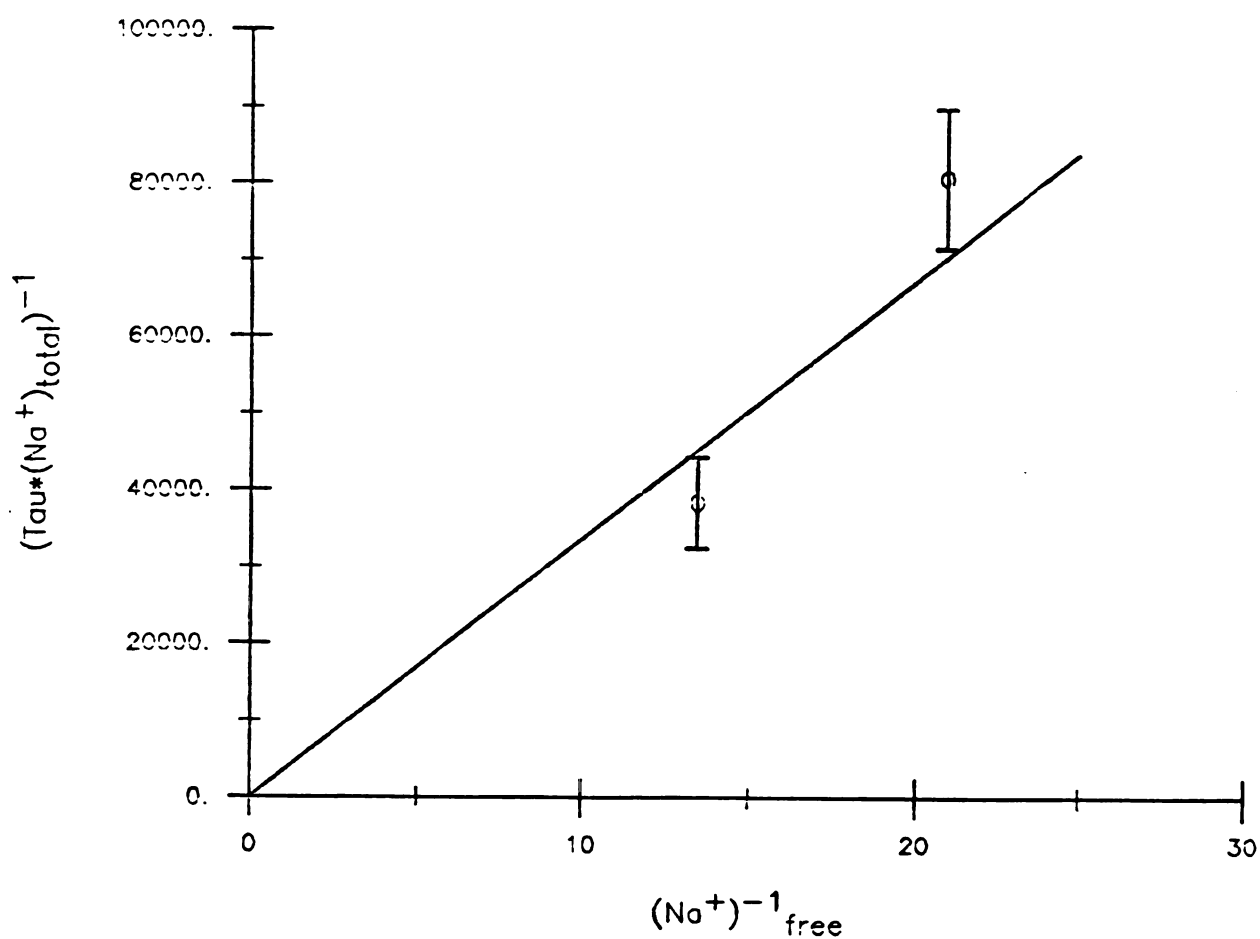


Figure 25. Plot of $1/(\tau[\text{Na}^+]_{\text{total}})$ vs. the inverse of the free sodium ion concentration for $\text{NaBPh}_4 \cdot 18\text{C6}$ in a 40-60 mole % MeOH-THF mixture at 25°C.

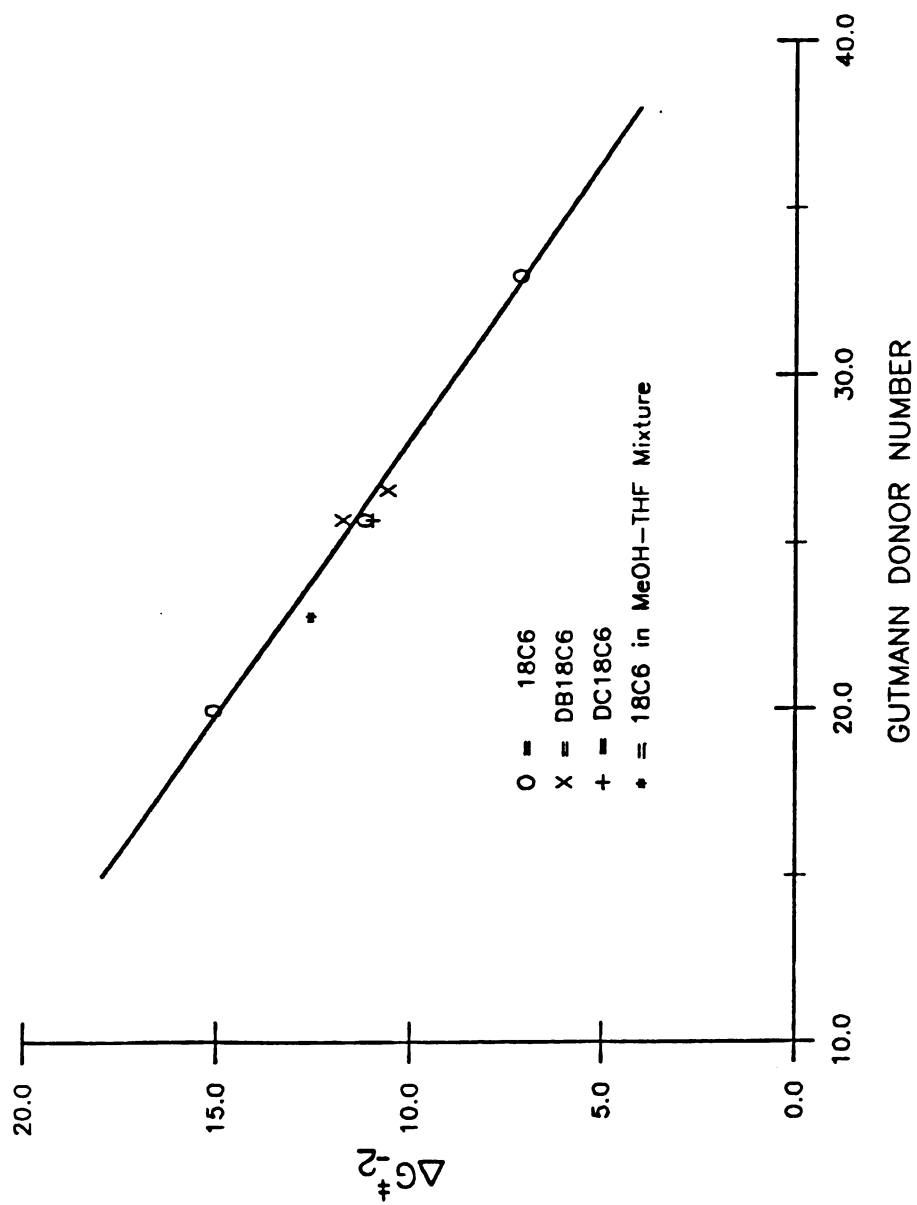


Figure 26. Plot of ΔG^+_2 vs Gutmann donor number for $\text{Na}^+\cdot\text{crown}$ in various solvents (references 10, 25, 78).

solvating ability of a solvent as expressed by the Gutmann donor number. Secondly, and perhaps just as important, it strengthens the concept of isosolvation. We are able to calculate the approximate solvent donor number of the mixture based on the isosolvation curve.

9. Results in PC-THF Mixtures

Tables 31 and 32 list mean lifetimes as a function of temperature for $\text{NaBPh}_4 \cdot 18\text{C6}$ in PC-THF mixtures (20-80 mole % PC-THF and 60-40 mole % PC-THF solutions). Figures 27 and 28 are Arrhenius plots for these systems. The predominant exchange mechanisms are determined from Figures 29 and 30.

Results presented earlier in this chapter have shown that in THF solutions the primary exchange process is the dissociative one when NaBPh_4 is the salt. In PC solutions, the predominant exchange mechanism is the bimolecular process. As may be deduced from Figures 29 and 30, the predominant one is determined by the larger solvent component of the mixture. In the 20-80 mole % PC-THF mixture the predominant exchange process is the dissociative one as is found in neat THF solutions. In the 60-40 mole % PC-THF mixture the predominant exchange mechanism is the bimolecular process as is found in neat PC solutions.

It was concluded from the study of sodium ion complexation kinetics with 18C6 in the neat solvents that high dielectric constant, low donor number solvents will tend

Table 31. Mean Lifetimes as a Function of Temperature
for the System $\text{NaBPh}_4 \cdot 18\text{C6}$ in a 20-80 Mole %
PC-THF Mixture.^a

P_{Na^+}	T (°C)	$\tau \times 10^4$ (s)
0.283	40.8 (± 1)	1.57 (0.04) ^(b)
"	33.1	1.95 (0.04)
"	25.4	3.43 (0.05)
"	18.9	4.41 (0.08)
"	11.2	6.57 (0.14)
"	4.0	10.1 (0.40)
"	-2.2	15.5 (0.7)
"	-9.5	23.4 (1.3)
0.415	40.8	1.82 (0.04)
"	32.9	2.77 (0.03)
"	25.3	4.64 (0.06)
"	18.9	6.62 (0.10)
"	11.2	10.1 (0.2)
"	3.9	16.2 (3.8)
"	-2.2	24.8 (0.9)
"	-9.6	46.9 (2.0)
0.646	40.8	2.99 (0.04)
"	33.0	5.01 (0.15)
"	25.3	6.65 (0.16)
"	18.9	9.03 (0.13)
"	11.3	14.1 (0.3)
"	4.0	24.0 (0.7)
"	-4.8	45.5 (2.0)
"	-12.5	99.5 (7.8)

^a0.1 M in salt.

^bStandard deviation estimate.

Table 32. Mean Lifetimes as a Function of Temperature for the System $\text{NaBPh}_4 \cdot 18\text{C6}$ in a 60-40 Mole % PC-THF Mixture.^a

P_{Na^+}	T (°C)	$\tau \times 10^4$ (s)
0.270	32.0 (± 1)	0.666(0.032) ^(b)
"	24.8	1.07 (0.03)
"	16.4	1.28 (0.05)
"	9.5	1.87 (0.03)
"	1.0	3.33 (0.07)
"	-8.5	6.43 (0.15)
0.406	32.4	0.723(0.04)
"	25.2	1.05 (0.04)
"	20.1	1.19 (0.03)
"	13.0	1.65 (0.02)
"	6.2	2.43 (0.03)
"	0.2	3.57 (0.06)
"	-6.8	6.83 (0.18)
"	-12.2	11.7 (0.3)
0.663	32.0	0.996(0.02)
"	24.7	1.17 (0.04)
"	20.6	1.41 (0.04)
"	14.6	1.57 (0.05)
"	4.4	3.38 (0.04)
"	-5.9	8.60 (0.13)

^a0.1 M in salt.

^bStandard deviation estimate.

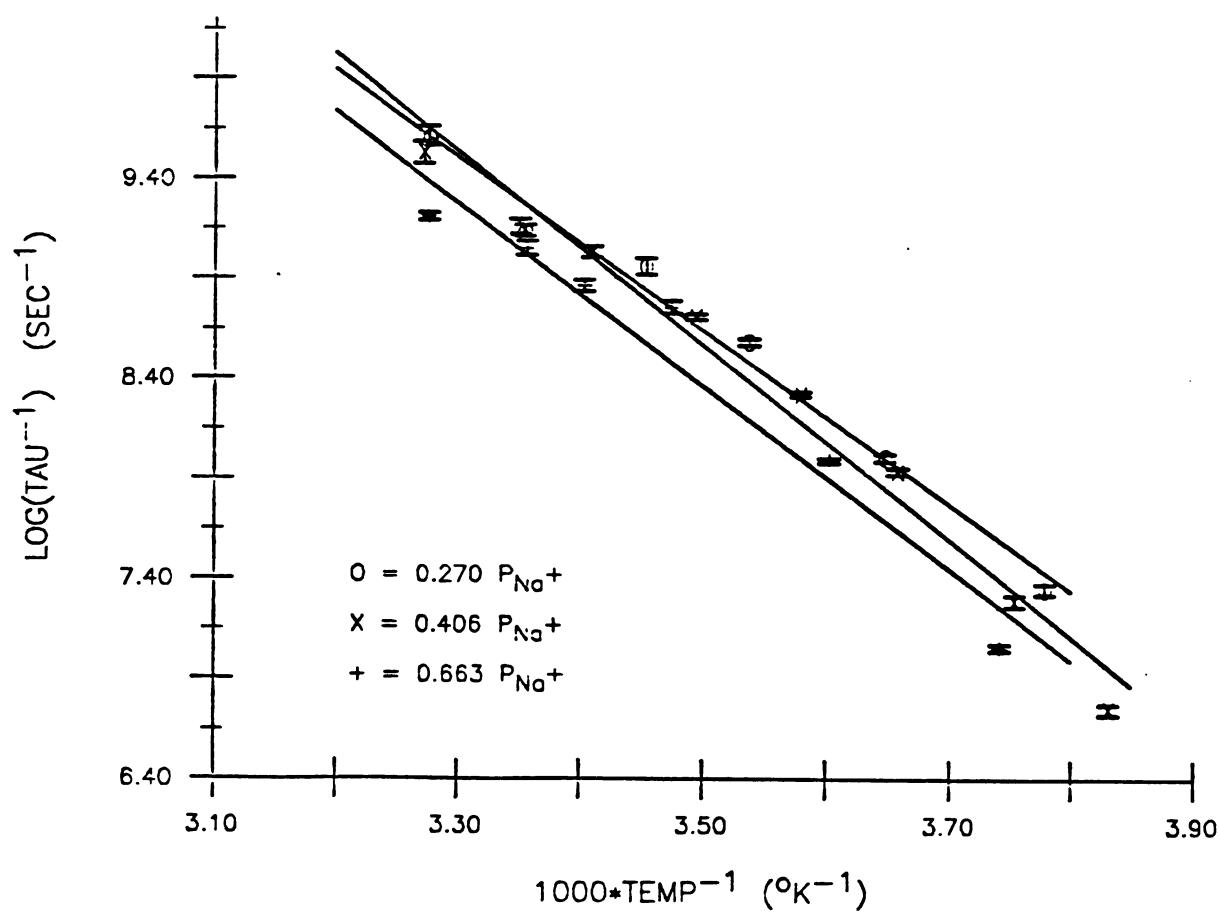


Figure 27. Semilog plots of $1/\tau$ vs $1/T$ for $\text{NaBPh}_4 \cdot 18\text{C6}$ in 60-40 mole % PC-THF solutions.

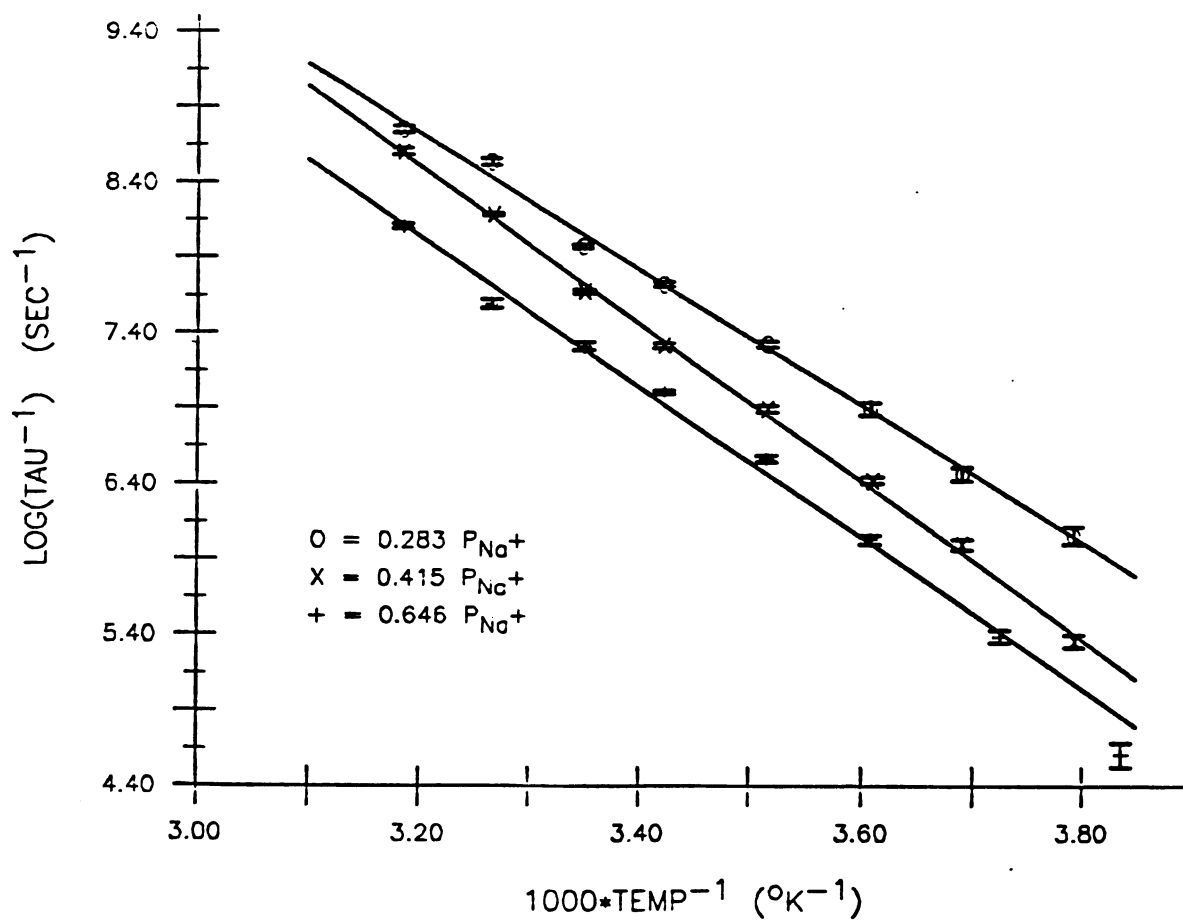


Figure 28. Semilog plots of $1/\tau$ vs. $1/T$ for $NaBPh_4 \cdot 18C6$ in 20-80 mole % PC-THF solutions.

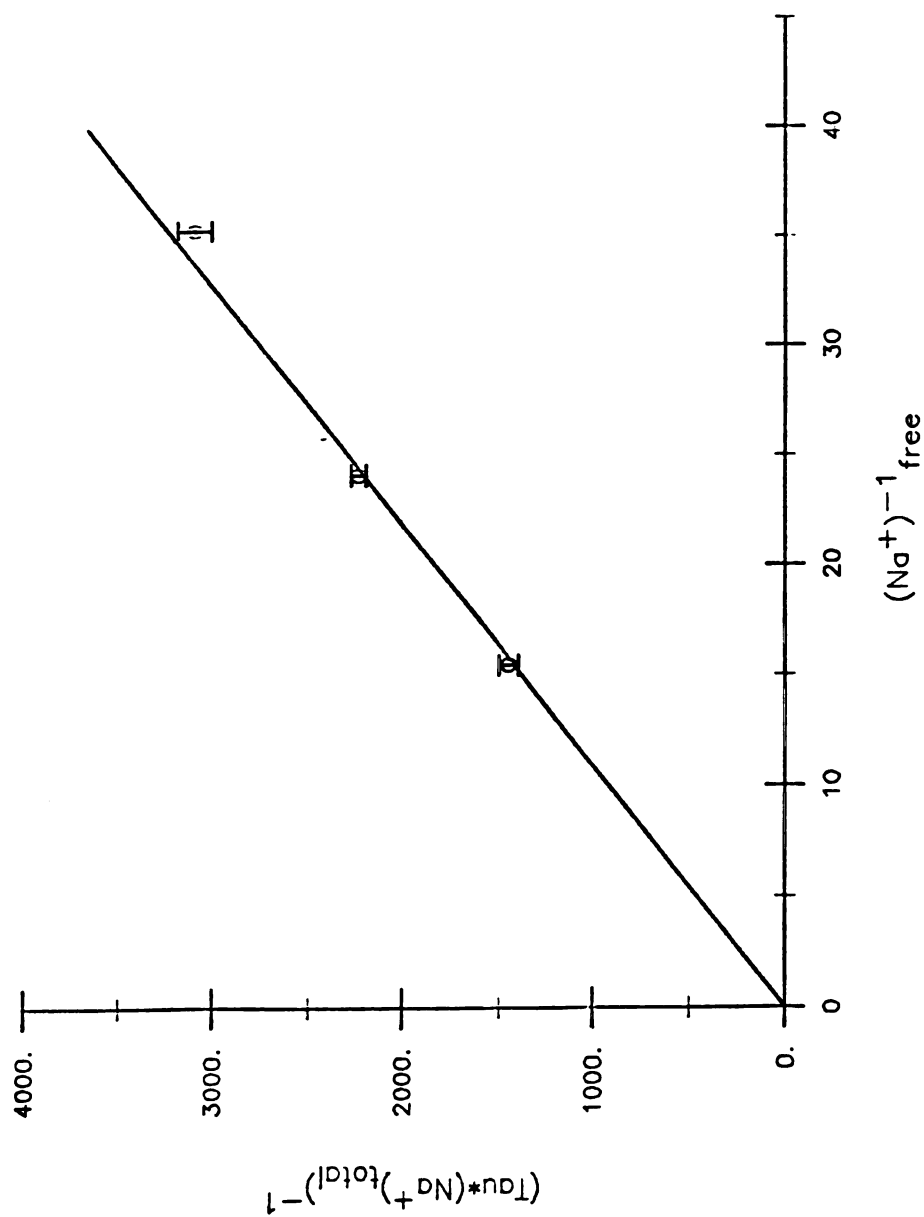


Figure 29. Plot of $1/(\tau[Na^+]_{total})$ vs. the inverse free sodium ion concentration for $NaBPh_4 \cdot 18C6$ in 20-80 mole % PC-THF mixtures at 25°C.

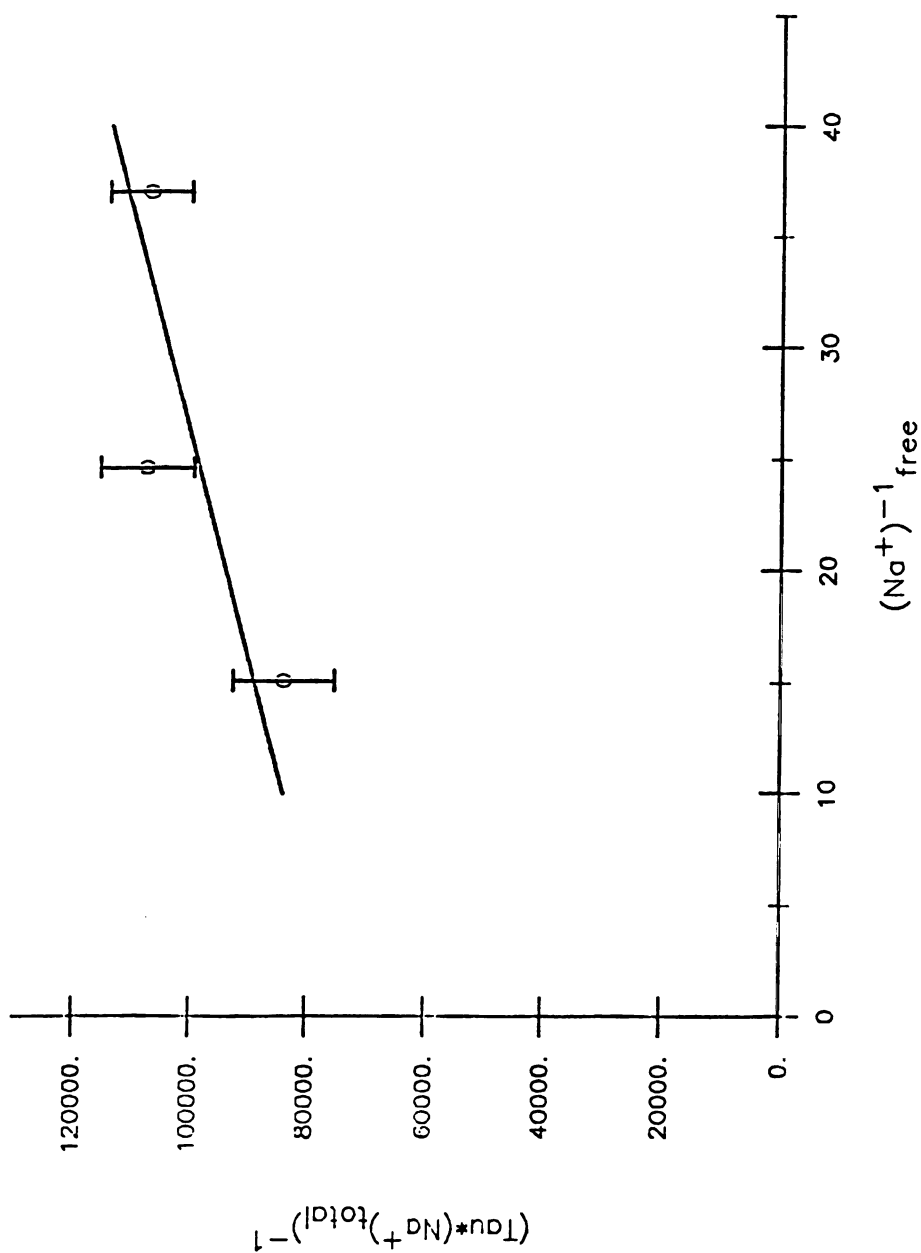


Figure 30. Plot of $1/(\tau[\text{Na}^+]_{\text{total}})$ vs. $(\text{Na}^+)^{-1}_{\text{free}}$ for $\text{NaBPh}_4 \cdot 18\text{C}6$ in 60-40 mole % PC-THF mixtures at 25°C .

to favor the bimolecular process. As the PC composition of the mixture with THF is increased the dielectric constant most likely is increased. In addition, it is reasonable that the donor number of the mixture is decreasing upon increasing PC composition. Therefore, as observed in solutions with higher PC concentrations, the bimolecular process should predominate.

It is interesting to note that in the 60-40 mole % PC-THF solution the free energy of activation for the bimolecular process is essentially the same as those found in all other systems in which the bimolecular process predominates, i.e., ~ 11 kcal \cdot mol $^{-1}$. Thus, the free energy barrier for this mechanism appears to be independent of solvent.

The Arrhenius activation energy in the 60-40 mole % PC-THF mixture is the largest observed for sodium ion complexation with 18C6 when the bimolecular exchange process predominates. The activation entropy for this system is the most positive observed for this mechanism thus far.

It seems unusual that while exchange proceeds via the dissociative process in the 20-80 mole % PC-THF mixture, the free energy barrier is lower than that found in the neat THF. This was unexpected since the donor number of this mixture is likely to be lower than that of THF. Thus, according to the model presented above, the free energy barrier should be larger. However, the isosolvation curve

for PC-THF mixtures is not typical (Chapter 3). It is possible that ion pairing or some other unexplained interactions occur at high THF compositions. Thus, this particular mixture may not be a good test of the model for the dissociative mechanism discussed above.

CHAPTER 5

COMPLEXATION KINETICS OF CESIUM ION WITH DB21C7 and WITH DB24C8

Introduction

The use of nmr techniques have greatly advanced the field of complexation kinetics. The exchange of metal ions between solvated and complexed sites influences the nmr spectrum of the ion nucleus. Through application of appropriate exchange equations one may extract the mean lifetime, τ , of the ion from the nmr spectrum (see Chapter 4). Since τ is related to the rate constant for the exchange process one may then calculate this value.

Unfortunately, a problem arises in that many researchers tend to assume rather than demonstrate an exchange mechanism. Since knowledge of the mechanism is obviously important in the overall study of complexation kinetics this practice should be discouraged.

The usefulness of determining the mechanism of exchange is illustrated well by the results in Chapter 4. Had the mechanism been assumed to be the dissociative process in all systems investigated, the interpretation of the data would have been considerably in error.

Recently, Shamsipur (30) investigated the complexation kinetics of cesium ion with several large crown ethers in acetone and in methanol solutions. The assumption was made that exchange proceeded via the dissociative process in all systems examined. Since both K^+ ion (27) and Na^+

ion (Chapter 4) have been observed to exchange by way of the bimolecular mechanism, it is important to determine which process does indeed predominate for the large Cs^+ cation. Such information may also provide clues as to how the cation size affects which exchange process occurs.

Thus, it is the goal of the work presented in this chapter to discern which mechanism is predominant for cesium ion-crown ether complexation kinetics as investigated by Shamsipur (30). Specifically, the systems $\text{CsSCN}\cdot\text{DB21C7}$ and $\text{CsSCN}\cdot\text{DB24C8}$ have been studied in acetone and in methanol solutions.

Results and Discussion

A full cesium-133 lineshape analysis has been used to obtain all kinetic information presented in this chapter. Since a complete discussion of this technique has been presented in Chapter 4, only a discussion of the final results will follow.

A. Measurements in the Absence of Exchange.

Cesium-133 nmr chemical shifts and inverse spin-spin relaxation times for solutions containing solvated CsSCN and for solutions in which the ratio $(\text{crown})/(\text{CsSCN}) > 1$ in acetone and in methanol, where the crown ether is either DB21C7 or DB24C8 , are reported in Tables 33 and 34. Figures 31 and 32 are plots of $\log(1/T_2)$ vs. inverse

Table 33. Cesium-133 Chemical Shifts and Relaxation Rates of CsSCN and of its Complexes with DB21C7 and with DB24C8 in MeOH Solutions.^a

T (°C)	0.02 M CsSCN	
	$1/T_2$ (s ⁻¹)	δ (ppm)
25.5 (±1.)	7.5 (±10%)	-43.68 (±0.02)
-50.4	6.3	-30.01
-60.1	8.5	-28.40
-70.3	11.0	-26.61
-80.0	10.7	-24.92
-88.9	15.4	-23.54
0.015 M CsSCN, 0.016 M DB24C8		
24.7	7.5	-36.18
-29.8	22.9	-32.49
-40.5	29.5	-32.29
-50.6	38.9	-32.35
-60.3	43.7	-32.49
-70.4	51.2	-32.79
-82.7	87.0	-33.24

Table 33. Continued.

T (°C)	0.021 <u>M</u> CsSCN, 0.023 <u>M</u> DB21C7	
	$1/T_2$ (s ⁻¹)	δ (ppm)
25.5 ($\pm 1.$)	9.4 ($\pm 10\%$)	-18.70 (± 0.02)
-19.6	26.1	-12.98
-31.2	33.3	-11.79
-44.3	78.5	-10.48
-55.9	69.7	- 9.33
-67.7	62.2	- 8.39
-80.2	92.4	- 7.58

^aRef. to infinitely dilute aqueous Cs⁺.

Table 34. Cesium-133 Chemical Shifts and Relaxation Rates of CsSCN and of its Complexes with DB21C7 and with DB24C8 in AC solutions.^a

T (°C)	0.02 M CsSCN	
	$1/T_2$ (s ⁻¹)	δ (ppm)
25.3 (±1.)	8.5 (±10%)	-14.10 (±0.02)
-17.2	10.7	- 8.56
-28.2	8.8	- 6.94
-38.9	9.1	- 5.37
-49.8	10.4	- 3.73
-60.4	10.0	- 2.09
-72.4	10.7	- 0.16
	0.02 M CsSCN, 0.022 M DB24C8	
	$1/T_2$ (s ⁻¹)	δ (ppm)
25.1	6.9	-26.62
-17.3	10.7	-25.53
-29.2	13.8	-25.16
-38.9	20.4	-24.89
-49.9	22.0	-24.59
-60.0	20.1	-24.23
-72.7	22.3	-23.74
	0.02 M CsSCN, 0.024 M DB21C7	
	$1/T_2$ (s ⁻¹)	δ (ppm)
25.1	7.8	- 5.93
-17.2	27.0	- 2.10
-28.1	53.7	- 1.15
-38.9	94.9	0.09
-49.5	94.2	1.49
-60.5	60.3	2.65
-72.9	54.0	3.74

^aRef. to infinitely dilute aqueous Cs⁺.

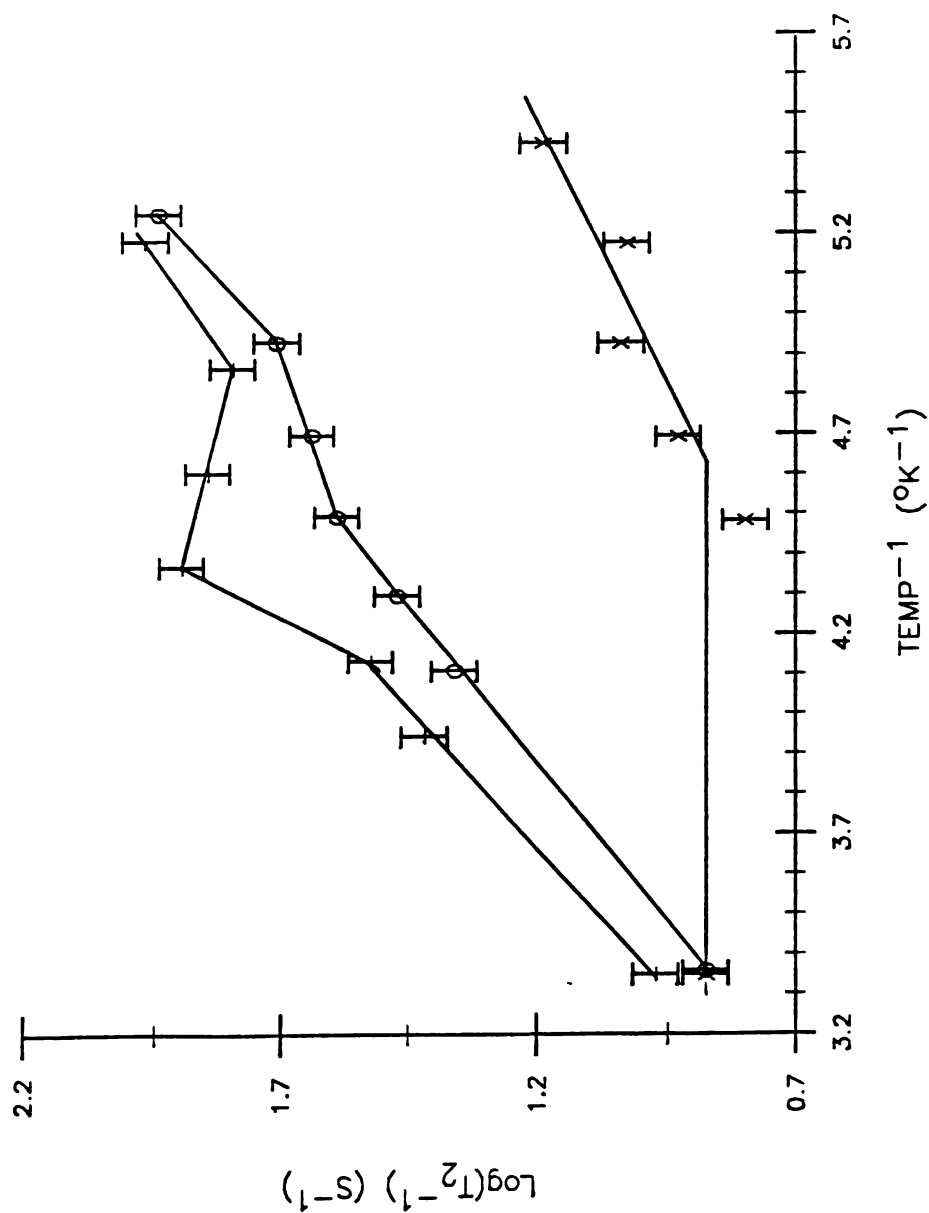


Figure 31. Semilog plots of $1/T_2$ vs. $1/T$ for solvated and complexed cesium ion in methanol solutions. (x) 0.02 M CsSCN; (o) 0.02 M Cs⁺·DB24C8, SCN⁻; (+) 0.02 M Cs⁺·DB21C7, SCN⁻.

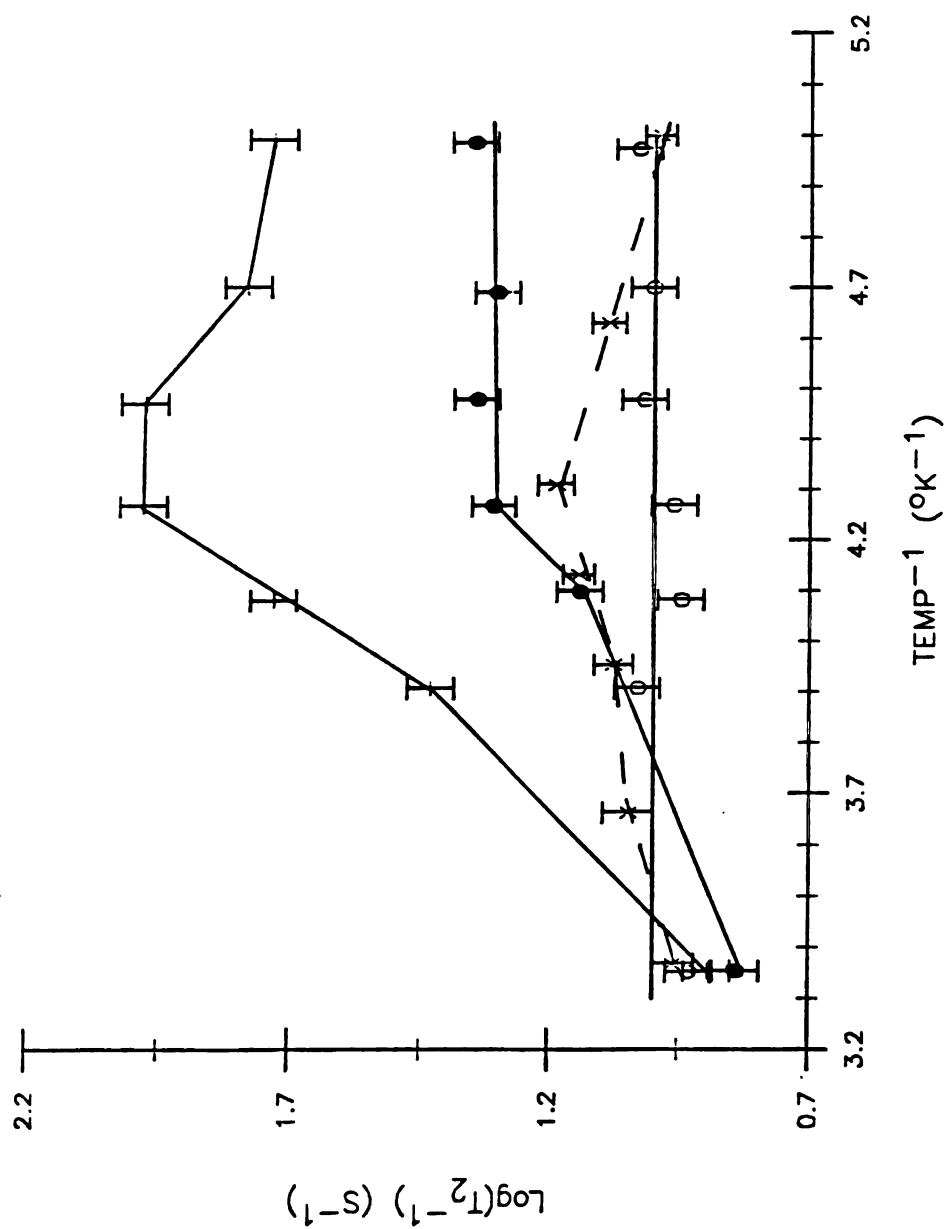


Figure 32. Semilog plots of $1/T_2$ vs. $1/T$ for solvated and complexed cesium ion in acetone solutions. (o) 0.02 M CsSCN; (x) 0.02 M CsBPH₄ (Reference 30); (●) 0.02 M Cs⁺·DB24C8, SCN⁻; (+) 0.02 M Cs⁺·DB21C7, SCN⁻.

temperature for these systems. Since, in all cases, the complex formation constants, K_f , are greater than 10^4 M^{-1} (81), solutions in which the crown ether concentration is greater than that of CsSCN contain only complexed Cs^+ ion. The inhomogeneity contribution to the relaxation rates is estimated to be $\leq 2 \text{ Hz}$.

The ^{133}Cs nucleus has a spin of $7/2$ and the predominant relaxation process has been shown to occur through quadrupolar relaxation (82). It is surprising to note, therefore, that in several systems investigated here the inverse relaxation time does not vary exponentially as a function of the absolute temperature. In fact, in both AC and MeOH solutions the $\text{Cs}^+\cdot\text{DB21C7}$ complex exhibits a maximum in the plot. Unfortunately, Shamsipur (30) does not report his results for comparison.

Deviations from linearity have been observed by ^{23}Na nmr for solvated Na^+ in pyridine (74) and in DMF (10). The authors suggested that changes in ion pairing might be responsible for the nonlinearity. Schmidt and Popov (27) observed deviations from linearity for solvated K^+ ion, but not for its complex with 18C6, in 1,3-dioxalane, MeOH, AC, and an acetone-THF mixture. They reasoned that in the low dielectric constant solvents such as 1,3-dioxalane changes in ion pairing may be responsible for the nonlinearity. However, in methanol solutions, changes in solvent structure with temperature was suggested as

the cause for deviation from theory. In going from acetone to acetone-THF mixtures a reverse in the curvature was observed for which no explanation could be given.

Mei (83) observed deviations from linearity of the ^{133}Cs relaxation time for free and complexed forms of CsBPh_4 in several solvent systems. However, the observed deviations may not, in fact, be real. The nonlinearity occurs at temperatures in which the relaxation rate is very slow and therefore, field inhomogeneity probably is responsible for most of the relaxation process in this region. Her results for the solvated Cs^+ ion in AC solutions are shown in Figure 32 for comparison. Our data are in agreement within experimental error if field inhomogeneity is considered.

In our case, the deviation from linearity of the relaxation rate as a function of temperature is real. There is a concentration dependence of the ^{133}Cs chemical shift of CsSCN in methanol and acetone solution at 25°C due to ion pairing (84). However, as shown in Figures 31 and 32, the effect of ion pairing on the relaxation rate of solvated CsSCN in these solvents at room temperature is minimal. Khaezali (85) studied ion pairing of CsSCN in methylamine at 25°C by cesium-133 nmr and found cesium linewidths always to be <2 Hz. The reason that the ion pairing does not significantly broaden the cesium-133 resonance is due to the very small quadrupole moment of

this nucleus (0.003 barns). As the temperature is lowered to the region where chemical exchange influences the cesium-133 spectrum ion pairing effects are expected to become even more minimal due to the fact that the dielectric constants of the solvents increase with decreasing temperature ($D = 29.5$ at -50°C ; $D = 48.5$ at -50°C (86)). It is reasonable to assume, therefore, that changes in ion pairing is not responsible for the observed behavior, especially since only the complexed Cs^+ ion and not the solvated cation exhibit nonlinearity.

The lack of deviation in the relaxation times of the solvated CsSCN as a function of temperature suggests that solvent structural changes with temperature (which would affect correlation times) are not responsible for the observed nonlinearity of the complexed sites. The large inhomogeneity contribution to the relaxation rate of the solvated site makes it difficult to fully eliminate this possibility. However, it is unlikely that both MeOH and AC would exhibit similar changes in structural properties as a function of temperature and in fact, the relaxation rates of the solvated sites in these two solvents do exhibit quite different behavior.

Three other possibilities remain which may explain the observed behavior. First, the quadrupolar coupling constant of the complexed salt may be changing with temperature. However, since the quadrupole moment is so small for cesium

ion it is unlikely that this would have a large effect. Second, the correlation time of the complexed site may not be changing as expected. As discussed in Chapter 4, the correlation time, τ_c , is expected to vary exponentially as a function of temperature. Contrary to expectations, the correlation time will change if the structure of the complexed site changes drastically with temperature. The third possibility is that there is an exchange process which is responsible for the variation in the relaxation time of the complexed site. For example, an exchange between two different conformers of the $\text{Cs}^+\cdot\text{DB21C7}$ complex may be slow enough to effect the ^{133}Cs nmr spectrum. At low temperatures one conformer may predominate while at high temperatures the exchange is rapid between different forms of the complex. It is interesting to note that for complexed $\text{Cs}^+\cdot\text{DB21C7}$ in AC and in MeOH solutions the relaxation rate goes through a maximum as a function of temperature, with the maximum relaxation rate occurring at essentially the same temperature and it is independent of solvent. Such behavior would be expected if the above exchange process were occurring. The $\text{Cs}^+\cdot\text{DB24C8}$ relaxation rate does not show such drastic deviation from expected behavior in AC or in MeOH solutions. Since the cavity of DB24C8 is larger than the diameter of the Cs^+ ion, it is reasonable to expect that any conformational changes of the complex would be more rapid than that of the DB21C7 complex at any temperature.

Of the above possibilities to explain the nonlinearity of the complexed Cs^+ ion relaxation rate as a function of temperature, the last two seem to be most likely. However, more study is needed to elucidate the cause of these interesting results.

B. Kinetic Results

Tables 35 and 36 list values as a function of temperature for these systems. Figures 33 and 34 show plots of $\log(1/\tau)$ vs. inverse temperatures for CsSCN complexation with DB21C7 and with DB24C8 in AC and in MeOH solutions at various relative free cesium ion populations. Figures 35-38 are plots used to determine whether the predominant exchange mechanism is the dissociative or the bimolecular process. In all systems investigated the bimolecular mechanism was found to predominate (the slope of the plots are essentially zero). The Arrhenius activation energies and other kinetic parameters were calculated from the data and are presented in Table 37, along with those of Shamsipur (calculated from his data on the basis of the bimolecular mechanism) for comparison. As may be seen, all results are in agreement with those of Shamsipur with the exception of the system $\text{CsSCN} \cdot \text{DB24C8}$ in methanol solutions. The origin of this discrepancy is unknown, but may be due to the small difference in chemical shift between solvated and complexed sites for this system. With the approximate nmr technique used by

Table 35. Mean Lifetimes as a Function of Temperature for CsSCN-Crown in MeOH Solutions.^a

Crown	P _{Cs+}	T (°C)	$\tau \times 10^4$ (s)
DB24C8	0.378	-51.0 (± 1)	7.80 (0.42) ^(b)
"	"	-59.4	7.75 (0.31)
"	"	-67.2	11.2 (0.2)
"	"	-76.4	16.0 (0.3)
"	"	-80.8	24.4 (0.6)
"	0.684	-59.6	7.99 (0.44)
"	"	-67.2	11.4 (0.7)
DB21C7	0.383	-19.9	1.62 (0.04)
"	"	-31.2	3.64 (0.07)
"	"	-36.6	4.83 (0.19)
"	"	-45.4	7.95 (0.20)
"	"	-60.7	20.7 (0.9)
"	0.686	-19.8	1.69 (0.05)
"	"	-36.7	5.65 (0.15)
"	"	-43.2	8.02 (0.24)
"	"	-55.1	16.9 (0.5)
"	"	-65.6	27.1 (1.3)

^a0.02 M in salt.^bStandard deviation estimate.

Table 36. Mean Lifetimes as a Function of Temperature for CsSCN·Crown in AC Solutions.^a

Crown	P _{Cs+}	T (°C)	$\tau \times 10^4$ (s)
DB24C8	0.384	-17.8 (±1)	0.417 (0.013) ^(b)
"	"	-34.2	1.11 (0.04)
"	"	-50.0	3.51 (0.08)
"	"	-60.4	8.84 (0.17)
"	"	-72.5	21.3 (1.0)
"	0.608	-17.7	0.536 (0.012)
"	"	-28.8	1.09 (0.06)
"	"	-39.2	1.81 (0.04)
"	"	-55.4	7.05 (0.22)
"	"	-72.6	24.8 (1.6)
DB21C7	0.385	-17.7	1.49 (0.04)
"	"	-29.6	5.81 (0.26)
"	"	-39.0	9.61 (0.22)
"	"	-49.9	30.0 (1.0)
"	"	-60.5	76.3 (4.4)
"	0.663	-17.7	3.34 (0.10)
"	"	-28.5	5.70 (0.20)
"	"	-39.1	14.4 (0.6)
"	"	-49.9	28.9 (0.7)
"	"	-60.4	66.2 (3.2)
"	"	-72.5	261. (41.)

^a0.02 M in salt.^bStandard deviation estimate.

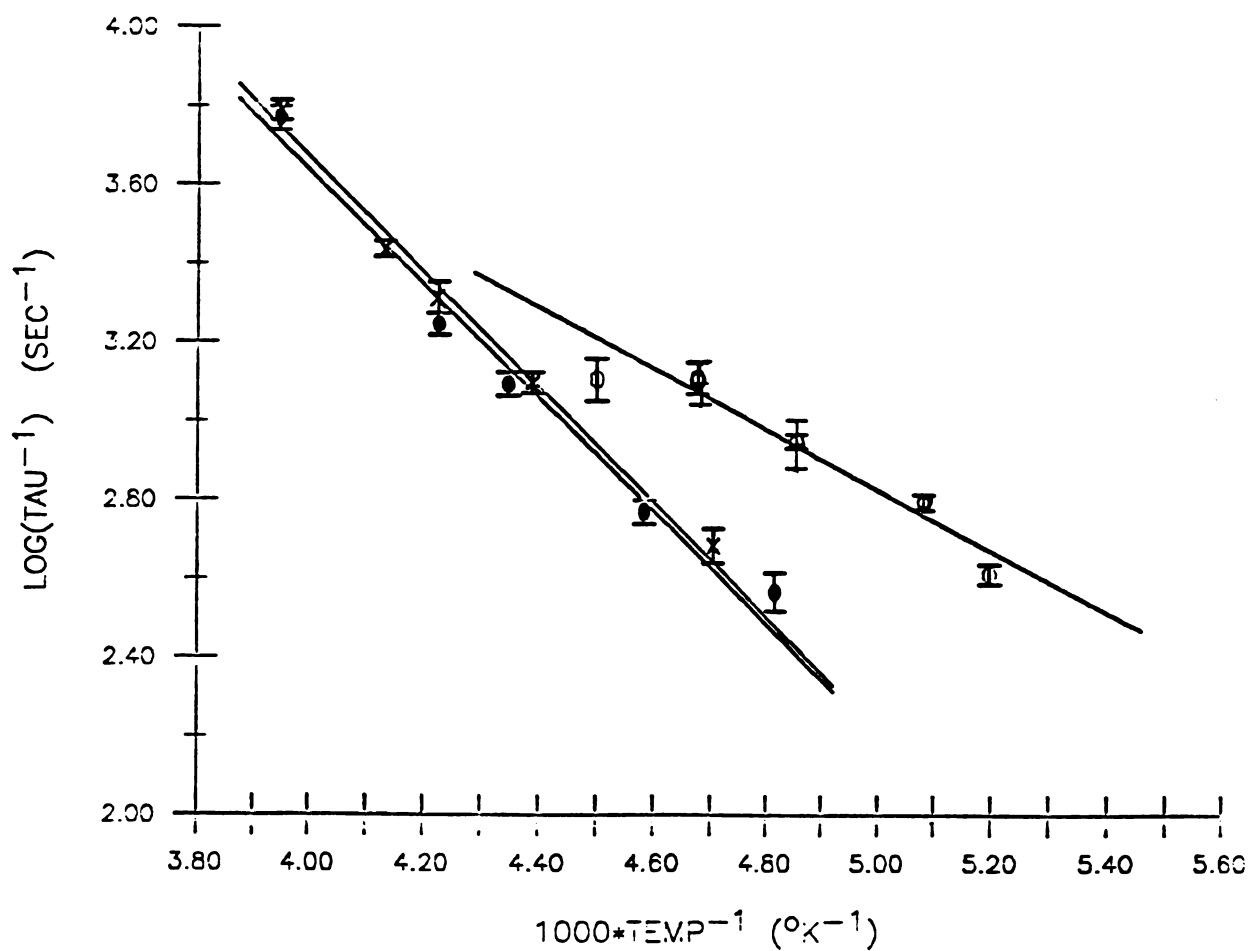


Figure 33. Semilog plots of $1/\tau$ vs. $1/T$ for CsSCN·DB21C7 and for CsSCN·DB24C8 in methanol solutions. (●) $[\text{CsSCN}]/[\text{DB21C7}] = 3.18$; (x) $[\text{CsSCN}]/[\text{DB21C7}] = 1.62$; (o) $[\text{CsSCN}]/[\text{DB24C8}] = 1.61$; (+) $[\text{CsSCN}]/[\text{DB24C8}] = 3.16$; all DB24C8 data used for fit.

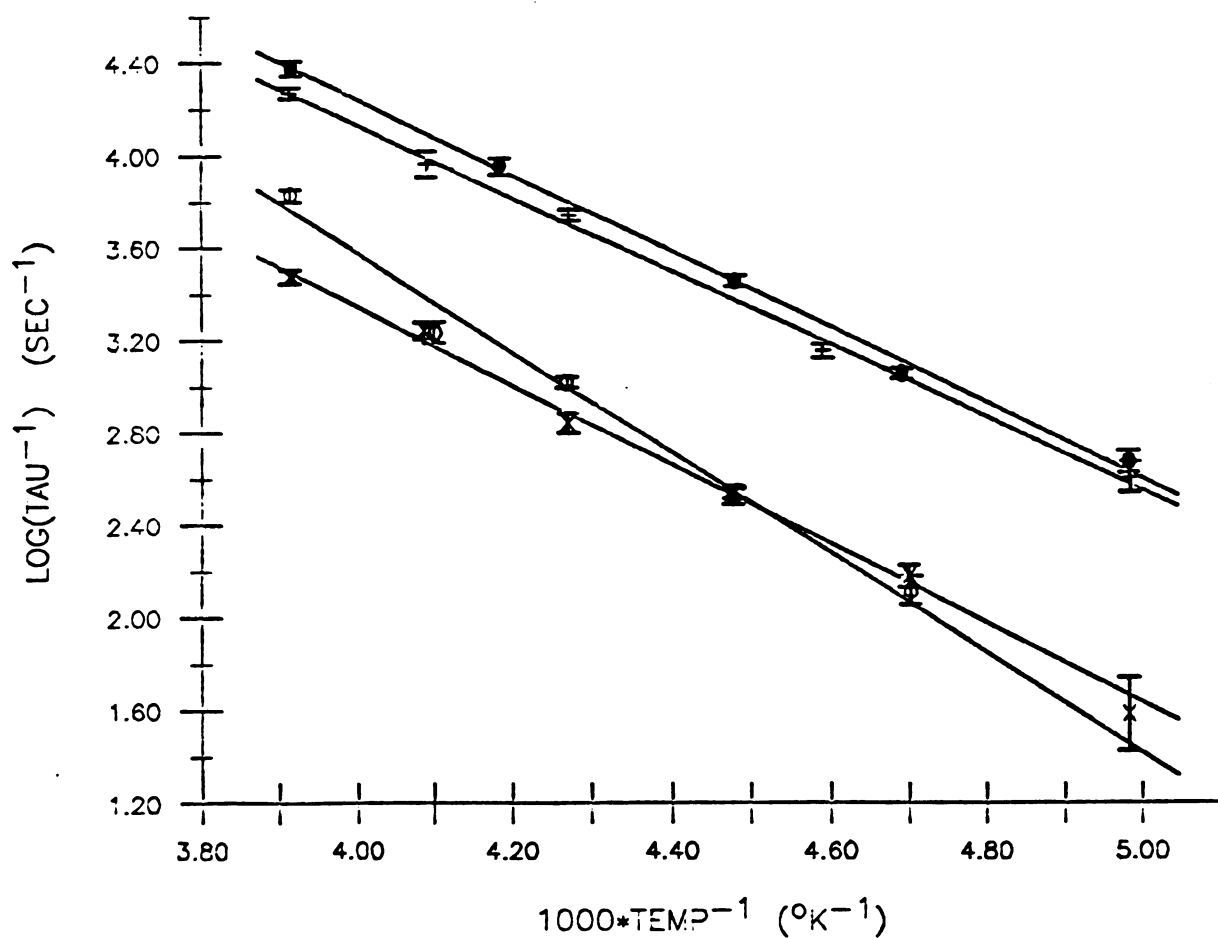


Figure 34. Semilog plots of $1/\tau$ vs. $1/T$ for CsSCN·DB21C7 and for CsSCN·DB24C8 in acetone solutions. (●)[CsSCN]/[DB24C8] = 1.62; (+)[CsSCN]/[DB24C8] = 2.55; (x)[CsSCN]/[DB21C7] = 2.97; (o)[CsSCN]/[DB21C7] = 1.62.

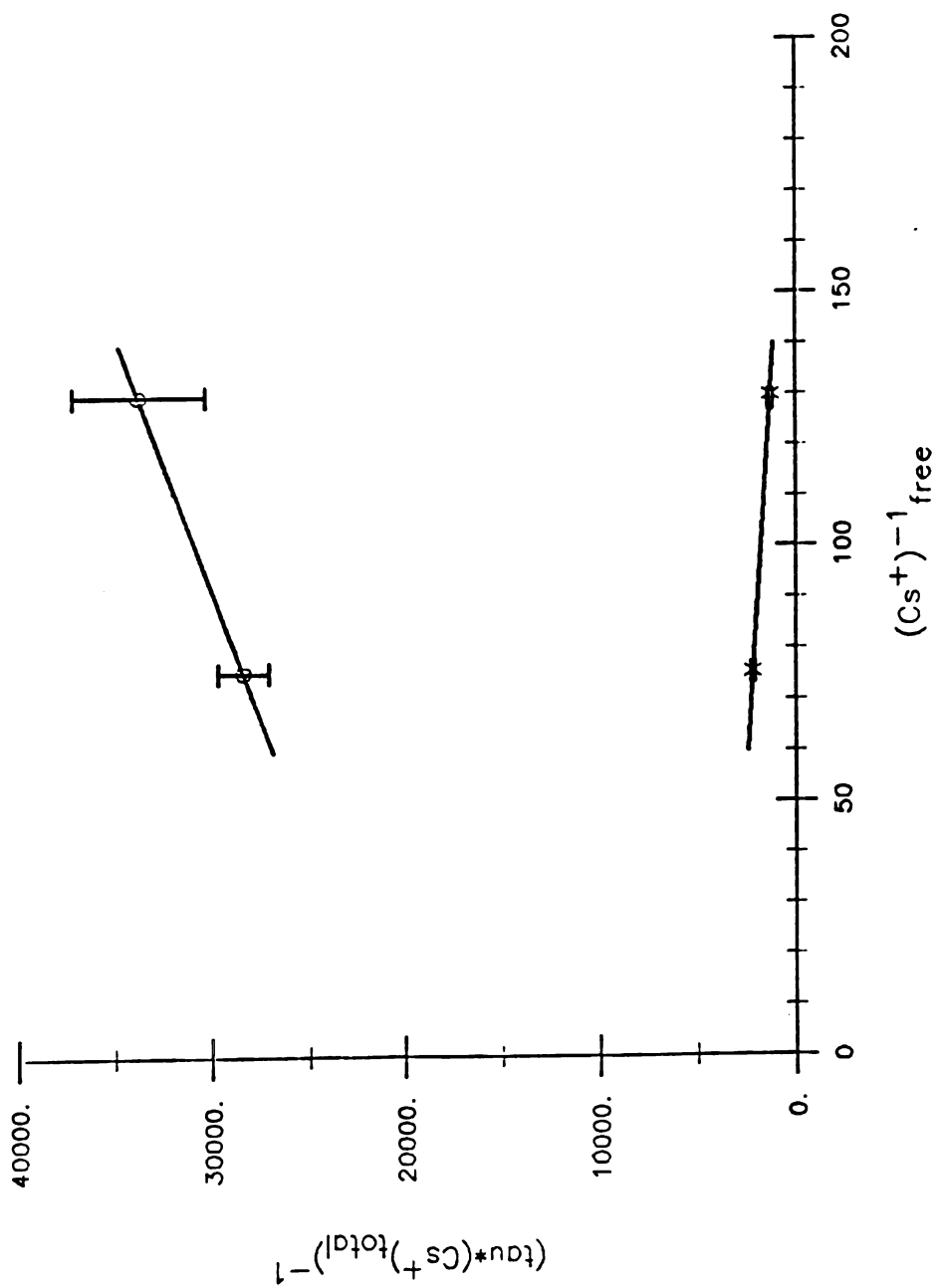


Figure 35. Plots of $1/(\tau[\text{Cs}^+]_{\text{total}})$ vs. the inverse free cesium ion concentration for $\text{CsSCN} \cdot \text{DB21C7}$ in acetone solutions at various temperatures. (o) 215°K; (x) 200°K.

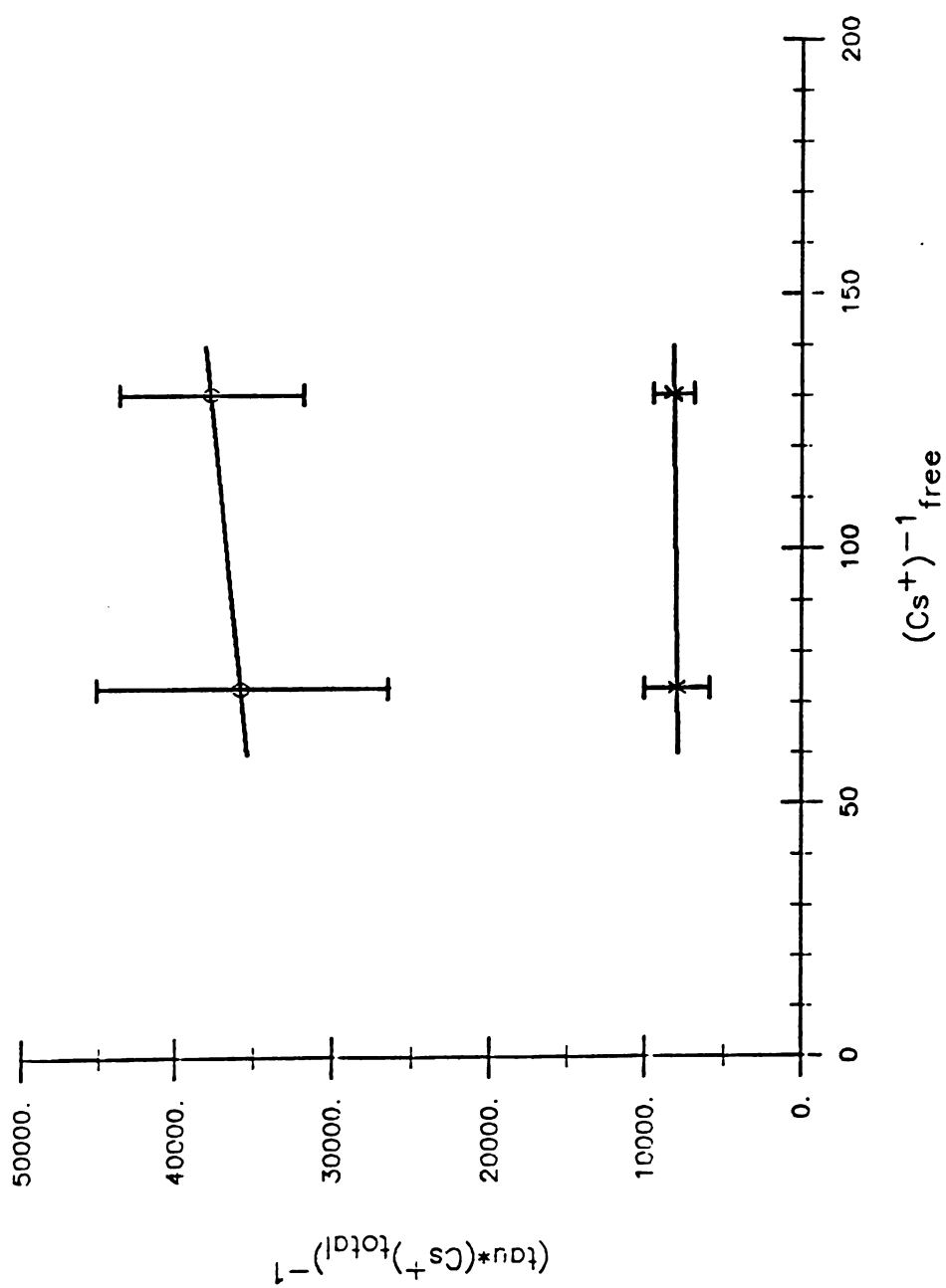


Figure 36. Plots of $1/(\tau[\text{Cs}^+]_{\text{total}})$ vs. the inverse free cesium ion concentration for CsSCN-DB21C7 in methanol solutions at various temperatures. (o) 220 K; (x) 200°K.

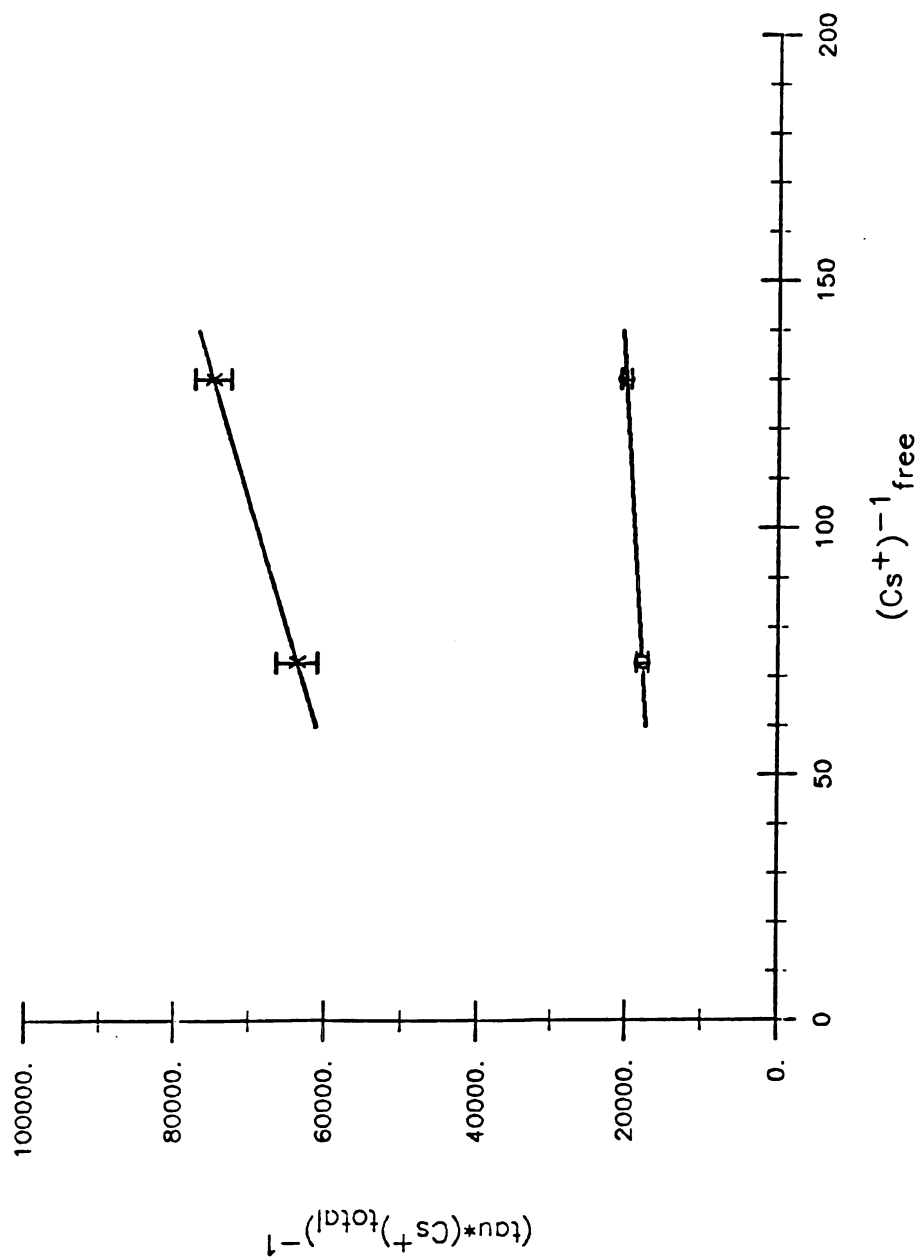


Figure 37. Plots of $1/(\tau[\text{Cs}^+]_{\text{total}})$ vs. the inverse free cesium ion concentration for $\text{CsSCN} \cdot \text{DB24C8}$ in acetone solutions at various temperatures. (x) 215°K; (o) 200°K.

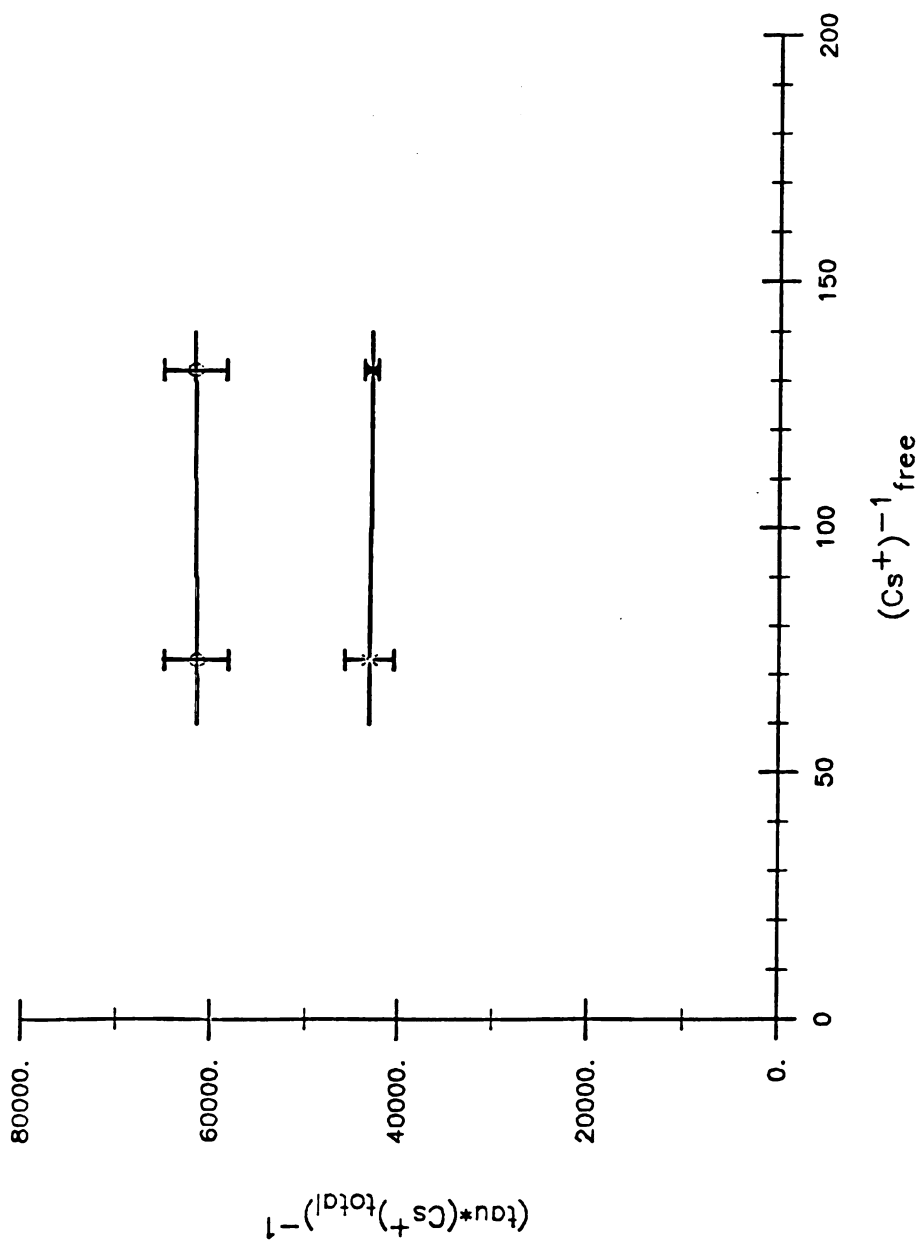


Figure 38. Plots of $1/(\tau[\text{Cs}^+]_{\text{total}})$ vs. the inverse free cesium ion concentration for CsSCN·DB24C8 in methanol solutions at various temperatures. (o) 214°K; (x) 206°K.

Table 37. Kinetic Parameters for the Complexation of Cs^+ with Several Crown Ethers in AC and in MeOH Solutions at 220°K.

Solv.	Crown	E_a (a)	ΔH^\ddagger (a)	ΔS^\ddagger (b)	ΔG^\ddagger (a)	$k_1 \times 10^{-4}$ (c)
AC	DB21C7 ^(e)	9.3(0.8) ^d	8.7(0.8)	0.9(3.7)	8.5(0.1)	1.6 (0.3)
"	"	8.7(0.5)	8.1(0.5)	-2.7(2.5)	8.7(0.2)	0.94(0.3)
"	DB24C8 ^(e)	8.2(0.6)	7.6(0.6)	-1.8(2.8)	8.0(0.1)	5.5 (1.0)
"	"	7.3(0.3)	6.7(0.3)	-5.0(1.5)	7.8(0.1)	7.4 (1.0)
MeOH	DB21C7 ^(e)	6.7(0.5)	6.1(0.5)	-10.9(2.3)	8.5(0.1)	1.8 (0.4)
"	"	6.6(0.3)	6.0(0.3)	-10.5(1.5)	8.3(0.1)	2.7 (0.4)
"	DB24C8 ^(e)	6.3(0.6)	5.7(0.6)	-26.8(2.8)	11.6(0.1)	14.5 (3.0)
"	"	3.5(0.5)	2.9(0.5)	-23.2(2.5)	8.0(0.2)	5.6 (2.0)

^a kcal·mol⁻¹

^b e.u.

^c M⁻¹s⁻¹.

^d Standard deviation estimate.

^e Reference 30.

Shamsipur (30), positive errors in the activation energies have been shown to occur when the chemical shift difference of the exchanging sites is small (87).

It is interesting to note that the free energy of activation, ΔG^\ddagger , is independent of solvent for the two crown complexes. This is due to lack of active solvent participation in the exchange process (see Chapter 4). However, there are solvent influences on the activation energies and entropies of the kinetic process. The activation energies are higher for the two complexes in acetone solutions while the activation entropies are more positive in this solvent. Since acetone has both a lower donor number (DN = 17.0) and dielectric constant than does methanol (DN = 25.7), it is reasonable to assume that in the transition state acetone cannot reduce the charge-charge repulsion of the cesium ions as well as methanol and thus, the activation energy is higher in this solvent. The activation entropy is more positive in acetone due to more breathing room of the crown in the transition state due to the larger separation of the Cs^+ ions. This observation has been made by Schmidt and Popov (27) for K^+ ion complexation kinetics and by us for sodium ion complexation kinetics with 18C6 (see Chapter 4).

The larger crown ether has the larger rate constant and lower ΔG^\ddagger , compared with DB21C7 regardless of solvent. Such behavior is expected since cesium ion has approximately the correct size for the cavity of DB21C7 but is smaller than

the cavity of DB24C8. The larger formation constant of the $\text{Cs}^+\cdot\text{DB21C7}$ complexed vs. that of the $\text{Cs}^+\cdot\text{DB24C8}$ complex also reflects the cavity size effect ($\log k_{\text{AC},\text{DB21C7}}^{25^\circ\text{C}} = 3.98$; $\log k_{\text{AC},\text{DB24C8}}^{25^\circ\text{C}} = 3.71$; $\log k_{\text{MeOH},\text{DB21C7}}^{25^\circ\text{C}} = 3.96$; $\log k_{\text{MeOH},\text{DB24C8}}^{25^\circ\text{C}} = 3.60$ (81)).

It is known that in these solvents the solvated CsSCN is ion paired to some extent (84). Unfortunately, information is not available concerning the degree in which the complexes are ion paired. Thus, it is not possible to determine whether ion pairing allows the bimolecular exchange process to predominate.

If we compare the complexation kinetics of the alkali metal ions with crown ethers a trend emerges. As one goes through the series $\text{Na}^+ \text{--} \text{K}^+ \text{--} \text{Cs}^+$ the predominant exchange mechanism varies from that of either the dissociative or bimolecular process for Na^+ ion to primarily the bimolecular process for Cs^+ ion. Assuming ion pairing is not responsible, this is likely due to the decrease in charge density as one goes to the larger cation in this series. Such a decrease in charge density will minimize the charge-charge repulsion in the bimolecular exchange process and thus, allow it to predominate. It would be interesting to investigate Li^+ ion complexation kinetics to see if the above hypothesis is correct. One would expect that this ion would exhibit primarily the dissociative mechanism in the absence of ion pairing.

In summary, it is important to investigate not only the rates of exchange involved in the complexation kinetics of crown ethers, but also the mechanism of exchange. Such information is invaluable in determining the kinetic processes of these complexes.

APPENDICES

APPENDIX A

DATA TRANSFER PROGRAMS FOR THE WH-180 NMR

The programs MOVE and NTCDTL were used to transfer data out serial port B of the Nicolet 1180 computer on the WH-180 nmr spectrometer.

A listing of MOVE and an example of its use are shown below:

```
100 DIM A(2047),X(8000),R$(6)
110 PRINT "FIRST FIVE CHARS OF FILENAME";
120 INPUT R$(0)
130 PRINT "INPUT FINAL FIVE CHARS OF FILENAME";
140 INPUT R$(1)
150 LET R$(2)="\"
160 LET N2=8000
170 CALL BDEFINE(10,R$)
180 CALL FREAD(10,X,N2)
190 CALL FREAD(10,X,N2)
200 LET N1=N2
210 CALL FAINT (N1,1)
220 CALL IAFLT(X,N1)
230 PRINT "INPUT # OF POINTS";
240 INPUT N
250 PRINT "STARTING POINT";
260 INPUT S
270 PRINT "ENTER STEP SIZE"
280 INPUT S1
290 LET W=N+S
300 FOR K=S TO W
310 LET L=K-S
320 LET A(L)=X(K)
330 NEXT K
340 CALL FDISP(A,N,800)
350 PRINT "OK";
360 INPUT B$
370 IF B$="N" THEN 230
380 FOR I=S TO W STEP S1
390 PRINT #8:I,X(I)
400 NEXT I
410 PRINT "DONE"
420 END
```

Example of Move

```
RUN MOVE
FIRST FIVE CHARS OF FILENAME?NB251
INPUT FINAL FIVE CHARS OF FILENAME?.5
INPUT # OF POINTS?600
STARTING POINT?2500
ENTER STEP SIZE
?2
OK?Y
DONE
```

The spectrum to be transferred is stored along with the language BASIC on the hard storage disk. Program MOVE is run and the appropriate input given. In the example, the data to be transferred are in the file NB251.5. The number of points in the region to be transferred is 600. The starting point of the region is 2500. The step size, 2, tells the program to skip every other point. At this time, the program will display the region to be transferred determined from the input above. If the region is satisfactory, a "Y" response will begin the data transfer.

NTCDTL is a program written by Nicolet to transfer data out serial port B. This program was used when the WH-180 software was upgraded in 1984. The following example demonstrates its use:

NTCDTL Example

```

RUN NTCDTL
DATE-TRANSFER PROGRAM
VERSION #10903
COMMAND:
BI,BO,CP,AP,AR,KB,LP,LR,MO,TL,TT?
BO
WHAT FORMAT (A=ASCII,B=BINARY)?  A
WHAT PARITY (E,O,M,N)?  N
MAXIMUM RECORD LENGTH = 64
PROMPT = 12
ENTER TERMINAL MODE (Y,N)?  N
- Hold down "Line Feed" Button on the
  floppy drive -

```

The region of the spectrum to be transferred is chosen using the upgraded software. The program is then run. The command "BO" refers to serial B out. The data are transferred in ASCII format. The parity chosen is none (N). The prompt "12" requires a line feed character prompt from the PDP-11 computer for each point transferred. Once the "N" response is given for the terminal mode question, the first data point is transferred. The "line feed" key is held down on the PDP-11 to transfer the rest of the file.

APPENDIX B

FT-NMR TWO-SITE EXCHANGE EQUATIONS MODIFIED TO
INCLUDE LINE BROADENING AND DELAY TIME

Using the formalism of Gupta et al. (75) the magnetization may be written as:

$$G = G_A + G_B = C_1 e^{\Lambda_1 t} + C_2 e^{\Lambda_2 t}$$

where G is the total magnetization, G_A and G_B are the magnetizations of sites A and B respectively, t is the time after application of the pulse, and all other symbols have the same meaning as in Reference 75.

The Fourier transform, S , of the free induction decay (FID) is given by

$$S = \int_0^{\infty} G e^{-i(\omega - \omega_{rf})t} dt$$

To modify the equation for the loss of signal during the delay time period (the time between application of the pulse and collection of the FID) the integration is taken from $t = DE$ to $t = \infty$. Thus

$$S_{DE} = \int_{DE}^{\infty} G e^{-i(\omega - \omega_{rf})t} dt$$

where DE = delay time. When line broadening is applied to the FID, the FID is multiplied by $\exp(-LB \cdot t)$ where LB is the line broadening. Thus,

$$S_{LB} = \int_0^{\infty} Ge^{-i(\omega-\omega_{rf})t} e^{-(LB)t} dt$$

$$= \int_0^{\infty} Ge^{[-LB-i(\omega-\omega_{rf})]t} dt .$$

Including both line broadening and delay time

$$S_{DE,LB} = \int_{DE}^{\infty} Ge^{[-LB-i(\omega-\omega_{rf})]t} dt$$

Integrating gives the spectrum in the frequency domain:

$$S_{DE,LB} = \frac{-C_1 e^{[\Lambda_1 - LB - i(\omega - \omega_{rf})]DE}}{\Lambda_1 - LB - i(\omega - \omega_{rf})} - \frac{C_2 e^{[\Lambda_2 - LB - i(\omega - \omega_{rf})]DE}}{\Lambda_2 - LB - i(\omega - \omega_{rf})}$$

where all symbols are described in Reference 75. Redefining α_A and α_B as

$$\alpha_A = T_{2A}^{-1} + i(\omega_A - \omega); \quad \alpha_B = T_{2B}^{-1} + i(\omega_B - \omega)$$

Then,

$$S_{DE,LB} = \frac{-C_1 e^{(\Lambda_1 - LB)DE}}{\Lambda_1 - LB} - \frac{-C_2 e^{(\Lambda_2 - LB)DE}}{\Lambda_2 - LB}$$

Also, using the relationship

$$\tau = \frac{\tau_A \tau_B}{\tau_A + \tau_B} = \tau_A P_B = \tau_B P_A$$

Then,

$$\Lambda_1, \Lambda_2 = \{-(\alpha_A + \alpha_B + \tau^{-1}) \pm [(\alpha_A - \alpha_B + \tau P_B^{-1} - \tau P_A^{-1})^2 + 4\tau^2 P_A^{-1} P_B^{-1}]^{1/2}\} / 2$$

Using these new definitions and $S_{DE, LB}$ we can program the computer in complex Fortran to solve the spectrum for τ .

Szczygiel has shown (8) that the delay time modification introduces a first order phase influence on the transformed spectrum. This has the form

$$\theta_1 = \cos (\omega - \omega_C) DE$$

where ω_C is a constant. Due to instrumental contributions to the first order phasing of the spectra which could not be included in the above equations, the first order phasing was done visually. The modified exchange equations used had the delay time contribution to the phasing eliminated when the spectra were fit.

The nonlinear least squares program KINFIT (49) was used to fit the data to the above modified equations. The subroutine EQN for the program is listed on the following pages.

```

PNC CARD
J03 CARD
PASS WORD CARD
HA, BANNER, STRASSER.
ATTACH, TAPE62, FILE.
REJIND, TAPE62.
ATTACH, READER, READERBINARY.
RETURN, KINFT4, LGO.
HAL, L=DYE, KINFT4=KINFT4.
FTV4, R=LGO.
LOAD, KINFT4.
LOAD, READER.
LGO.
7

```

```

8
3 CARD
SUBROUTINE EGN
COMMON KOUNT, ITAPE, JTAPE, IWT, LAP, XINCR, NOPT, NOVAR, NOUNK, X, U, ITMAX,
1WTX, TEST, I, AV, RESID, IAR, EPS, ITYP, XX, RXTYP, DX11, FOP, FO, FU, P, ZL, TO, E
2IGVAL, XST, T, DT, L, M, JJJ, Y, DY, VECT, NCST, CONST, NDAT, JDAT, MOPT, LOPT,
3YYY, CONSTS
COMMON/FREDT/IMETH
COMMON/POINT/KOPT, JOPT, XXX
COMPLEX ALPHA, ALPHB, XLAMA, XLAMB, C1, C2, XS, BRUCE, ALEX, AL, FRED
DIMENSION X(4,300), J(20), WTX(4,300), XX(14), FOP(300), FO(300), FU(300)
1P(20,21), VECT(20,21), ZL(300), TO(20), EIGVAL(20), XST(300), Y(10),
2DY(10), CONSTS(50,16), NCST(50), ISMIN(50), RXTYP(50), DX11(50), IRX(50)
3MOPT(50), LOPT(50), YYY(50), CONST(16), XXX(15)
GO TO (2,3,4,5,1,7,8,9,10,11,12) ITYP
1 CONTINUE
ITAPE=60
JTAPE=61
RETJRN
7 CONTINUE
NOUNK=5
NOVAR=2
RETJRN
8 CONTINUE
RETURN
2 CONTINUE

```

```

C=====
C=====

```

VMR TJD-SITE EXCHANGE WITH CORRECTION
FOR LINE BROADENING AND DELAY TIME.

PARAMETERS	U(1) = K	(INTENSITY)
	U(2) = C	(BASELINE)
	U(3) = THETA	(ZERO ORDER PHASE CORRECTION)
	U(4) = DELTA	(FREQUENCY CORRECTION)
	U(5) = TAU	(EXCHANGE RATE)
CONSTANTS	CONST(1) = PA	(POP. OF SITE A)
	CONST(2) = T2A	
	CONST(3) = WA	
	CONST(4) = PB	
	CONST(5) = T2B	
	CONST(6) = WB	
	CONST(7) = DE	(DELAY TIME)
	CONST(8) = LB	(LINE BROADENING)

```

C=====
C=====

```

```

IF(U(5).GT.0.)60 TO 1000
U(5)=.0001
1070 CONTINUE
PI=2*3.14159
ALPHA=1./CONST(2)+CMPLX(0.,1.)*(CONST(3)-XX(1)*PI+U(4))
ALPHB=1./CONST(5)+CMPLX(0.,1.)*(CONST(6)-XX(1)*PI+U(4))
BRUCE=-(ALPHA+ALPHB+1./U(5))
FRED=(ALPHA-ALPHB+CONST(4)/U(5)-CONST(1)/U(5))*2
BOB=4*CONST(1)*CONST(4)/(U(5)*U(5))
ALEX=FRED+BOB
AL=EXP(CLOG(ALEX)/2.)
XLAMA=(BRUCE+AL)/2.
XLAMB=(BRUCE-AL)/2.
C1=CMPLX(0.,1.)*(XLAMB+CONST(1)*ALPHA+CONST(4)*ALPHB)/(-XLAMA+
1XLAMB)
C2=CMPLX(0.,1.)*(XLAMA+CONST(1)*ALPHA+CONST(4)*ALPHB)/(XLAMA-
1XLAMB)
XS=-C1*(EXP((XLAMA-CONST(8))*CONST(7)))/(XLAMA-CONST(8))+
1(-C2)*(EXP((XLAMB-CONST(8))*CONST(7)))/(XLAMB-CONST(8))
REAP=REAL(XS)
AMAG=AMAG(XS)
CALC=U(1)*(-REAP*SIN(U(3)-(CONST(3)-XX(1)*PI+U(4))*CONST(7)))+
1AMAG*COS(U(3)-(CONST(3)-XX(1)*PI+U(4))*CONST(7))*U(2)
IF(IMETH.NE.-1) GO TO 35
RETURN
35 CONTINUE
RESID=CALC-XX(2)
RETURN

```

```

EGN4
EGN4
EGN4
EGN4

```


APPENDIX C

SUGGESTIONS FOR FUTURE WORK

There are four areas of research that are suggested from these studies.

1. Ion Pairing of Complexes by Infrared Spectroscopy.

The observation of the ion paired complex $\text{Na}^+ \cdot 18\text{C}6$, NCS^- in tetrahydrofuran solutions by infrared spectroscopy (Chapter 3) appears to be the first such observation by this technique. It would be interesting to use infrared spectroscopy to investigate ionic association of complexed metal ions and compare these results with those of other techniques.

2. NaAlEt_4 Complexation. This salt is soluble in a wide variety of low dielectric, low donor number solvents. In addition, the proton nmr of the anion provides information as to the type of ion pair the salt forms in a given solution (57). It would be interesting, therefore, to study ion pairing, complexation, and complexation kinetics of this salt in those solvents in which solubility problems prevent the use of the "normal" salts.

3. Cesium Ion Complexation Kinetics. It would be useful to determine if the dissociative exchange mechanism is predominant for Cs^+ complexation with DB30ClO in AC and in MeOH solutions as reported by Shamsipur (30). This

knowledge would complete the study initiated by Shamsipur concerning the kinetics of complexation of Cs^+ ion with the larger crowns in these solvents.

Mei et al. (28) assumed the dissociative mechanism to be predominant for Cs^+ ion complexation with 18C6 in pyridine solutions. A free energy of activation of $\Delta G_{-2}^\ddagger = 12.02 \text{ kcal}\cdot\text{mol}^{-1}$ was reported. However, if one assumes the bimolecular mechanism to be predominant, a value of $\Delta G_1^\ddagger = 9.3 \text{ kcal}\cdot\text{mol}^{-1}$ is calculated from their data. This value is of the approximate magnitude one would expect for the solvent independent free energy barrier for alkali metal ion complexation with 18C6 based on charge density arguments. The barrier varies from $\sim 10.5 \text{ kcal}\cdot\text{mol}^{-1}$ for Na^+ ion to $\sim 10.0 \text{ kcal}\cdot\text{mol}^{-1}$ for K^+ ion to $\sim 9.3 \text{ kcal}\cdot\text{mol}^{-1}$ for Cs^+ ion. One would expect the free energy barrier to be highest for Na^+ ion in this series due to its higher charge density which would result in the greatest amount of charge-charge repulsion in the transition state.

Therefore, it would be extremely interesting to determine the mechanism of Cs^+ ion complexation with 18C6 in several solvents in order to compare the results with the other alkali metal ions.

4. Lithium Ion Complexation Kinetics. To our knowledge no data exist in the literature concerning Li^+ ion complexation kinetics with crown ethers. It would be interesting to determine the kinetics of complexation of this ion

with the crown ethers and compare the results with the other alkali metal ions.

Thus far, only Na^+ ion has been demonstrated to exchange via the dissociative pathway. Since Li^+ has a higher charge density than does Na^+ , one would expect the free energy barrier for the bimolecular mechanism to be higher for Li^+ ion. Therefore, it seems reasonable for the dissociative mechanism to also occur for the ion. It would be interesting to see if the above predictions are correct.

REFERENCES

REFERENCES

1. Pedersen, C. J. J. Am. Chem. Soc. 1967, 89, 2495.
2. Pedersen, C. J. J. Am. Chem. Soc. 1967, 89, 7017.
3. Dietrich, B.; Lehn, J.-M.; Sauvage, J. P. Tetrahedron Lett. 1969, 2885.
4. Lehn, J.-M. Struct. Bonding (Berlin) 1973, 16, 1.
5. Lehn, J.-M. Acc. Chem. Res. 1978, 11, 49.
6. Liesegang, G. W. and Eyring, E. M. in "Synthetic Multidentate Macrocyclic Compounds" ed. by Izatt, R. M. and Christensen, J. J. Academic Press, New York, pp. 245-287 (1978).
7. Schmidt, E., Ph.D. Thesis, Michigan State University, East Lansing, MI, 1981.
8. Szczygiel, P. M. S. Thesis, Michigan State University, East Lansing, MI, 1984.
9. Wong, K. H.; Konizer, G.; Smid, J. J. Am. Chem. Soc. 1970, 92, 666.
10. Shchori, E.; Jagur-Grodzinski, J.; Luz, Z.; Shporer, M. J. Am. Chem. Soc. 1971, 93, 7133.
11. Chock, P. B. Proc. Nat. Acad. Sci USA 1972, 69, 1939.
12. Liesegang, G. W.; Farrow, M. M.; Rodriguez, L. J.; Burnam, R. K.; Eyring, E. M. Int. J. Chem. Kin. 1978, 10, 471.
13. Rodriguez, L. J.; Liesegang, G. W.; White, R. D.; Farrow, M. M.; Purdie, N.; Eyring, E. M. J. Phys. Chem. 1977, 81, 2118.
14. Farber, H.; Petrucci, S. J. Phys. Chem. 1981, 85, 1396.
15. Chen, C. C.; Petrucci, S. J. Phys. Chem. 1982, 86, 2601.

16. Maynard, K. J.; Irish, D. E.; Eyring, E. M.; Petrucci, S. J. Phys. Chem. 1984, 88, 729.
17. Chen, C.; Wallace, W.; Eyring, E.; Petrucci, S. J. Phys. Chem. 1984, 88, 2541.
18. Boss, P., Ph.D. Thesis, Michigan State University, East Lansing, MI, 1985.
19. Grell, E.; Funck, T.; Eggers, F. in "Membranes", ed. by G. Eisenman, Vol. III, Dekker, New York, pp. 1-171 (1975).
20. Gutmann, V., "Coordination Chemistry in Nonaqueous Solutions", New York, Springer-Verley (1968).
21. Popov, A. I. Pure and Appl. Chem. 1975, 41, 275.
22. Dickert, F. L.; Gumbrecht, W. Z. Naturforsch. 1984, 39b, 69.
23. Mei, E.; Popov, A. I.; Dye, J. L. J. Am. Chem. Soc. 1977, 99, 6532.
24. Kauffmann, E.; Dye, J. L.; Lehn, J.-M.; Popov, A. I. J. Am. Chem. Soc. 1980, 102, 2274.
25. Shchori, E.; Jagur-Grodzinski, J.; Shporer, M. J. Am. Chem. Soc. 1973, 95, 3842.
26. Shporer, M.; Luz, Z. J. Am. Chem. Soc. 1975, 97, 665.
27. Schmidt, E.; Popov, A. I. J. Am. Chem. Soc. 1983, 105, 1873.
28. Mei, E.; Popov, A. I.; Dye, J. L. J. Phys. Chem. 1977, 81, 1677.
29. Mei, E.; Dye, J. L.; Popov, A. I. J. Am. Chem. Soc. 1977, 99, 5308.
30. Shamsipur, M. Ph.D. Thesis, Michigan State University, East Lansing, MI, 1979.
31. Lin, J. D.; Popov, A. I. J. Am. Chem. Soc. 1981, 103, 3773.
32. Day, M. C., University of Louisiana, Baton Rouge, Louisiana.
33. Hohn, E. G.; Olander, J. A.; Day, M. C. J. Phys. Chem. 1969, 73, 3880.

34. Day, M. C. personal communication, 1984.
35. Gokel, G. W.; Cram, D. J.; Liotta, C. L.; Harris, H. P.; Cook, F. L. Org. Synth. 1977, 57, 30.
36. Gokel, G. W.; Cram, D. J.; Liotta, C. L.; Harris, H. P.; Cook, F. L. J. Org. Chem. 1974, 39, 2445.
37. Pedersen, C. J. J. Am. Chem. Soc. 1967, 89, 7017.
38. Pedersen, C. J.; Frensdorf, H. K. Angew. Chem. Int. Ed. 1972, 11, 16.
39. Wright, D. L. Ph.D. Thesis, Michigan State University, East Lansing, MI, 1974.
40. Martin, M. L.; Delpuech, J.-J.; Martin, G. J. in "Practical NMR Spectroscopy", Heyden & Son Ltd., Philadelphia, p. 178 (1980).
41. Templeman, G. L.; VanGeet, A. L. J. Am. Chem. Soc. 1970, 92, 5578.
42. Greenberg, M. S.; Popov, A. I. Spectrochim. Acta 1975, 31A, 697.
43. (a) Van Geet, A. L. Anal. Chem. 1968, 40, 227.
 (b) Van Geet, A. L. Anal. Chem. 1970, 42, 679.
 (c) Kaplan, M. L.; Bobey, F. A.; Chang, H. N. Anal. Chem. 1975, 47, 1703.
44. Hertz, H. G.; Tutsch, R.; Versmold, H. Ber Bunsenges Phys. Chem. 1971, 75, 1177.
45. Eisenstadt, M.; Friedman, H. L. J. Chem. Phys. 1966, 44, 1407.
46. Lindon, J. C.; Ferridge, A. G. Prog. in NMR Spectrosc. 1980, 14, 27.
47. Walmsley, J. A.; Atkinson, T. V. unpublished program.
48. Atkinson, T. V. unpublished program.
49. Nicely, V. A.; Dye, J. L. J. Chem. Educ. 1971, 48, 443.
50. Greenberg, M. S.; Badner, R. L.; Popov, A. I. J. Phys. Chem. 1973, 77, 2449.
51. Carvajal, C.; Tolle, K. J.; Smid, J.; Szwarc, M. J. Am. Chem. Soc. 1965, 87, 5548.

52. Comyn, J.; Dainton, F. S.; Ivin, K. J. Electrochim Acta 1963, 13, 1851.
53. Bhattacharyya, D. M.; Lee, C. L.; Smid, J.; Szwarc, M. J. Phys. Chem. 1965, 69, 608.
54. Tersag, G.; Boileau, S. J. Chim Phys. 1971, 68, 903.
55. Boileau, S.; Hemery, P.; Justice, J.-C. J. Soln. Chem. 1975, 4, 873.
56. Chabanel, M.; Wang, Z. J. Phys. Chem. 1984, 88, 1441.
57. Ahmad, N.; Day, M. C. J. Am. Chem. Soc. 1977, 99, 941.
58. Westmoreland, T. D. Jr.; Ahmad, N.; Day, M. C. J. Organometal. Chem. 1970, 25, 329.
59. Vaes, J.; Chabanel, M.; Martin, M. L. J. Phys. Chem. 1978, 82, 2420.
60. Menard, C.; Wojtkowiak, B.; Chabanel, M. Bull. Soc. Chim. Belges 1972, 81, 241.
61. Erlich, R. H.; Popov, A. I. J. Am. Chem. Soc. 1971, 93, 5620.
62. Popov, A. I. in "Solute-Solvent Interactions" v.2, New York, Marcel Dekker, ed. by Coetzee, J. F. and Ritchie, C. D. (1976).
63. Popovych, O. and Tomkins, R. P. T. in "Nonaqueous Solution Chemistry", New York, J. Wiley & Sons (1981).
64. Frankel, L. S.; Langford, C. H.; Stengle, T. R. J. Phys. Chem. 1970, 74, 1376.
65. Erlich, R. H.; Greenberg, M. S.; Popov, A. I. Spectrochim. Acta 1973, 29A, 543.
66. Kinsinger, J. B.; Tannahill, M. M.; Greenberg, M. S.; Popov, A. I. J. Phys. Chem. 1973, 77, 2444.
67. Wu, Y.-C.; Friedman, H. L. J. Phys. Chem. 1966, 70, 501.
68. Lin, J. D. Ph.D. Thesis, Michigan State University, East Lansing, MI, 1980.
69. Frensdorff, H. K. J. Am. Chem. Soc. 1971, 93, 600.
70. Abragam, A. "The Principles of Nuclear Magnetism", Oxford University Press, London (1961).

71. Deverell, C. Prog. Nucl. Magn. Reson. Spectrosc. 1969, 4, 278.
72. Arnold, M. St. J.; Packer, K. J. Mol. Phys. 1966, 10, 141.
73. Kintzinger, J.-P.; Lehn, J.-M. J. Am. Chem. Soc. 1974, 96, 3313.
74. Ceraso, J. M. Ph.D. Thesis, Michigan State University, East Lansing, MI, 1976.
75. Gupta, R. K.; Pitner, T. P.; Wasylshen, R. J. Magn. Res. 1974, 13, 383.
76. Woessner, D. E. J. Chem. Phys. 1961, 35, 41.
77. Ceraso, J. M.; Smith, P. B.; Landers, J. S.; Dye, J. L. J. Phys. Chem. 1977, 81, 760.
78. Liesegang, G. W.; Farrow, M. M.; Vazquez, F. A.; Purdie, N.; Eyring, E. M. J. Am. Chem. Soc. 1977, 99, 3240.
79. Cox, B. G.; Garcia-Rosas, J.; Schneider, H. J. Am. Chem. Soc. 1981, 103, 1054.
80. Shih, J. S.; Popov, A. I. Inorg. Nucl. Chem. Letts. 1977, 13, 105.
81. Shamsipur, M.; Rounaghi, G.; Popov, A. I. J. Soln. Chem. 1980, 9, 701.
82. (a) O'Reilly, D. E.; Petersen, E. M. J. Chem. Phys. 1969, 51, 4906.
(b) Wehrli, F. W. J. Magn. Res. 1977, 25, 575.
83. Mei, E. Ph.D. Thesis, Michigan State University, East Lansing, MI, 1977.
84. DeWitte, W. J.; Schoening, R. C.; Popov, A. I. Inorg. Nucl. Chem. Letts. 1976, 12, 251.
85. Khaezali, S. Ph.D. Thesis, Michigan State University, East Lansing, MI, 1982.
86. "Nonaqueous Electrolytes Handbook", Janz, G. J.; Tomkin, R. P. T. eds., Academic Press, vol. 1 (1972).
87. (a) Allerhand, A.; Gutowsky, H. S.; Jonas, J.; Meinzer, R. A. J. Am. Chem. Soc. 1966, 88, 3185.

87. (b) Allerhand, A.; Gutowsky, H. S. J. Chem. Phys.
1964, ~~40~~⁴¹, 2115.

MICHIGAN STATE UNIV. LIBRARIES



31293010967176